Status of G_M^n, G_E^n analysis

Andrew Puckett
University of Connecticut
SBS Collaboration Meeting
9/12/2024

UCONN

Acknowledgements

- This work supported in part by DOE Office of Science, Office of Nuclear Physics, award DE-SC0021200
- SBS Collaboration
- Materials/photos/analysis in this talk provided by:
  - Arun Tadepalli, Mark Jones, Bogdan Wojtsekhowski, Robin Wines, Eric Fuchey, Gordon Cates, David Hamilton, etc.
  - GMN analysis results/plots provided by GMN/nTPE thesis students: Provakar Datta, Sebastian Seeds, Anuruddha Rathnayake, Maria Satnik, Zeke Wertz, John Boyd *et al.*
  - GEN analysis results/plots from GEN thesis students: Faraz Chahili Kate Evans, Jack Jackson, Sean Jeffas, Gary Penman, Hunter Presley, *et al.*
- And many others…

Outline

- Overview of SBS neutron form factor experiments—apparatus, physics observables, methodology
- Overview of SBS software infrastructure
  - Monte Carlo simulation
  - Event reconstruction
  - Data analysis: detector calibration tools, physics analysis tools, Monte Carlo event generators, etc
- GMn/nTPE analysis details:
  - σ_n/σ_p extraction methodology
  - Systematic Uncertainties
  - Outstanding issues–HCAL efficiency, MC inconsistencies
- GEN analysis details:
  - Asymmetry and FFR extraction methodology
  - Inelastic contamination
  - Statistics challenges
  - Path forward
- Summary and conclusions

The SBS neutron Form Factor Experiments

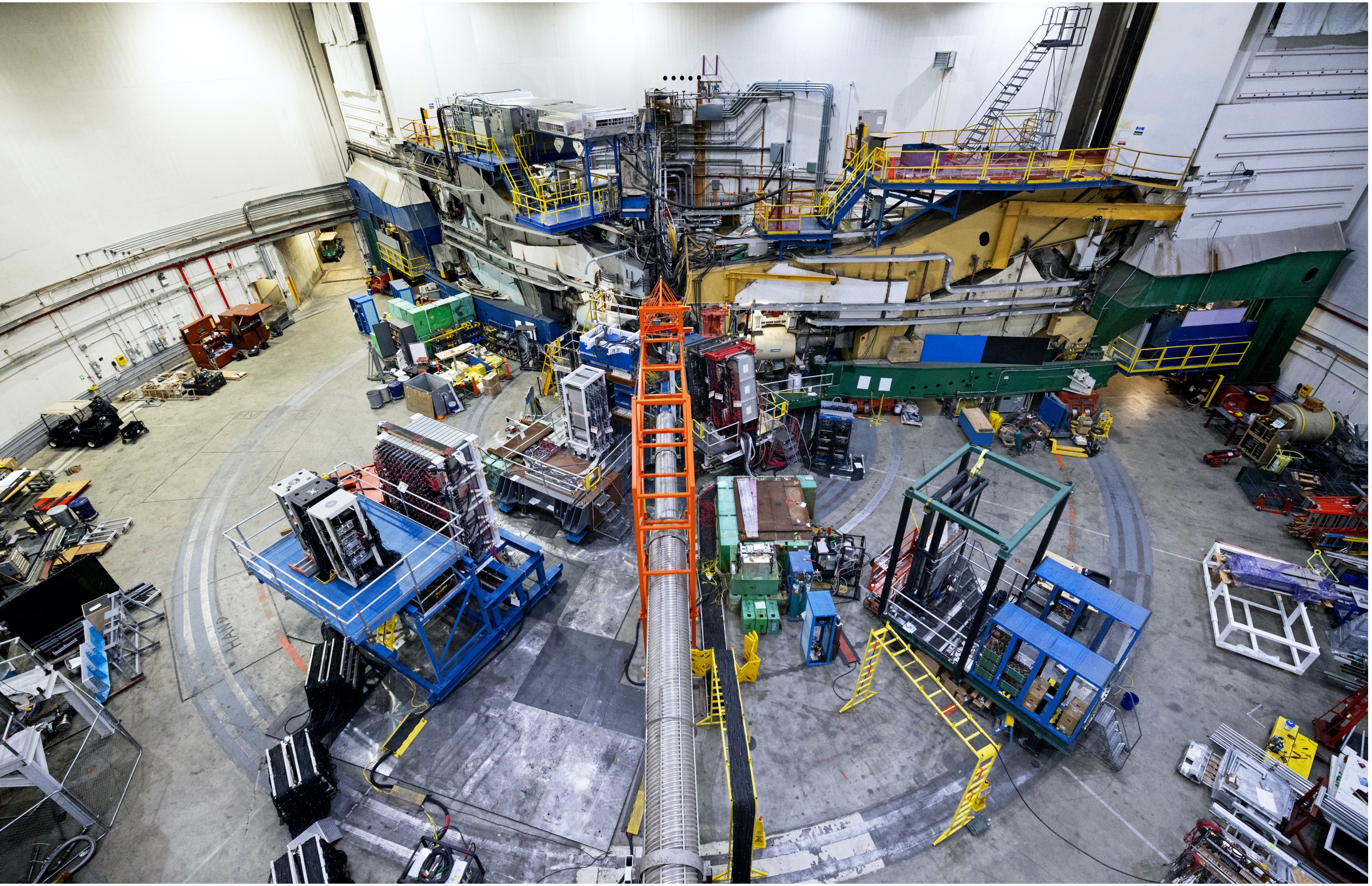

- Both GMN and GEN involve measurements of coincidence (e,e'N) reactions in quasi-elastic kinematics on light nuclear targets
- Common requirements include:
  - Scattered electron detection with tracking, PID, and full kinematic reconstruction
  - Nucleon detection and charge identification
- Key differences include:
  - Physics observables (cross section ratio versus polarized beam-target asymmetry)
  - Dominant sources of uncertainty:
    - nucleon acceptance/detection efficiency systematics (GMN)
    - Statistics and inelastic contamination! (GEN)

GMN/GEN Apparatus, I: Hadron Arm

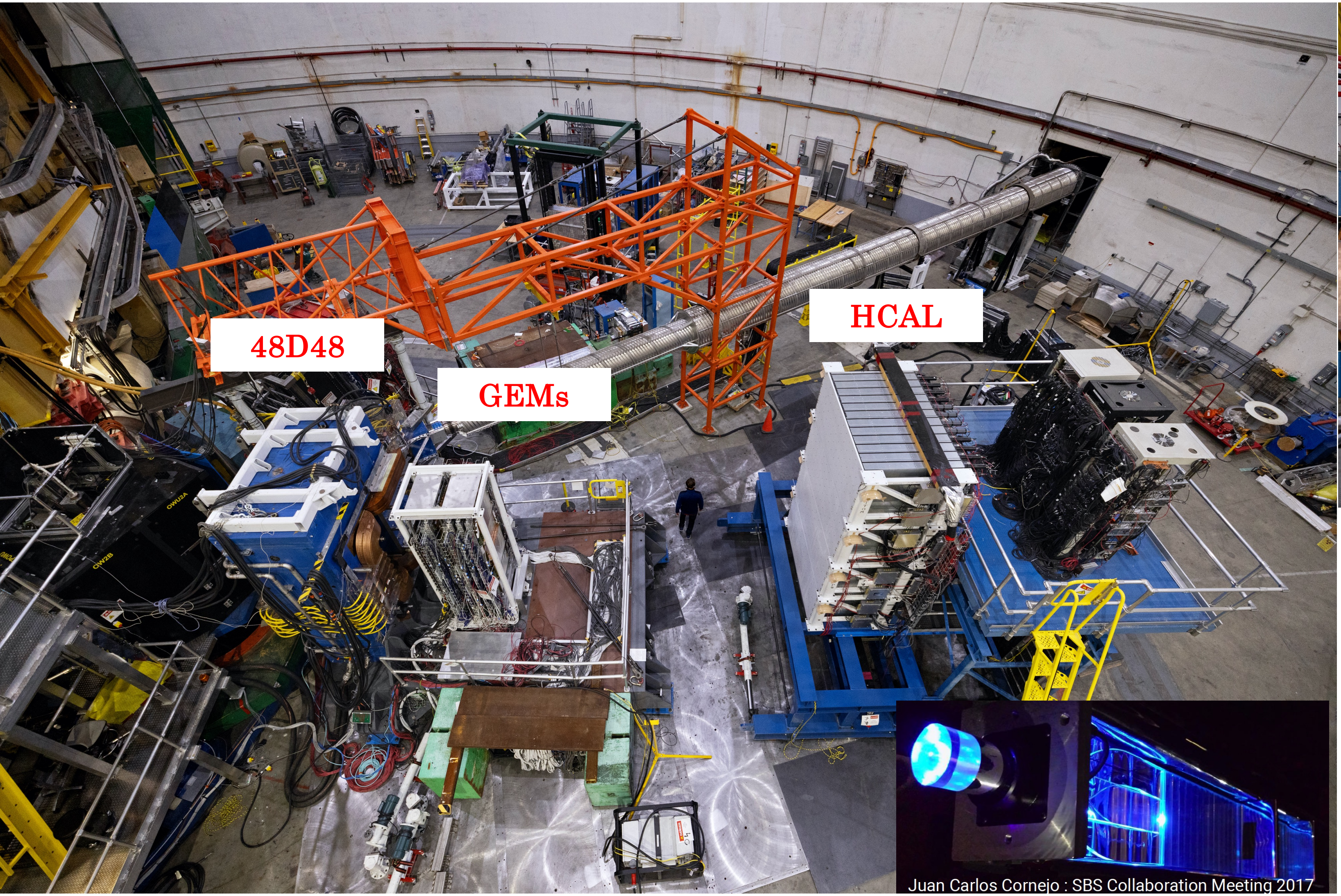

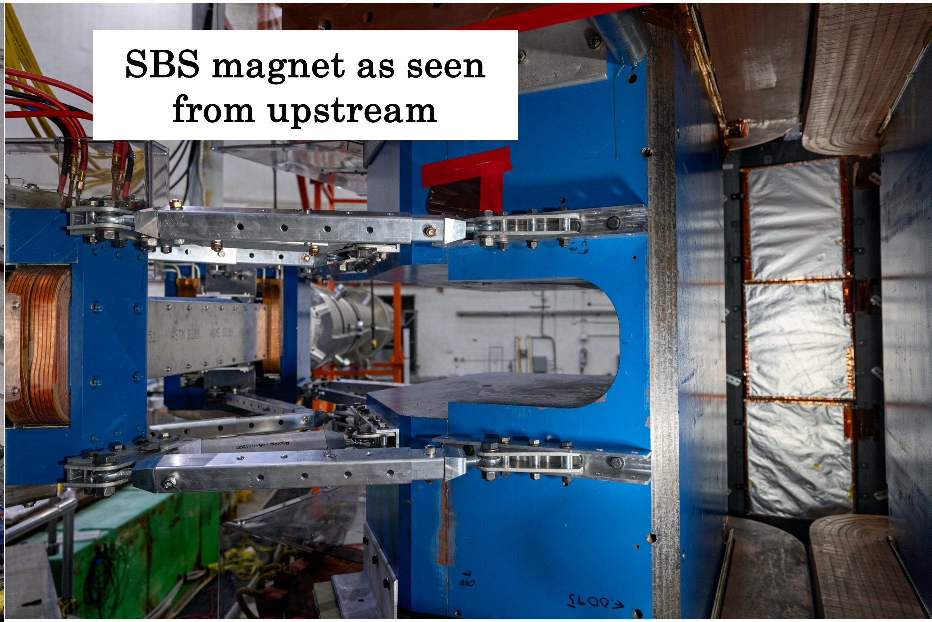

Common to ALL SBS experiments:

- 48D48 magnet: dipole with a cut in iron yoke for passage of the beam → reach forward scattering angles
- Hadron Calorimeter (HCAL) → efficient detector for high-energy hadrons (protons, neutrons, pions, etc)
- Gas Electron Multipliers (GEMs) → high-rate charged-particle tracking (not used in hadron arm during GMN)

GMN/GEN Apparatus, II: Electron Arm

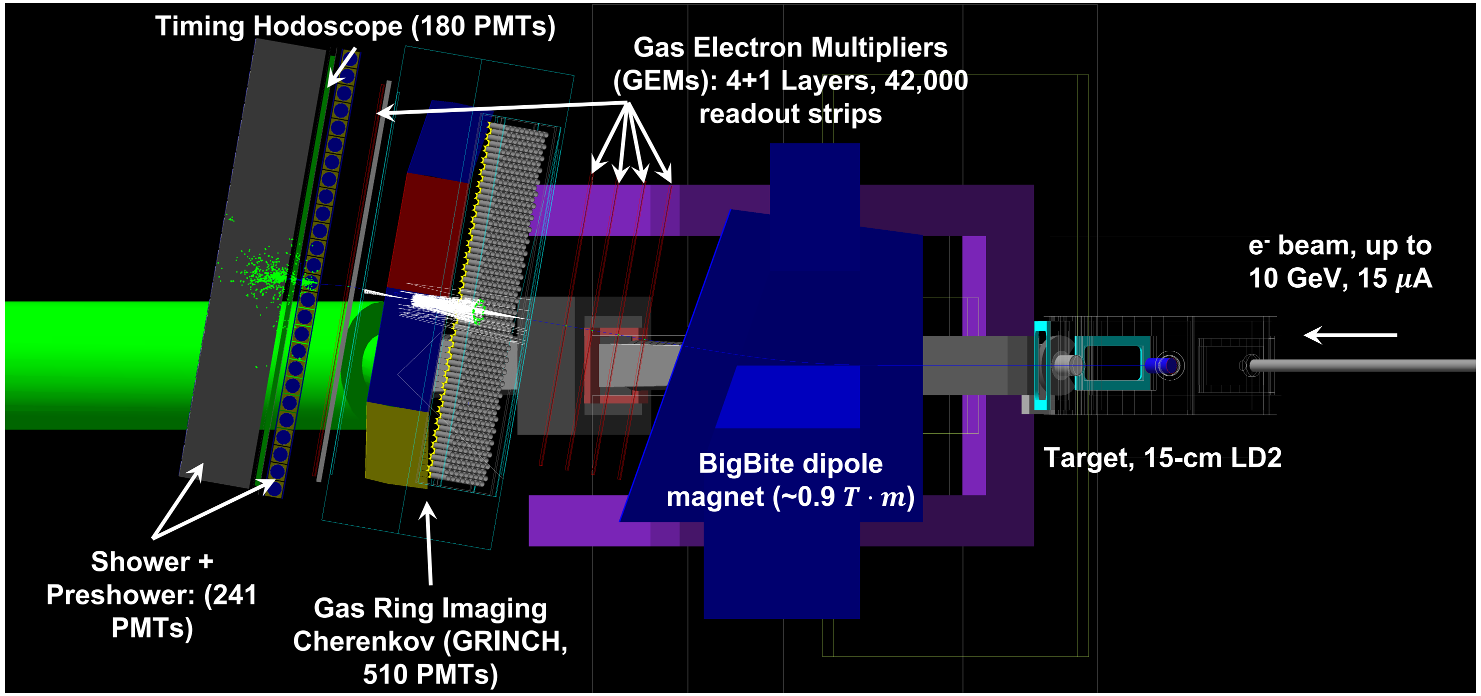

- BigBite spectrometer upgrades for 12-GeV era high-luminosity running:
  - GEM-based tracking—5 layers, 42,000 readout strips
  - Gas Cherenkov with high segmentation (510 PMTs) for pion rejection
  - Replace preshower lead-glass with rad-hard blocks from HERMES
  - Highly-segmented scintillator hodoscope (89 paddles) for precise time-of-flight measurement

GMN/GEN Apparatus, III: Targets

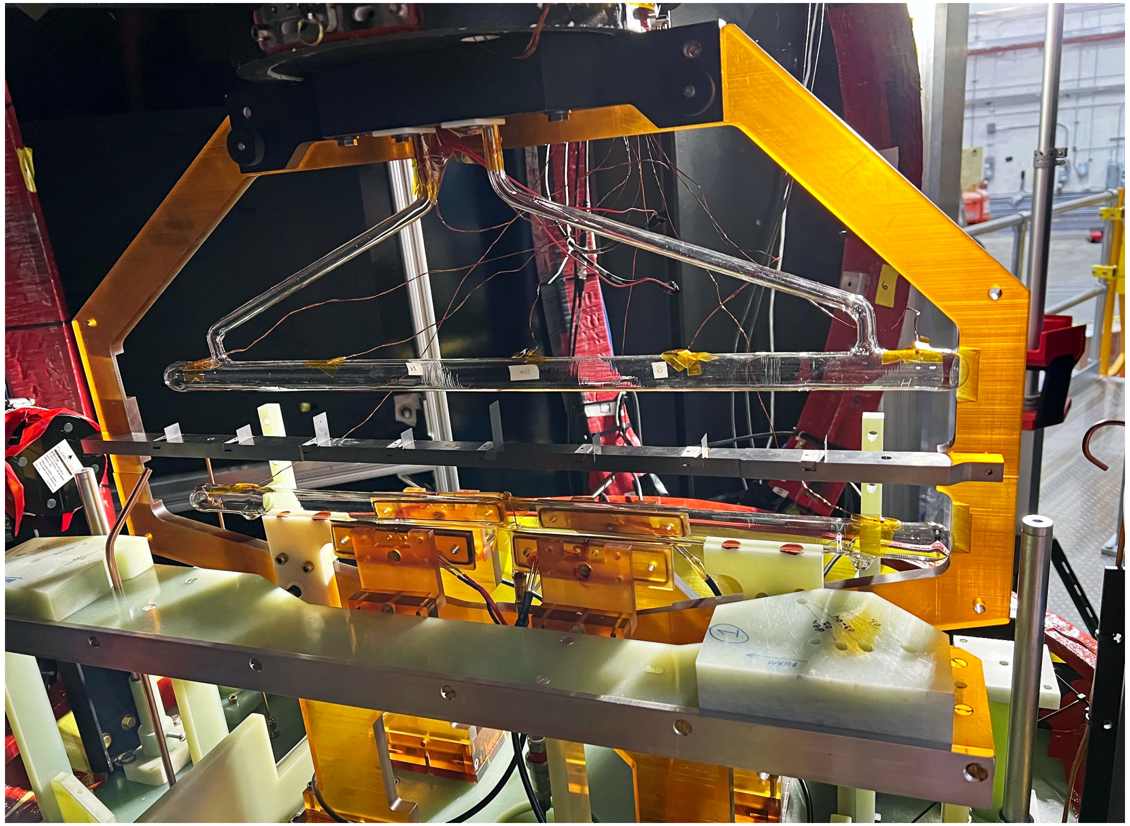

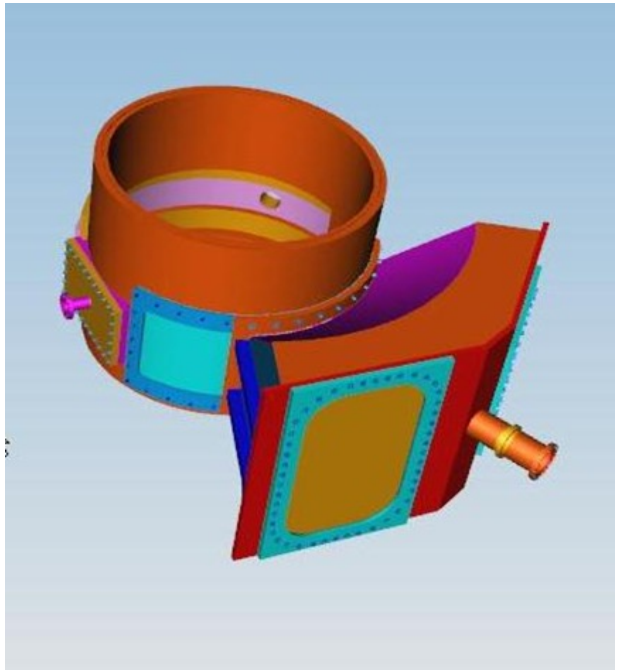

- Above: cryotarget (LH2/LD2) and optics ladder for GMN/GEN-RP/Pion-KLL
- Middle: scattering chamber “vacuum snout” for GEP

- Above: Polarized Helium-3 target for GEN with optics foils/reference cell/NMR pickup coils/etc.

SBS Software Infrastructure

- SBS online/offline analysis software is based on Podd, the standard C++/ROOT-based Hall A analysis framework
- Important/"official" repositories (these are the codes that are developed/supported/maintained by the SBS software "czar" (me)):
  - **SBS-offline**: https://github.com/JeffersonLab/SBS-Offline Main repository of SBS-specific reconstruction libraries and source code. Includes raw data decoders that aren't yet standardized under Podd for new readout modules such as MPD w/VTP and VETROC
  - SBS-replay: https://github.com/JeffersonLab/SBS-replay Repository for analyzer database files, replay scripts, analysis and calibration macros, online GUI configuration files, etc. No build system. Just a collection of files. This repo is needed for all SBS analysis.
  - **Libsbsdig**: https://github.com/JeffersonLab/libsbsdig Main library for digitization of simulation output; translates *g4sbs* output (hit time, position, energy deposit, etc) into simulated raw detector signals ("pseudo-data"), populates "hit" data structures used by reconstruction (ADC, TDC, crate, slot, channel, etc); purpose is for testing and developing event reconstruction algorithms and for physics analysis; analyzing simulated events using identical algorithms to those used for real data.
  - **G4sbs**: https://github.com/JeffersonLab/g4sbs GEANT4-based simulation of all of the major SBS experiments. Documentation at https://hallaweb.jlab.org/wiki/index.php/Documentation_of_g4sbs
  - SIMC: https://github.com/MarkKJones/simc_gfortran/tree/bigbite custom SIMC for use in SBS analysis; the main use case in SBS analysis is elastic/quasi-elastic event generation with realistic nuclear and radiative effects.
  - **SBSGEM_standalone**: https://github.com/ajpuckett/SBSGEM_standalone standalone GEM reconstruction code. Was useful during GEM cosmic commissioning before GMN, but superseded by SBS-offline. No longer under active development, maintenance, or end-user support.
- There are several other "unofficial" repositories for analysis support written by SBS thesis students that have proven highly useful.

Event Reconstuction in GMN/GEN: Common Aspects

- Electron reconstruction in BigBite
  - BBCAL clustering: energy, position, time reconstruction (FADC). Pion rejection via preshower. Define region of interest for tracking
  - Hodoscope: precise timing analysis (TDC)
  - GEMs: Tracking
  - BigBite optics: reconstruct kinematics and vertex
  - GRINCH: pion rejection
- Nucleon reconstruction in HCAL
  - HCAL clustering: energy, position, time (FADC and TDC)

BigBite Tracking

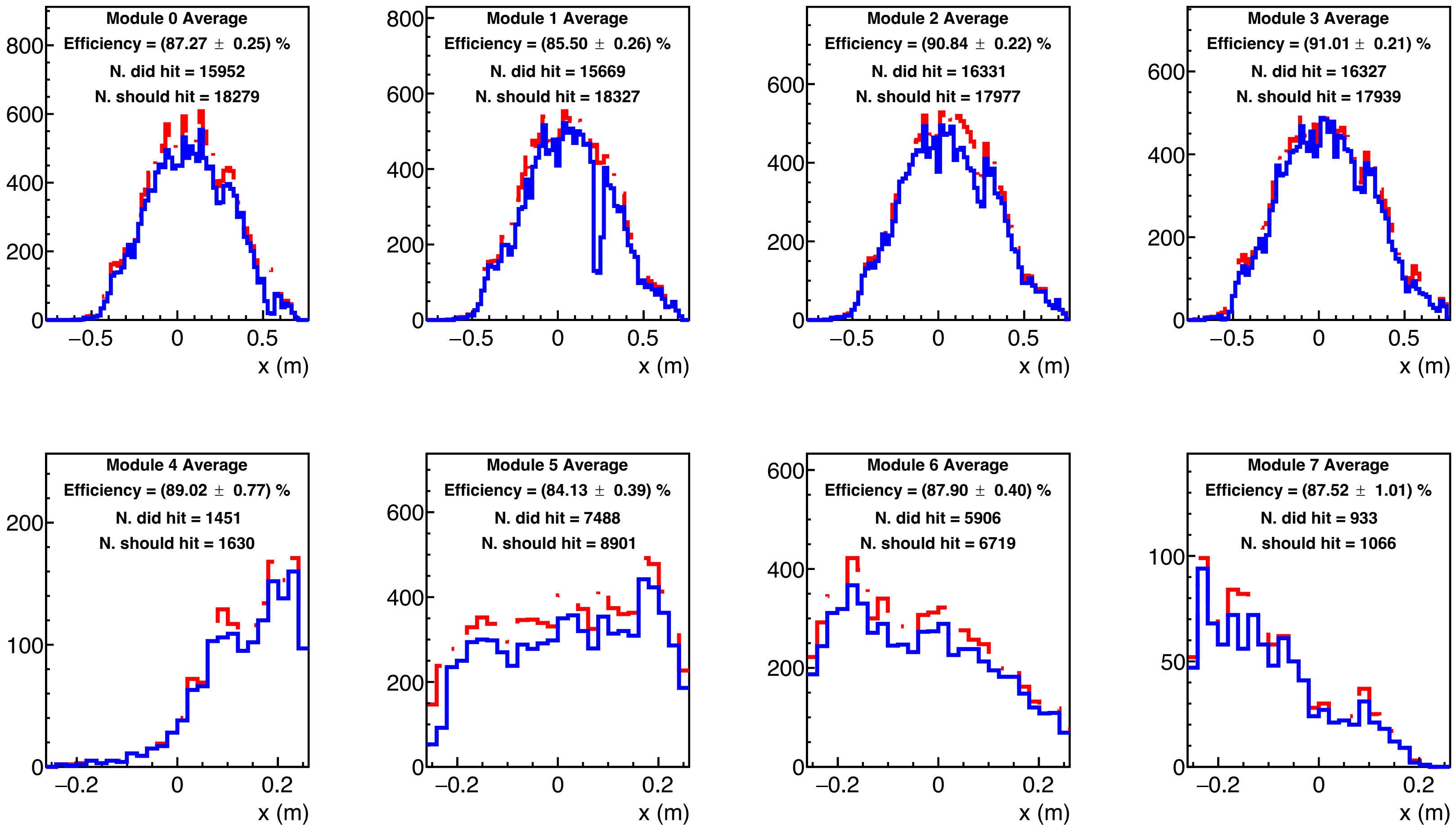

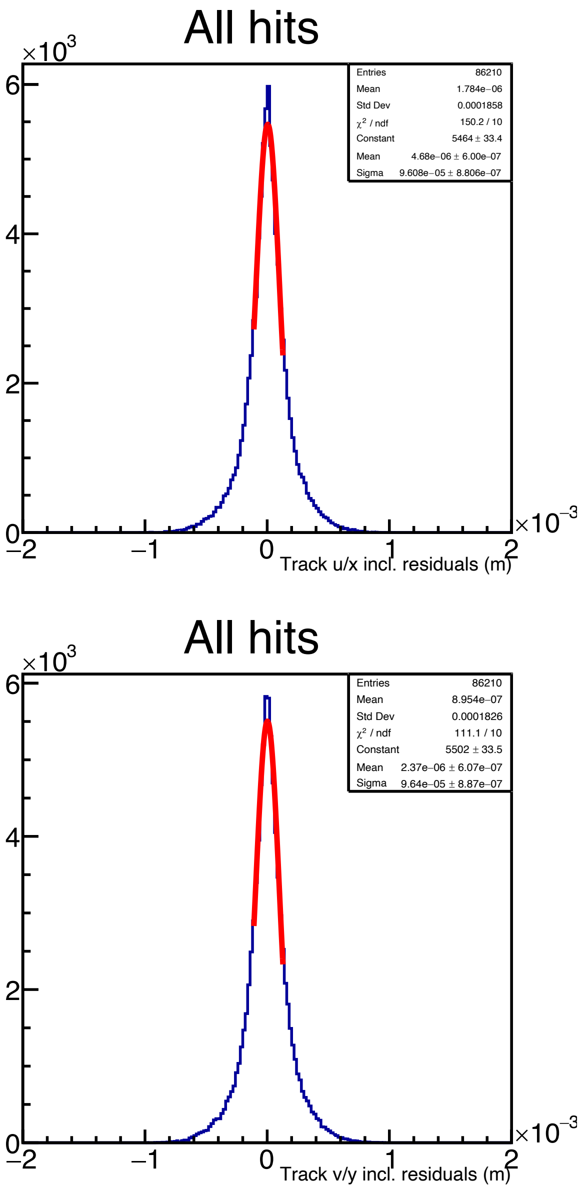

- Typical track-based efficiencies and residuals in well-calibrated tracking.
- For more details, see my talk from Hall A Winter Meeting 2024

BigBite Optics

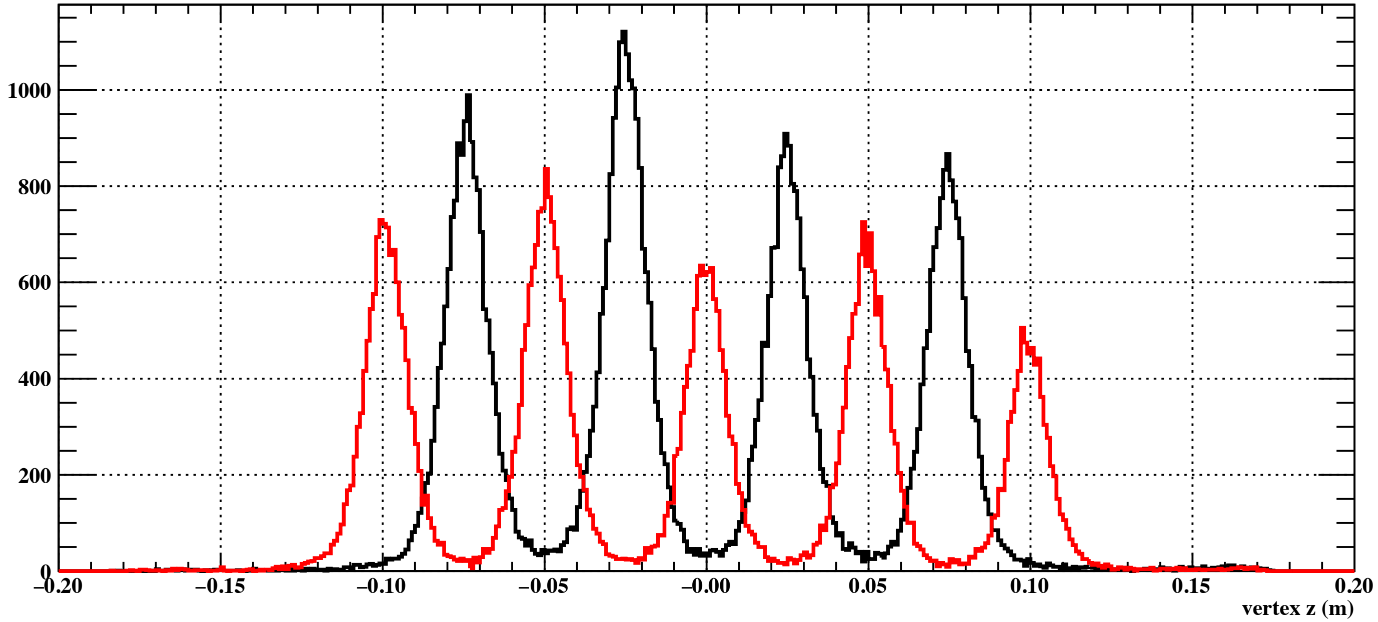

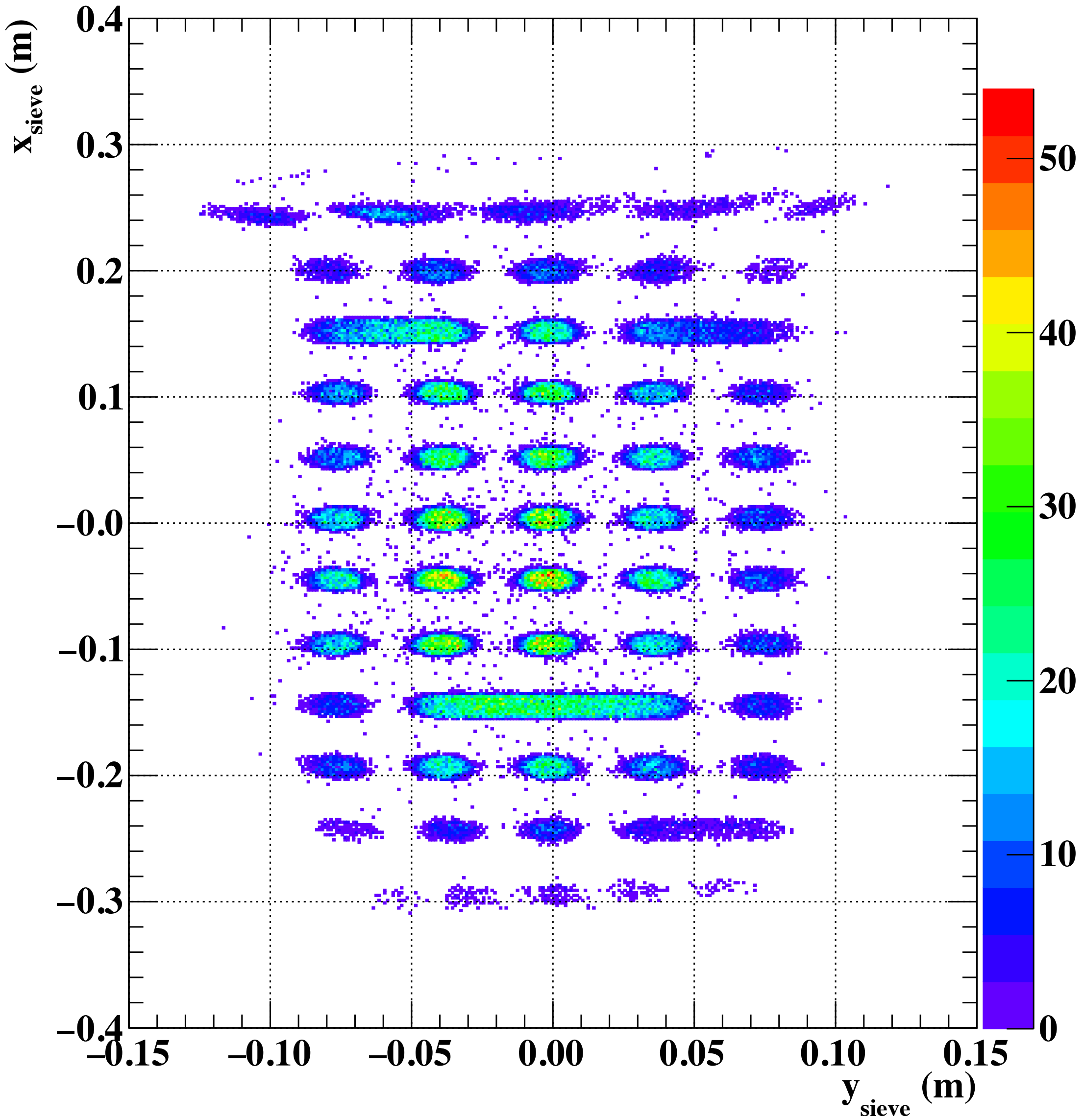

- Above, left: vertex z reconstruction from optics-foil targets (4-foil and 5-foil data from GEN-RP)
- Right: reconstructed sieve hole pattern, GEN-RP

BigBite PID example: "SBS-9", run 13747 (15 uA LH2)

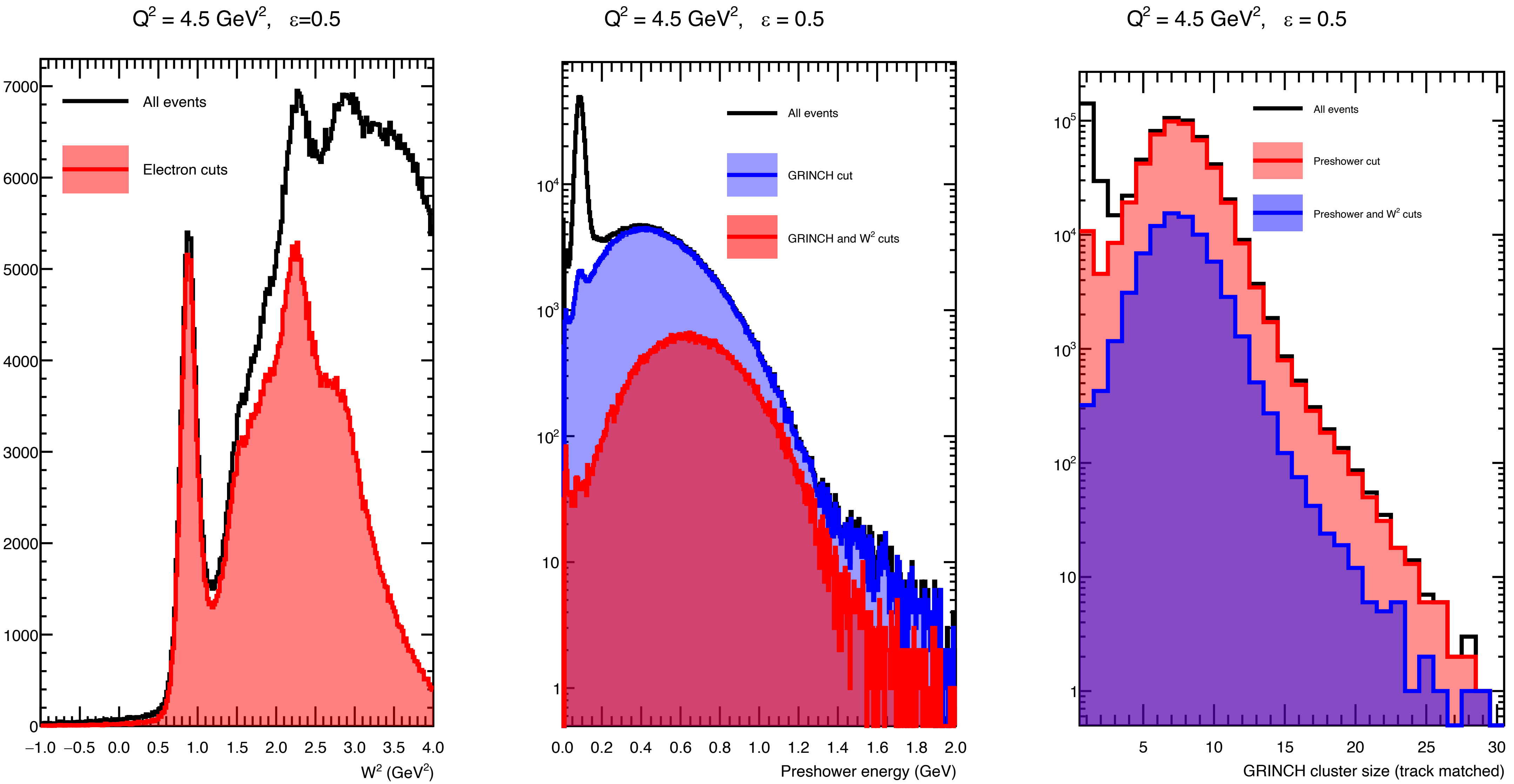

Neutron/proton separation

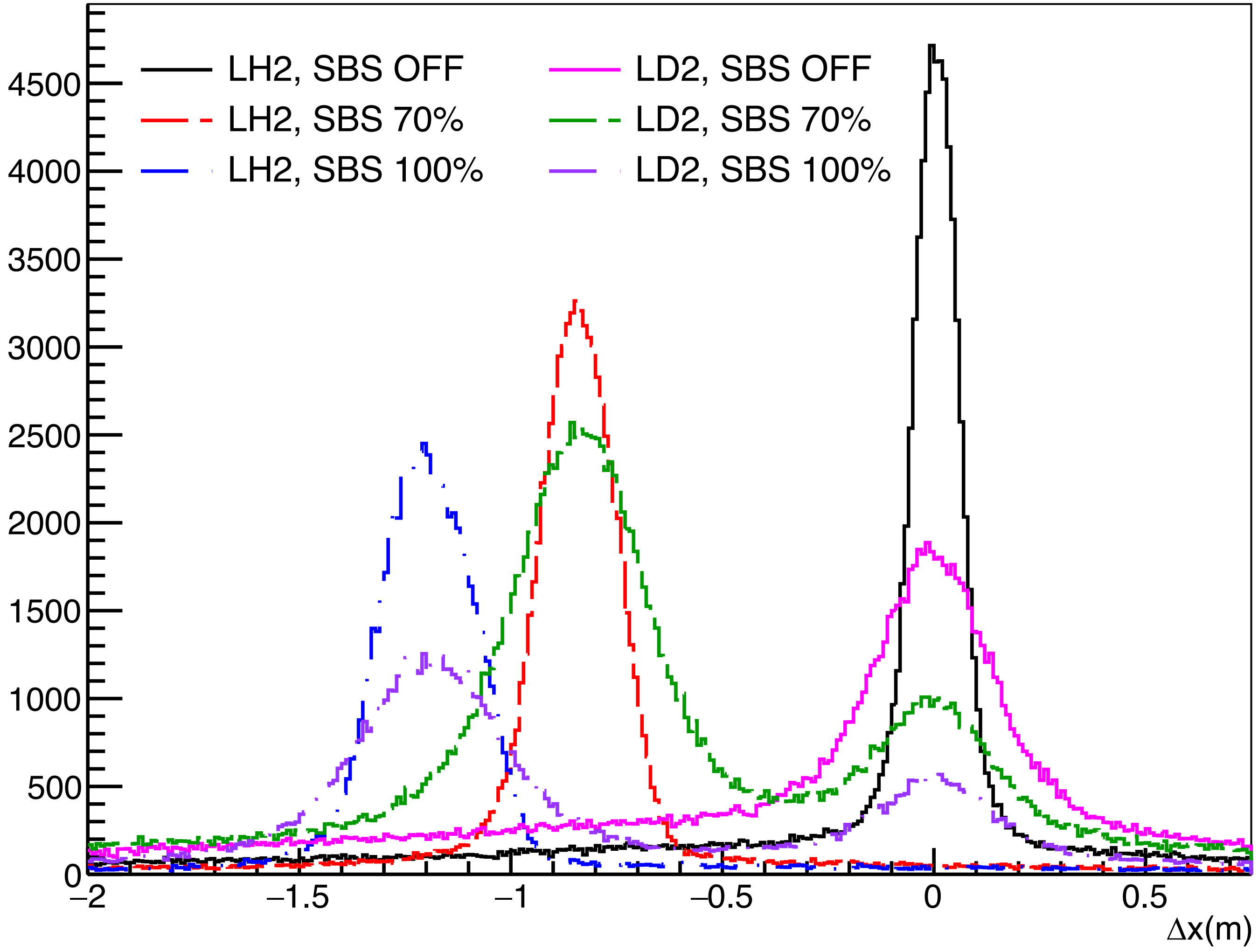

- Nucleon charge ID is accomplished by a small vertical deflection of protons in SBS magnet
- Optimal deflection is that which gives ”clean” n/p separation while minimizing acceptance/efficiency difference between neutrons and protons
- “Fiducial cut” is calculated based on reconstructed *electron* kinematics—requires that both proton and neutron in quasi-elastic kinematics would hit HCAL active area with a safety margin equivalent to ~100 MeV Fermi smearing

HCAL reconstruction and elastic event selection, $Q^2 = 4.5, \epsilon = 0.5$ (SBS-9)

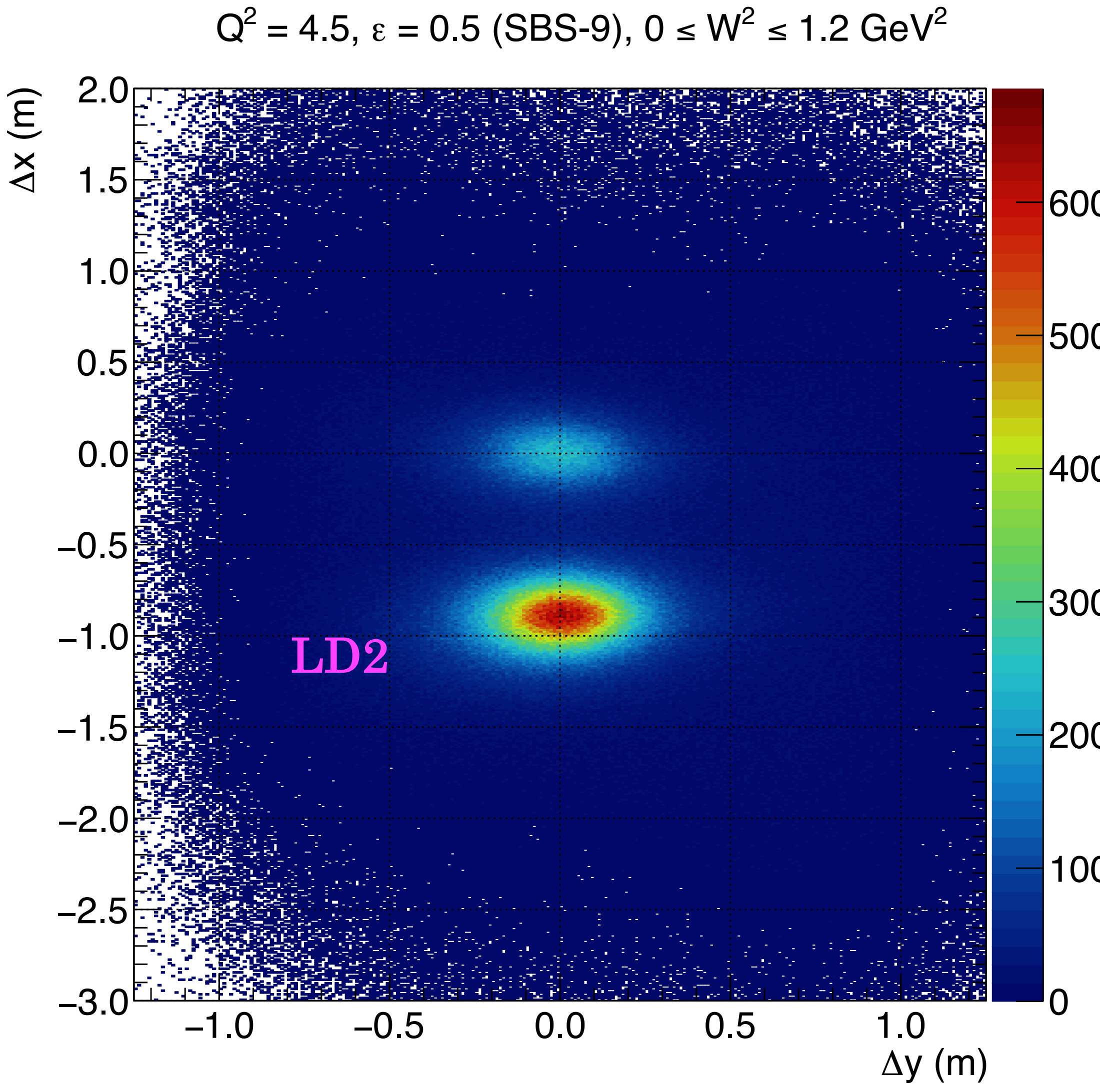

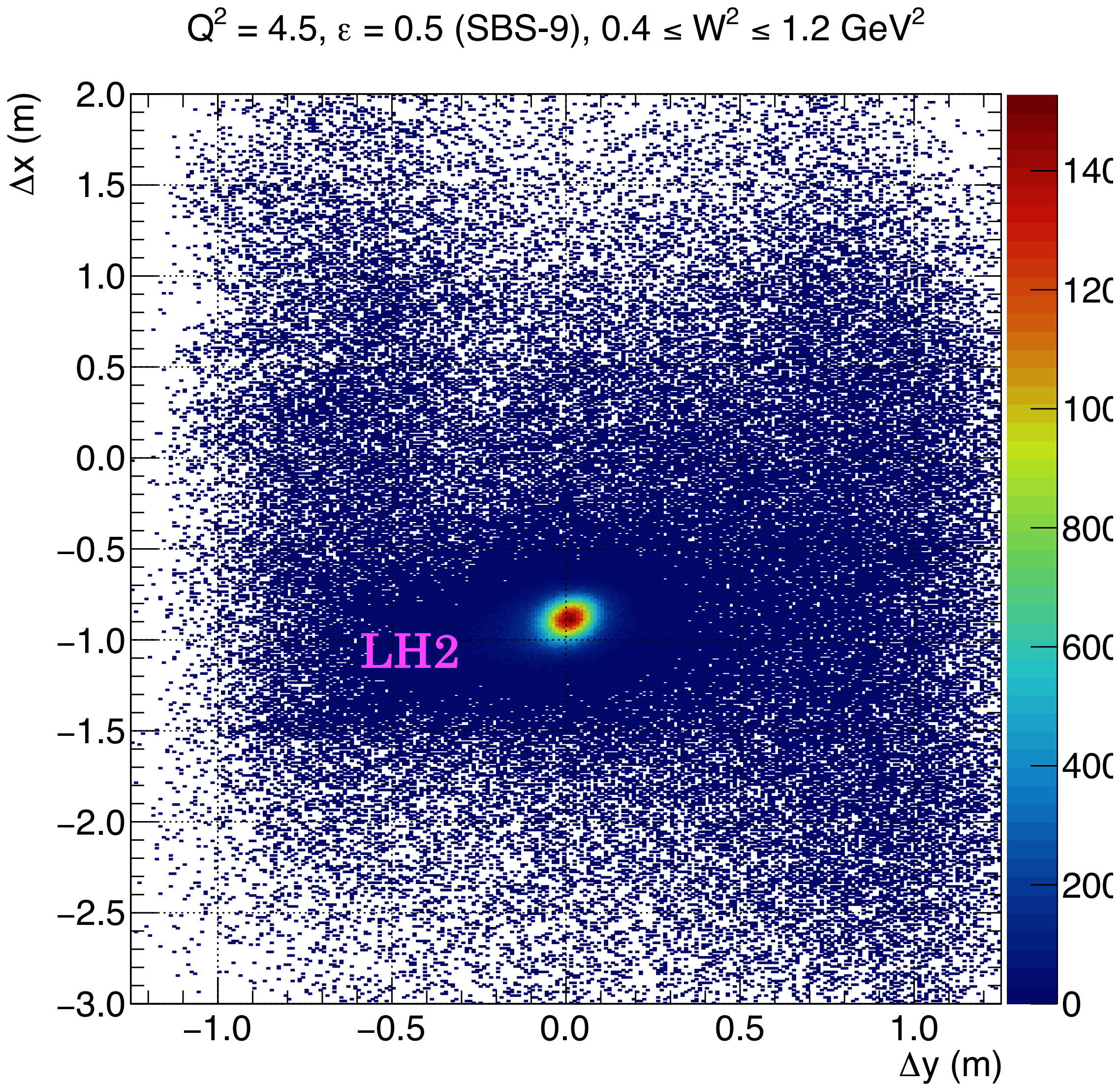

Experiments E12-09-019/E12-20-010 (GMN/nTPE)

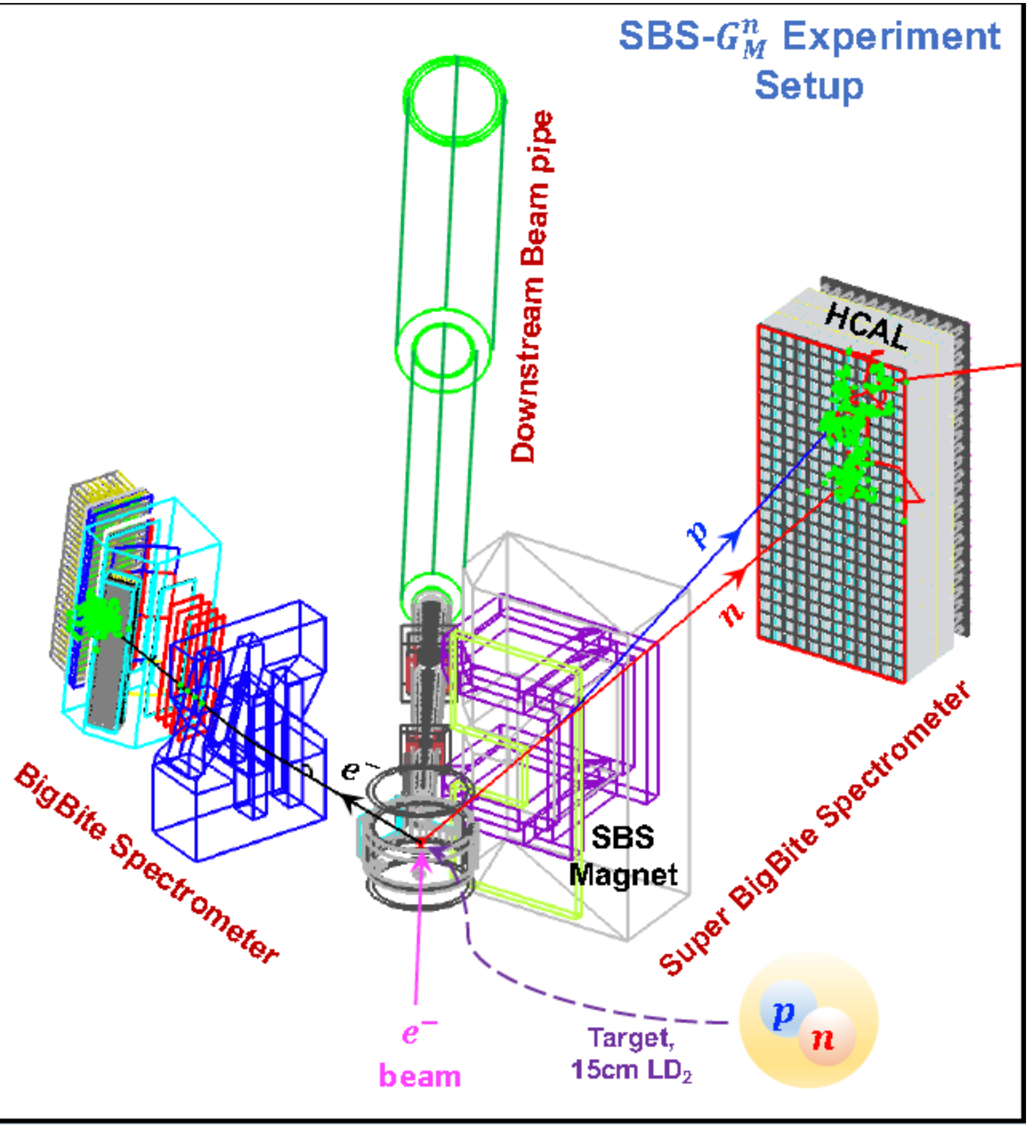

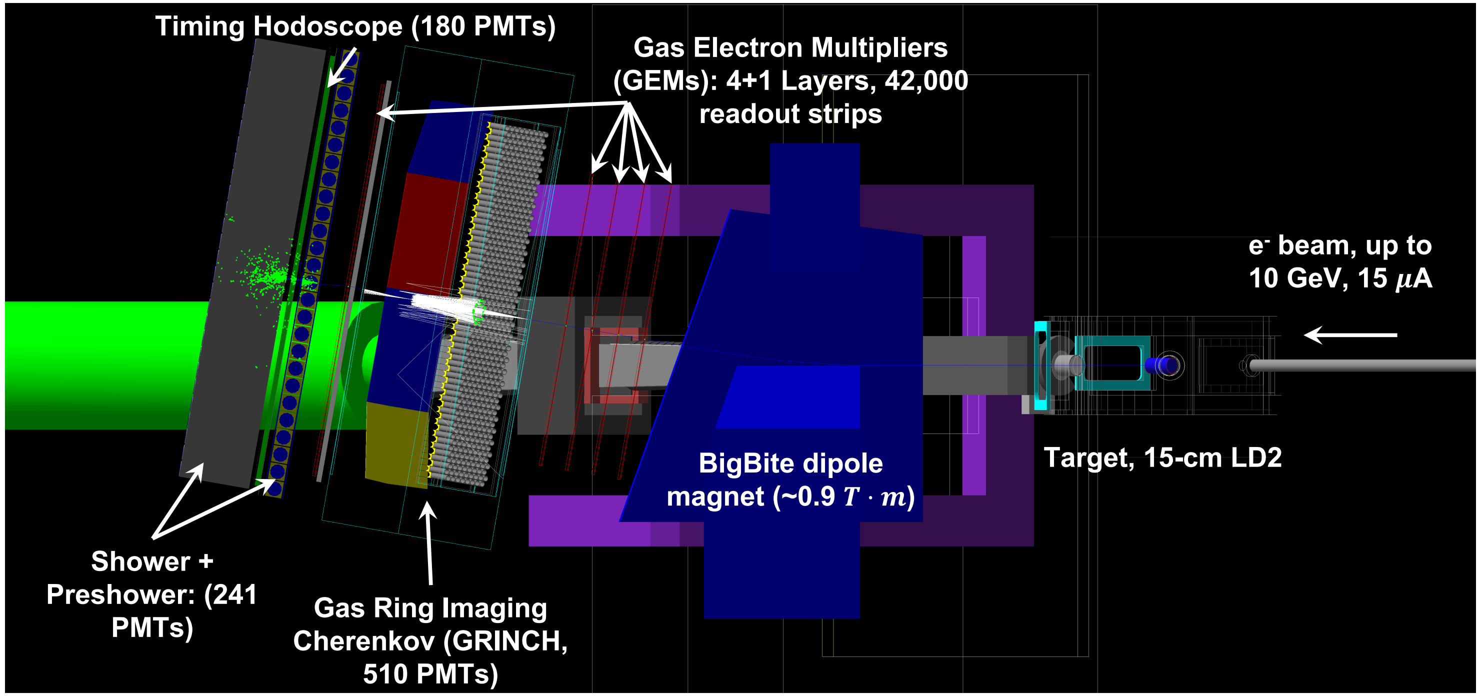

- Measure cross section ratio d(e,e'n)/d(e,e'p) on liquid deuterium.
- e^- arm: BigBite with upgraded detectors for high-luminosity running
- n/p arm: SBS with HCAL
- Ran Oct. 2021-Feb. 2022

“Ratio” method for G_M^n

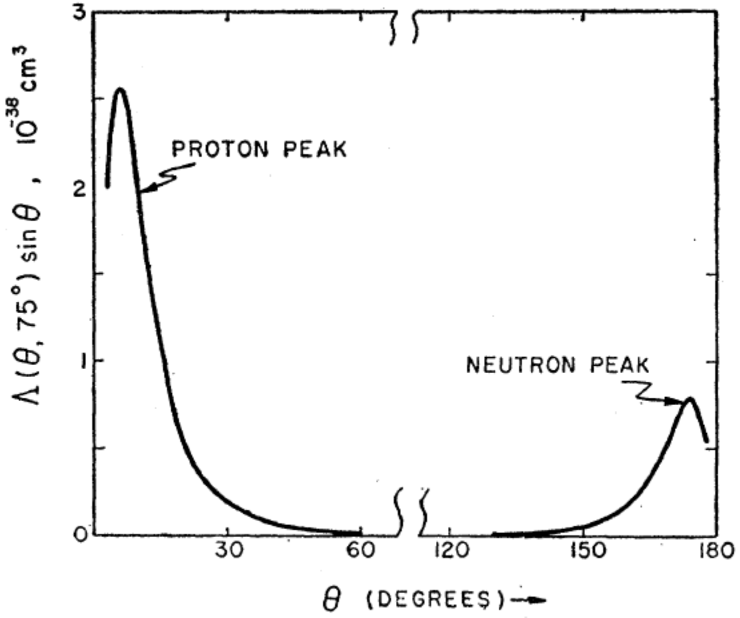

FIG. 1. The angular distribution function $\Lambda(\theta,\vartheta)\sin\theta$ in the absence of final-state interactions is plotted as a function of the proton scattering angle in the nucleon center-of-mass system [$\cos\theta=\hat{p}\cdot\hat{q}$] for the scattering of 500-Mev electrons through an angle $\vartheta=75°$ with a momentum transfer giving $p=\frac{1}{2}q=1.3\times10^{13}$ cm^{-1}. $\Lambda(\theta,\vartheta)$ is defined in Eq. (11.2); the function $F(\theta)$ entering the definition was evaluated using a Hulthén wave function for the deuteron. The cross section $d^3\sigma/(d\theta d\Omega_e dE_e')$ is given by (4.71×10^5 cm^{-1} rad^{-1} sterad^{-1} Mev^{-1}) $\Lambda(\theta,\vartheta)\sin\theta$. No nucleon form factors have been introduced into the results.

Figure from Durand, 1959 (Phys. Rev. 115, 1020 (1959))

- Idea: simultaneous measurement of $d(e,e'n)p$ and $d(e,e'p)n$ in quasi-elastic kinematics
- Simultaneous measurement cancels many sources of experimental systematic uncertainty (electron acceptance/detection efficiency, luminosity, detector and DAQ livetime, etc).
- Small nuclear model dependence—nuclear (and radiative) effects similar/nearly identical for (e,e’n) and (e,e’p) cross sections
- Combine with existing knowledge of free proton cross section to extract free neutron cross section
- **Major remaining source of systematic uncertainty is the relative acceptance/efficiency between protons and neutrons! → SBS-HCAL was designed to minimize this**

nTPE experiment: Precision Rosenbluth Separation of $en \to en$

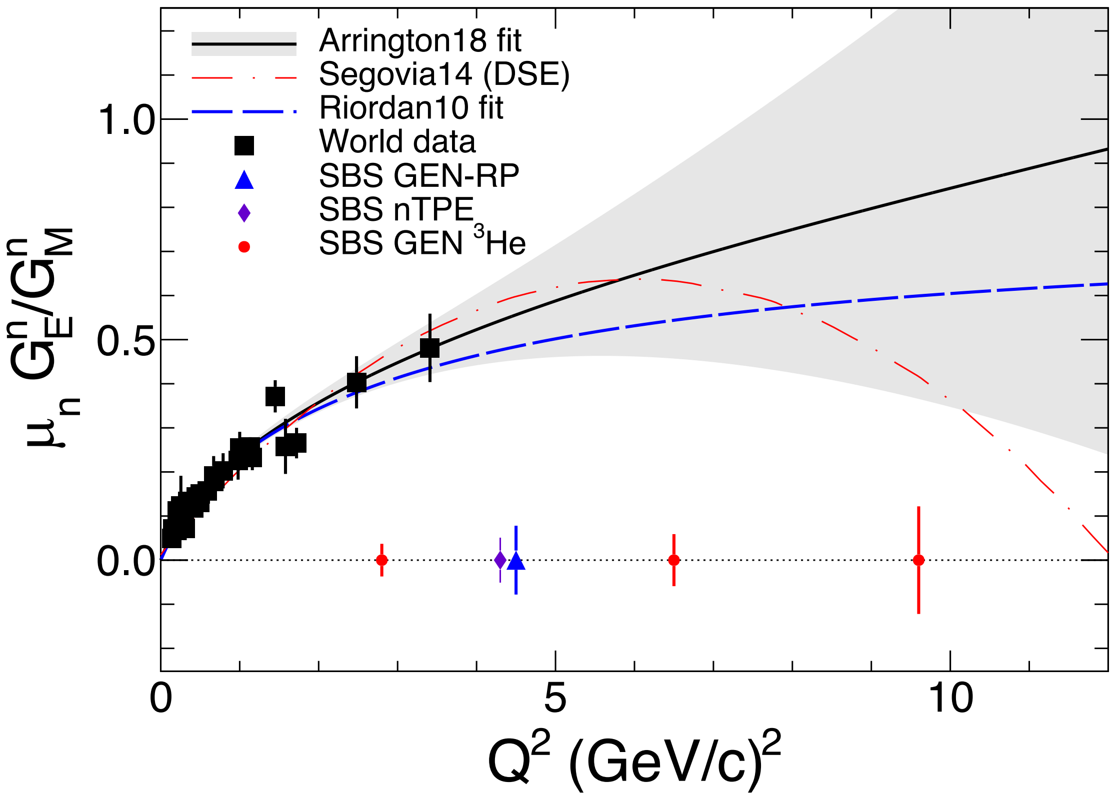

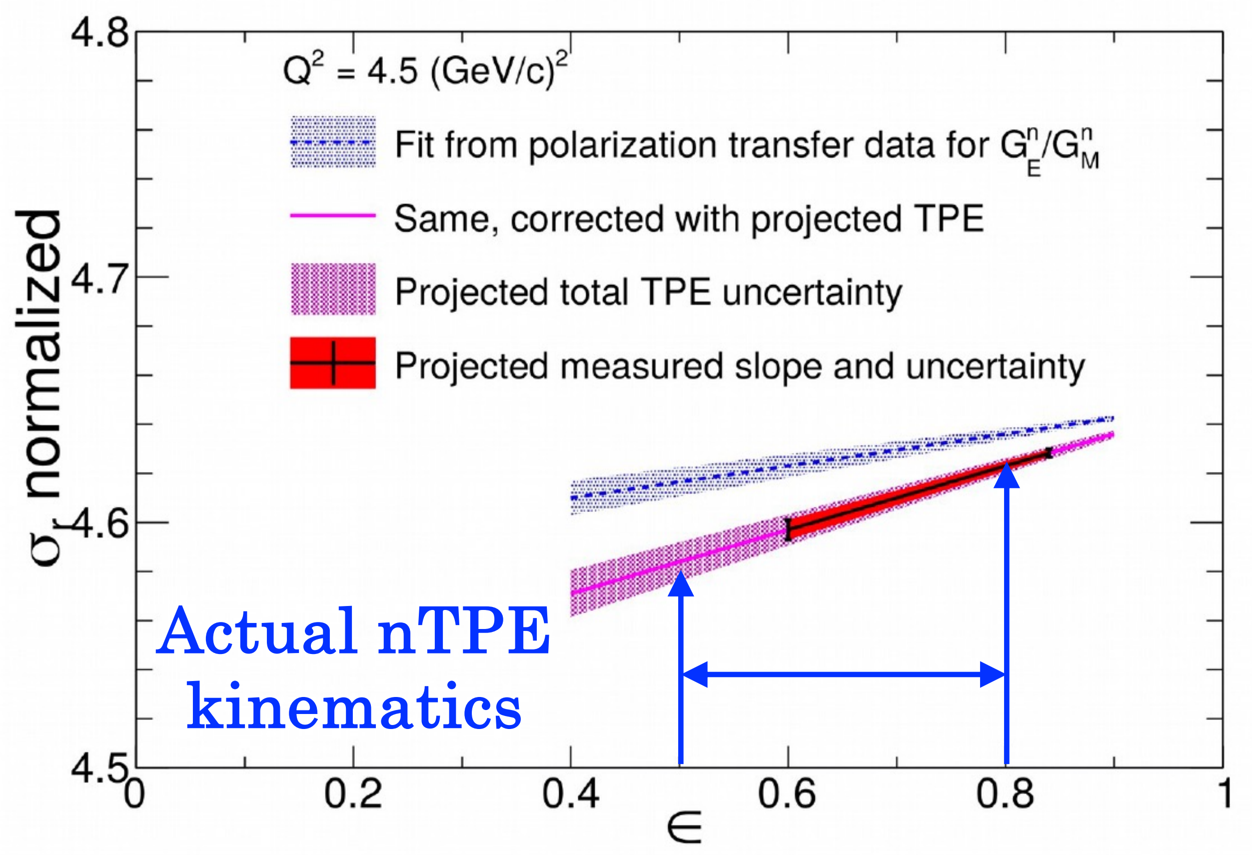

- Left: $\mu_n G_E^n / G_M^n$ world data and projected uncertainties from SBS program
- Right: projected nTPE sensitivity from proposal 12-20-010 (**Eric Fuchey contact**)
- Actual kinematics have $\Delta\epsilon \approx 0.3$, compared to 0.24 from the proposal

GMN extraction using ratio method—basic idea

- Goal is to extract σ_n/σ_p in quasi-elastic kinematics with small uncertainties.
- Nuclear and radiative effects are expected to (mostly) cancel in the ratio, especially at high Q^2
- Electron acceptance, efficiency, luminosity/etc also cancel
- Most important known sources of systematic uncertainty:
  - Differences in acceptance/efficiency between neutrons and protons (if any)
  - Inelastic contamination (and other backgrounds, e.g., accidentals, fake GEM tracks/etc)
- SBS HCAL was designed to minimize n/p acceptance/efficiency difference!
  - Large acceptance
  - High (and very similar) efficiencies for p, n (by design)

$$R_{np} \equiv \frac{\sigma_{d(e,e'n)p}}{\sigma_{d(e,e'p)n}} \approx \frac{\sigma_{en\rightarrow en}}{\sigma_{ep\rightarrow ep}}$$

$$\approx \frac{\epsilon {G_E^n}^2 + \tau {G_M^n}^2}{\epsilon {G_E^p}^2 + \tau {G_M^p}^2}$$

$$\implies G_M^n \approx \sqrt{\frac{R_{np}\sigma_R^p - \epsilon {G_E^n}^2}{\tau}}$$

- BigBite gives $\vec{q}$ vector and interaction vertex
- Project to the surface of HCAL and compare to detected nucleon position/energy/time.

SBS GMN analysis methodology

- All relevant (known) physics and detector effects are built in to the Monte Carlo simulation:
  - SIMC: quasi-elastic $d(e,e'N)$ event generation with realistic nuclear and radiative effects (suitable modifications for GMN analysis by Provakar Datta, Mark Jones)
  - G4sbs: SBS detector simulation (GEANT4-based) (many contributors)
  - Libsbsdig: translate simulation output to pseudo-raw data that can be processed by the same reconstruction code as the real data (Eric Fuchey)
  - SBS-offline: event reconstruction (A. Puckett, E. Fuchey, J.-C. Cornejo, many others)
- Fit real data to the sum of simulated quasi-elastic n and p scattering (plus inelastic background)
  - We interpret the relative normalization between MC n and p distributions required to match data as the ratio of the "measured" σ_n/σ_p to the "predicted" ratio from the MC cross section model.

$Q^2 = 7.4$ GeV^2, $0.25 \leq W^2 \leq 1.32$ GeV^2, Fiducial Cuts

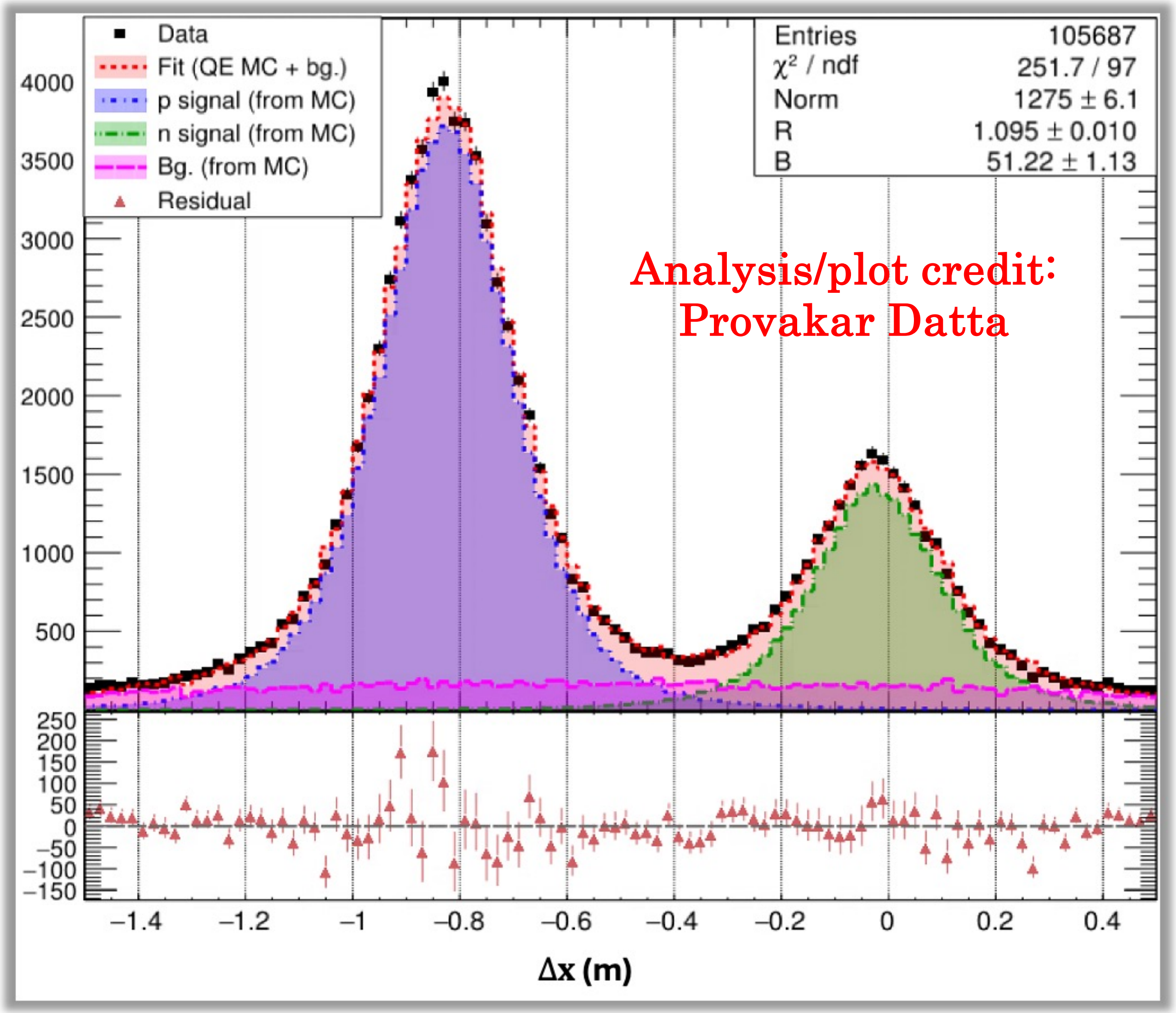

High-Q^2 GMN Data

Q^2 = 9.9 GeV^2, $0.2 \leq W^2 \leq 1.32$ GeV^2, Fiducial Cuts

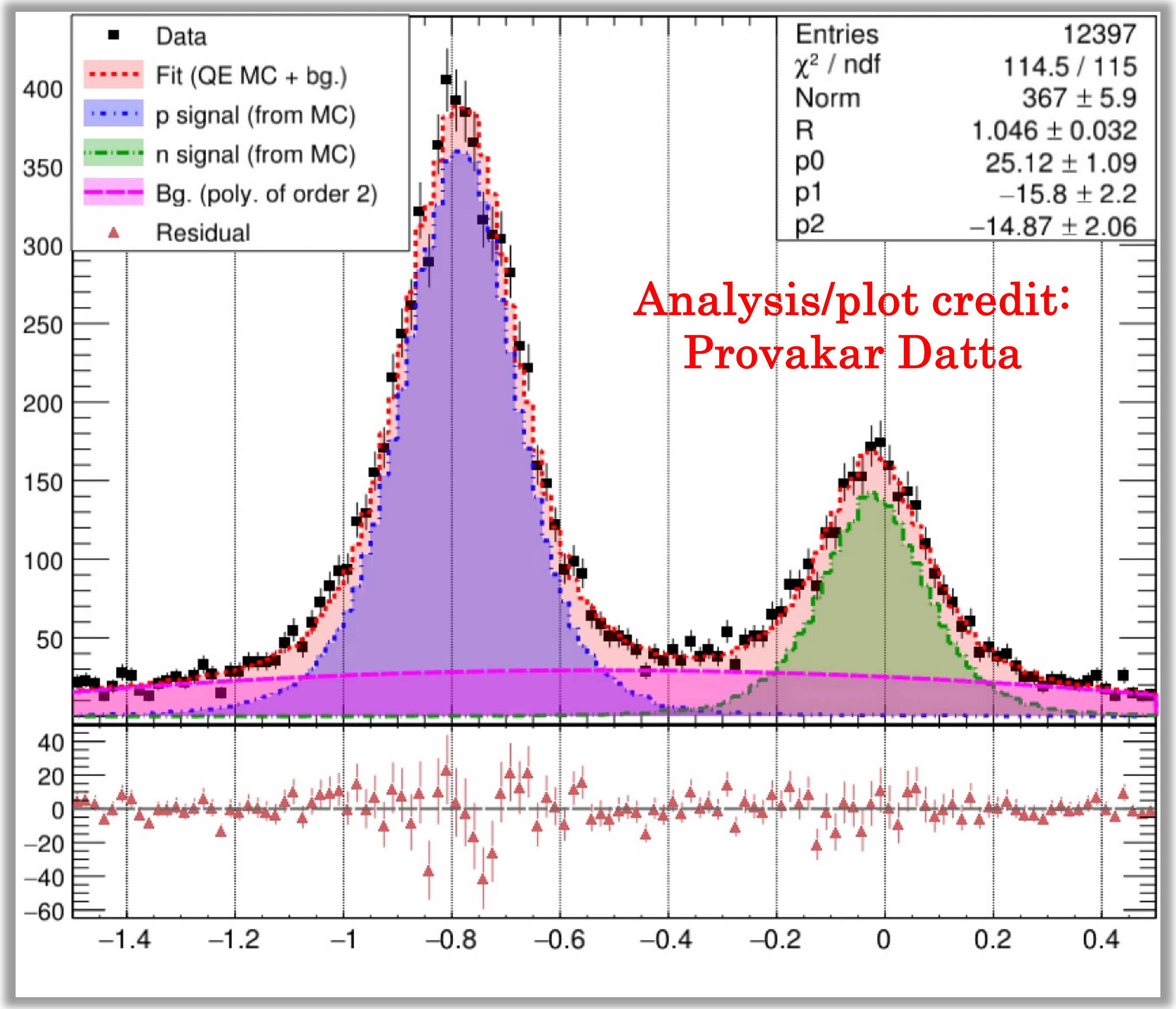

Q^2 = 13.6 GeV^2, $0.16 \leq W^2 \leq 1.44$ GeV^2, Fiducial Cuts

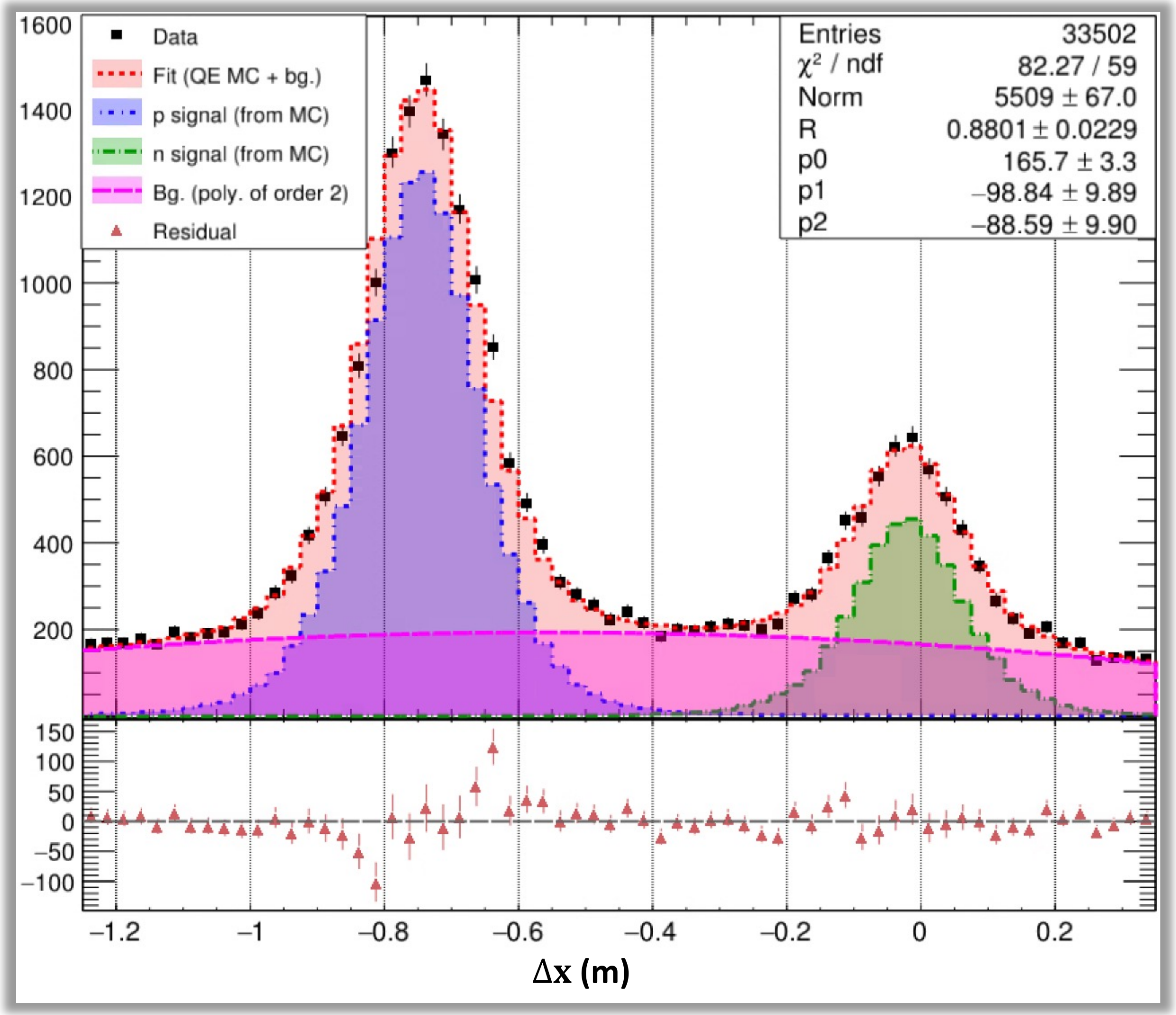

Data/MC comparison for W^2 distribution

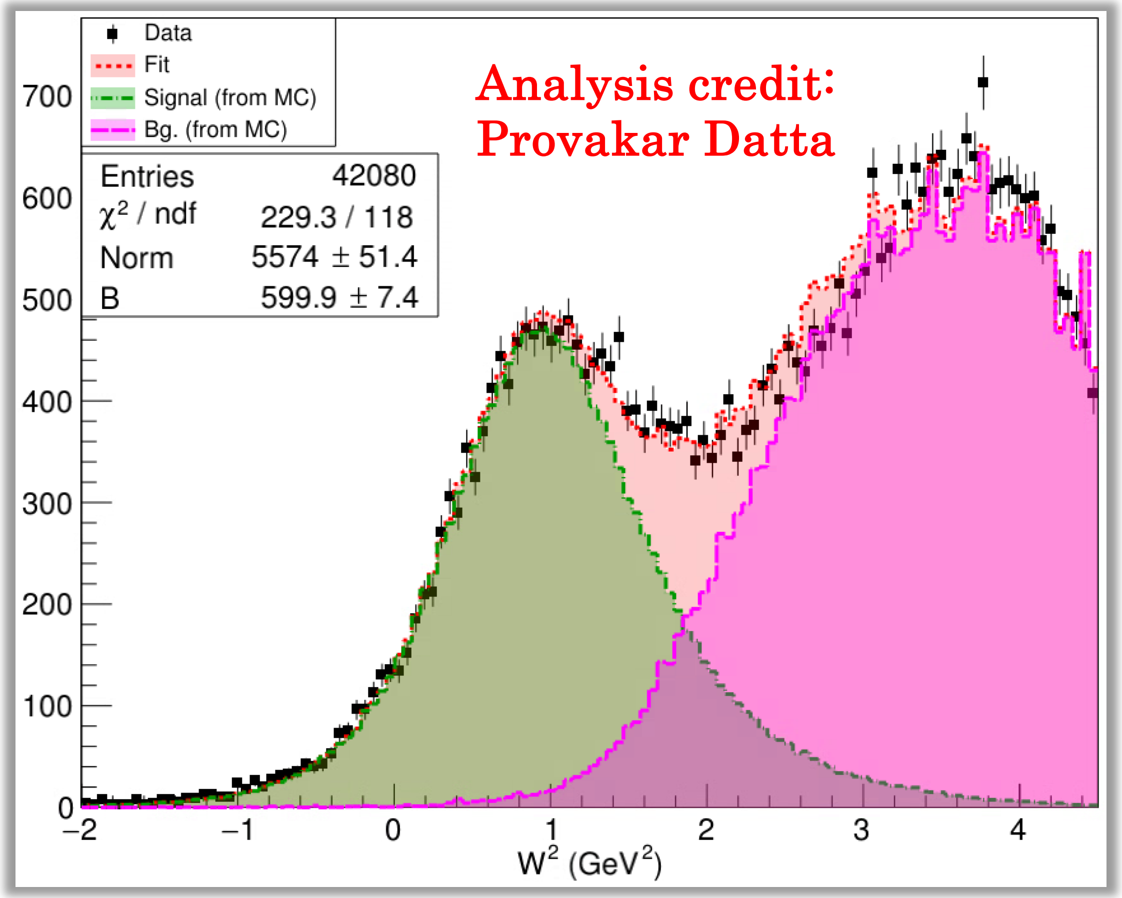

Q^2 = 13.6 (GeV/c)^2

- At high-Q^2, Fermi-smearing and kinematic broadening lead to very wide W^2 distribution for quasi-elastic scattering from deuterium.
- SIMC (quasi-elastic) plus built-in *g4sbs* inelastic generator (based on Christy-Bosted F2F107 fit) qualitatively reproduce the shape of the W^2 distribution very well even at the highest Q^2

GMn systematics: HCAL efficiency

- LH2 elastic data give us a clean sample of tagged protons we can use to estimate HCAL efficiency
- No dedicated calibration data for neutron detection efficiency
- We can achieve a (relatively) clean selection of elastically scattered electrons based on BigBite variables alone (especially at low Q^2)
- We use the LH2 elastic data to benchmark the Monte Carlo calculation of proton detection efficiency
- To the extent that data and Monte Carlo agree on the proton detection efficiency, we deem the Monte Carlo simulation trustworthy for both proton and neutron.
- For "SBS-8" $(Q^2, \epsilon) = (4.5, 0.8)$, we have plenty of LH2 and LD2 data across multiple field settings of SBS, to populate the entire useful active area of HCAL.

Methods for Proton Detection efficiency (PDE) analysis

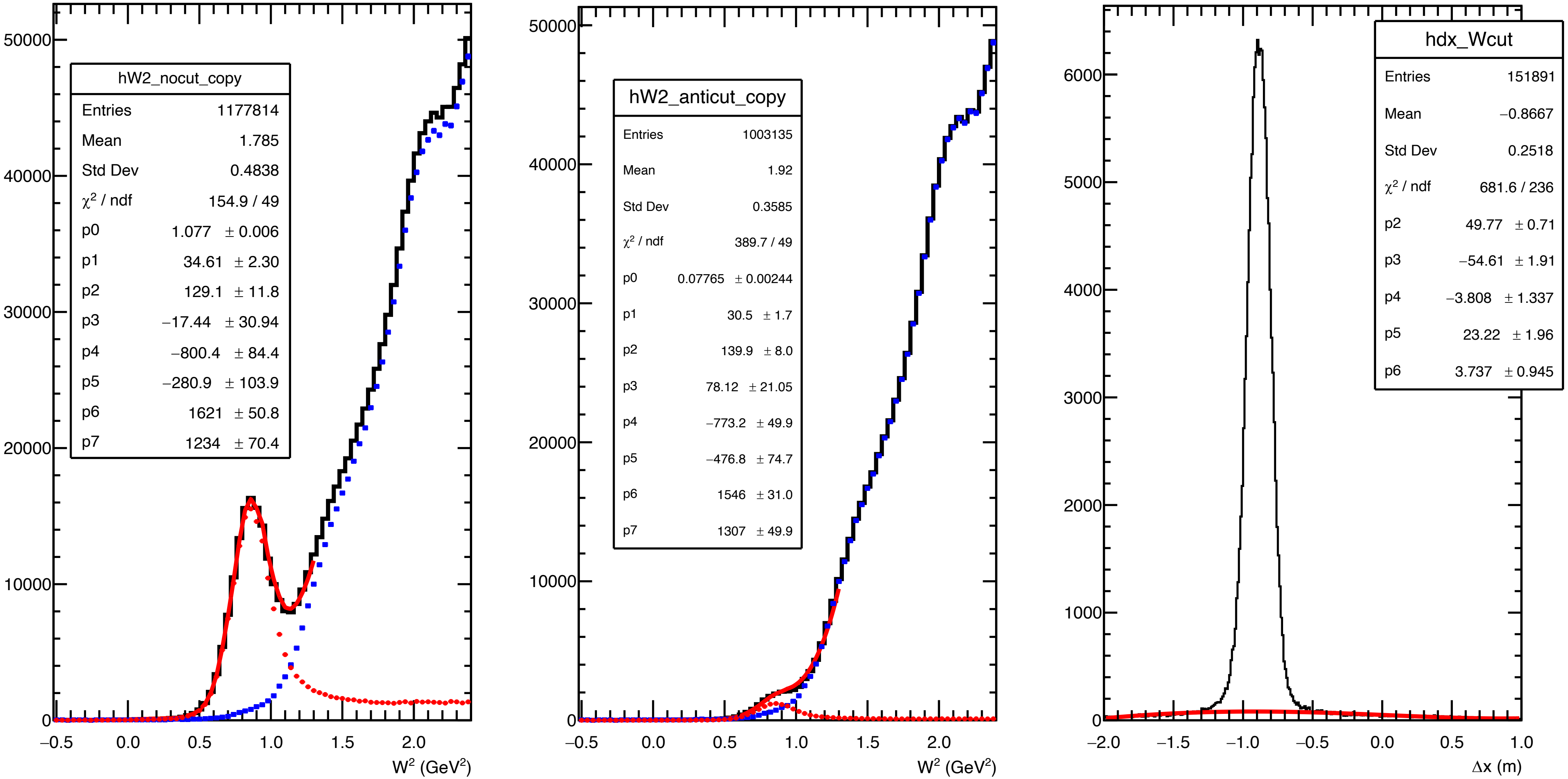

- All methods of extracting PDE involve attempting to estimate the number of elastically scattered protons from electron information alone ("denominator")
- Example at left shows "inclusive W^2 anticut" method
- Pros: Includes background estimation and subtraction
- Cons: very sensitive to cuts and fitting

Pure cut-based method for PDE

- Since January 2024, we have adopted a new strategy for proton efficiency analysis
- Idea is to use aggressive cuts on BigBite variables alone to obtain a "clean" selection of elastically scattered electrons
- In addition to track quality and BigBite PID cuts (preshower, GRINCH, etc), we also apply fiducial cuts on the track midplane projection ("optics validity"), vertex z (reject small end window contribution), and W^2, as well as the usual "fiducial" cuts on the predicted proton position at HCAL (accounting for magnetic deflection)
- Pros: allows us to study detailed position dependence of efficiency
- Cons: Neglects inelastic background; less reliable for high Q^2

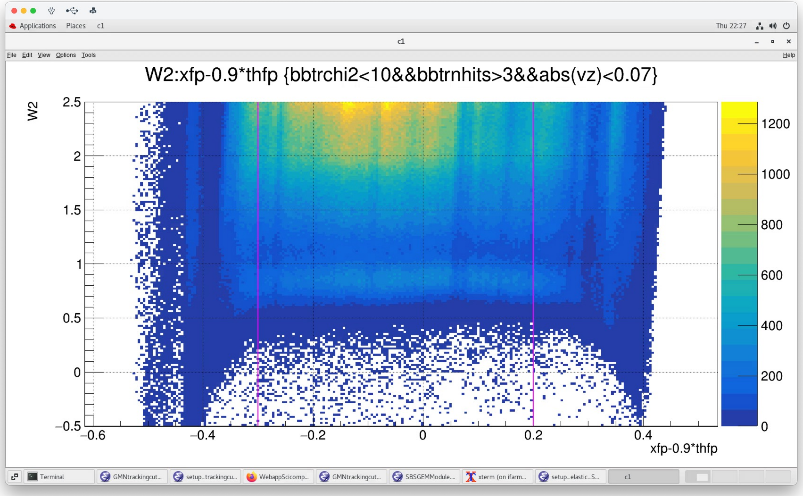

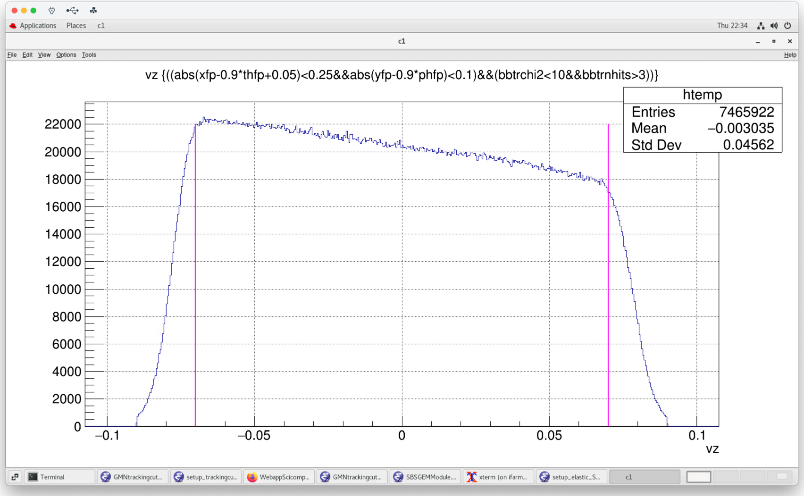

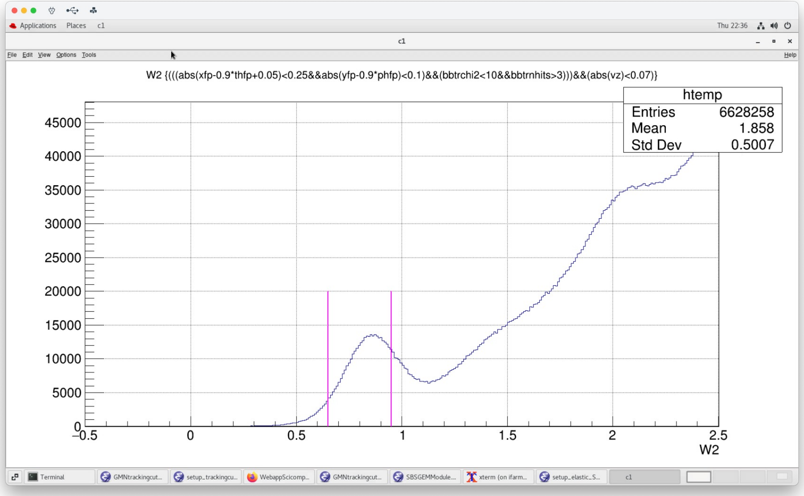

Cut-based HCAL proton detection efficiency example results

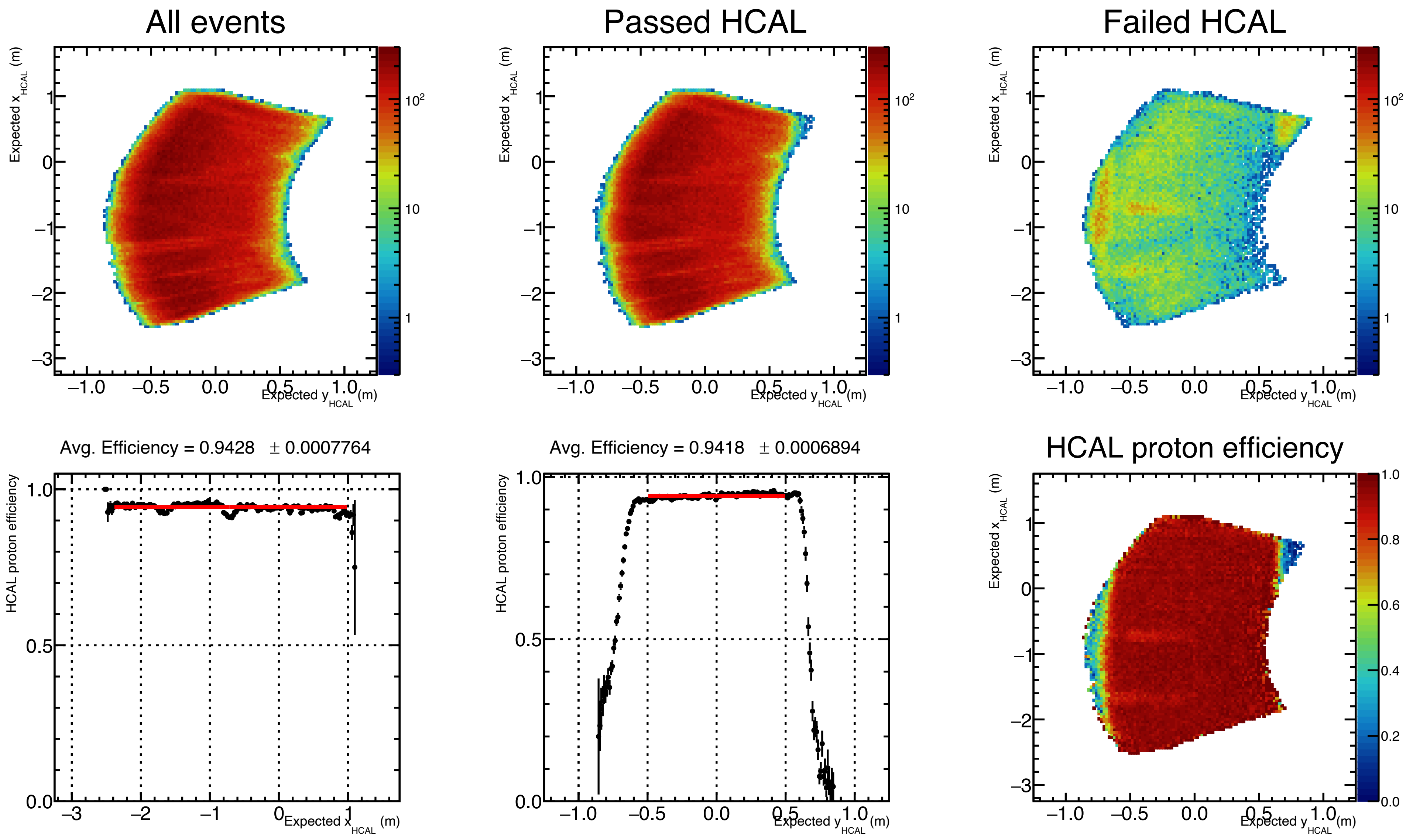

- These results are for $Q^2 = 4.5\ GeV^2, \epsilon = 0.8$ ("SBS-8")
- This analysis, done for the first time in January 2024, reveals low-efficiency regions of HCAL corresponding to known faulty HCAL modules
- Need to quantify impact on σ_n/σ_p ratio extraction
- Particularly important for nTPE

Summary of HCAL proton efficiencies from cut-based method

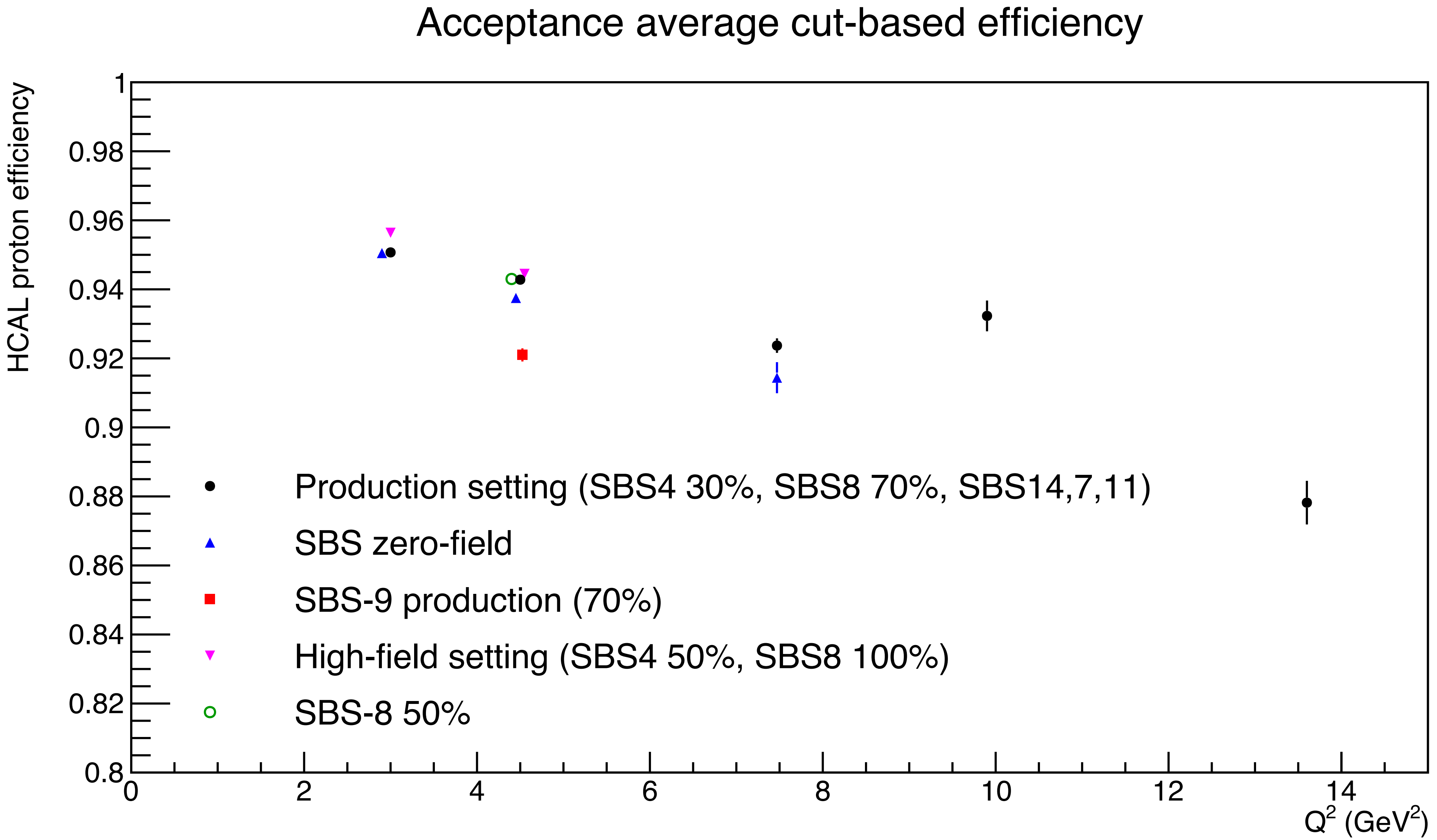

HCAL proton efficiency map, ALL nTPE LH2 data combined

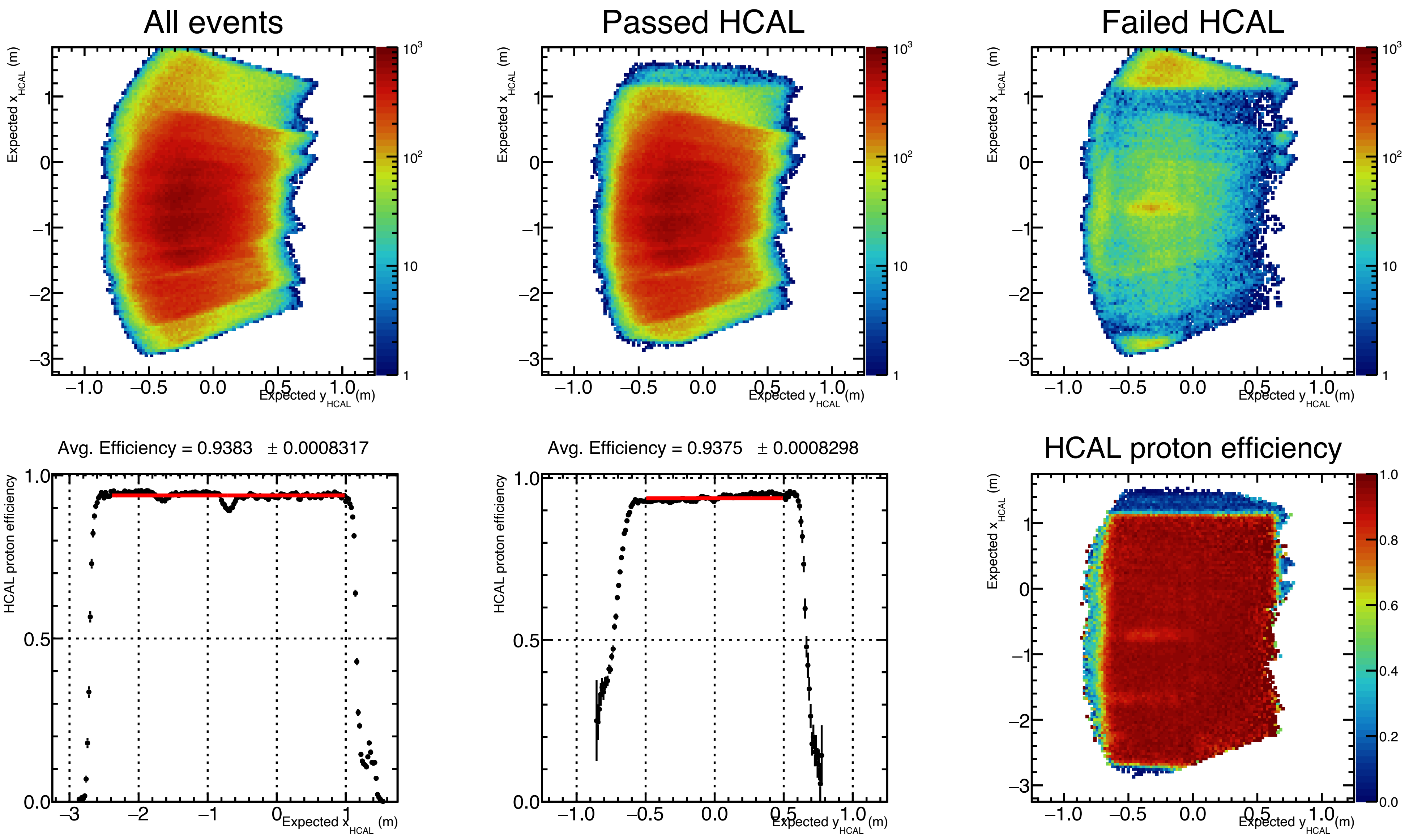

Example of "coarse-grained" proton efficiency map from data, SBS8/9, all field settings combined

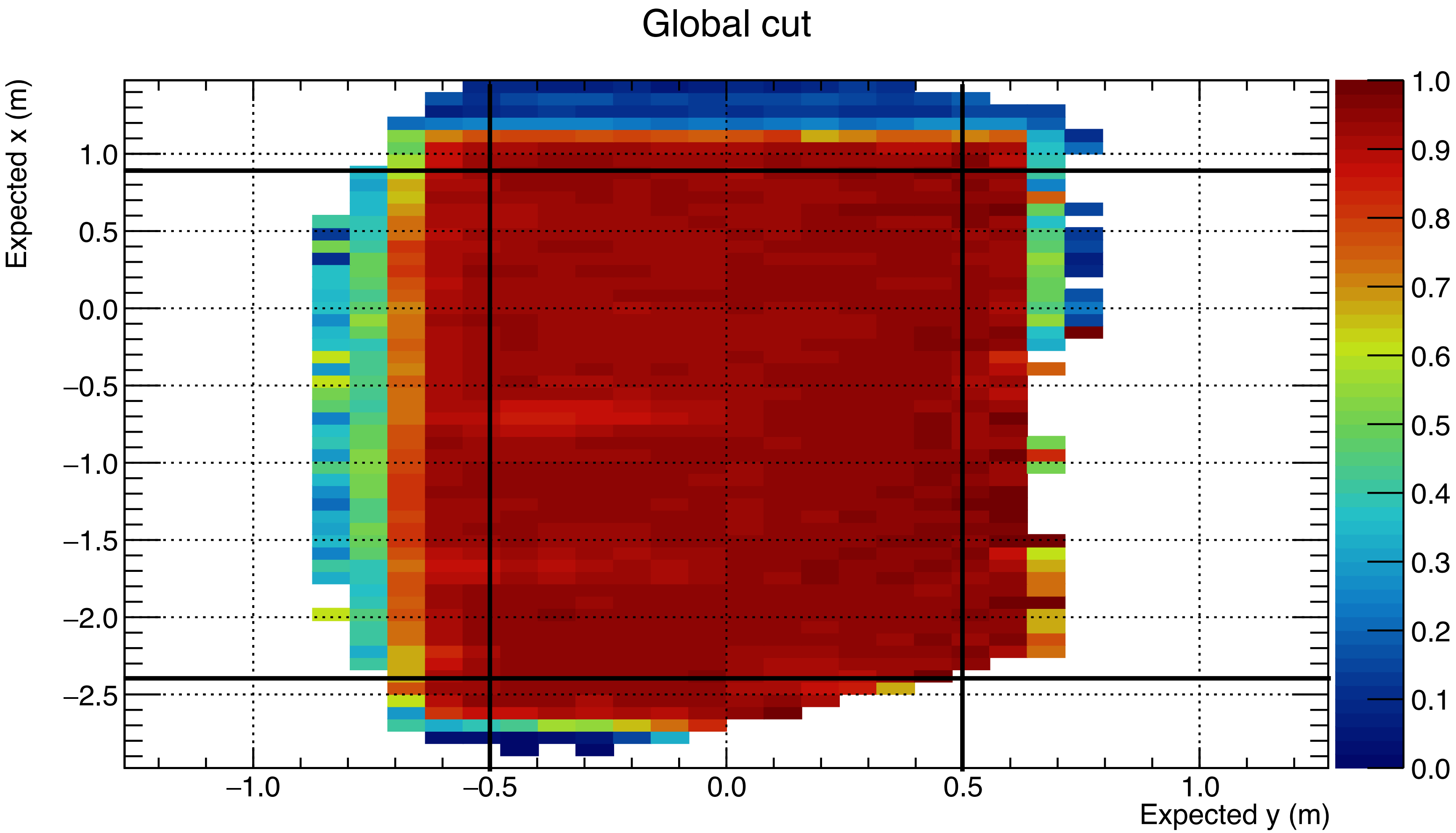

- "Coarse-grained" efficiency map uses bin size of ¼ of HCAL block size (i.e., 4 bins/block).
- Combination of SBS field settings covers entire useful area for all kinematics
- Black lines indicate typical fiducial cut boundary

Formalism for applying *ad hoc* efficiency corrections to MC, II:

For each Monte Carlo event, we calculate the following ratio (possible variations on this theme to be discussed later):

$$\begin{aligned}
\text{Relative efficiency correction factor } c &\equiv \frac{\epsilon^{\text{data}}_{\text{cut-based}}(x,y)}{\left\langle \epsilon^{\text{data}}_{\text{cut-based}} \right\rangle}, \\
\text{where } \epsilon^{\text{data}}_{\text{cut-based}}(x,y) &\equiv \text{Interpolated cut-based proton efficiency at position} \\
&\quad (x,y) \text{ from grid/histogram} \\
\langle \mathcal{O} \rangle &\equiv \text{acceptance-average value of observable } \mathcal{O}
\end{aligned}$$

- The acceptance-averaged value of the position-dependent correction factor is 1 by construction.
- Our baseline assumption is that the correction factor is charge-independent; i.e., the same for protons and neutrons, depending only on position and not on field setting or incident angle or anything else.
- In constructing weighted Monte Carlo distributions for comparison to real data, we *multiply* each simulated event by the correction factor *c* before filling the standard "dx" histograms and fitting to data.
- We can also attempt to correct for the *absolute* efficiency difference between real data and MC by introducing a modified correction factor:

$$\text{Modified correction factor } c' \equiv c \frac{\left\langle \epsilon^{data}_{\text{cut-based}} \right\rangle}{\left\langle \epsilon^{\text{MC}}_{\text{cut-based}} \right\rangle} = \frac{\epsilon^{\text{data}}_{\text{cut-based}}(x,y)}{\left\langle \epsilon^{\text{MC}}_{\text{cut-based}} \right\rangle}$$

Data/SIMC comparison of PDE (SBS-8, 70% field), II (Provakar)

SBS8 – SBS70p H(ee'p)

Data **SIMC**

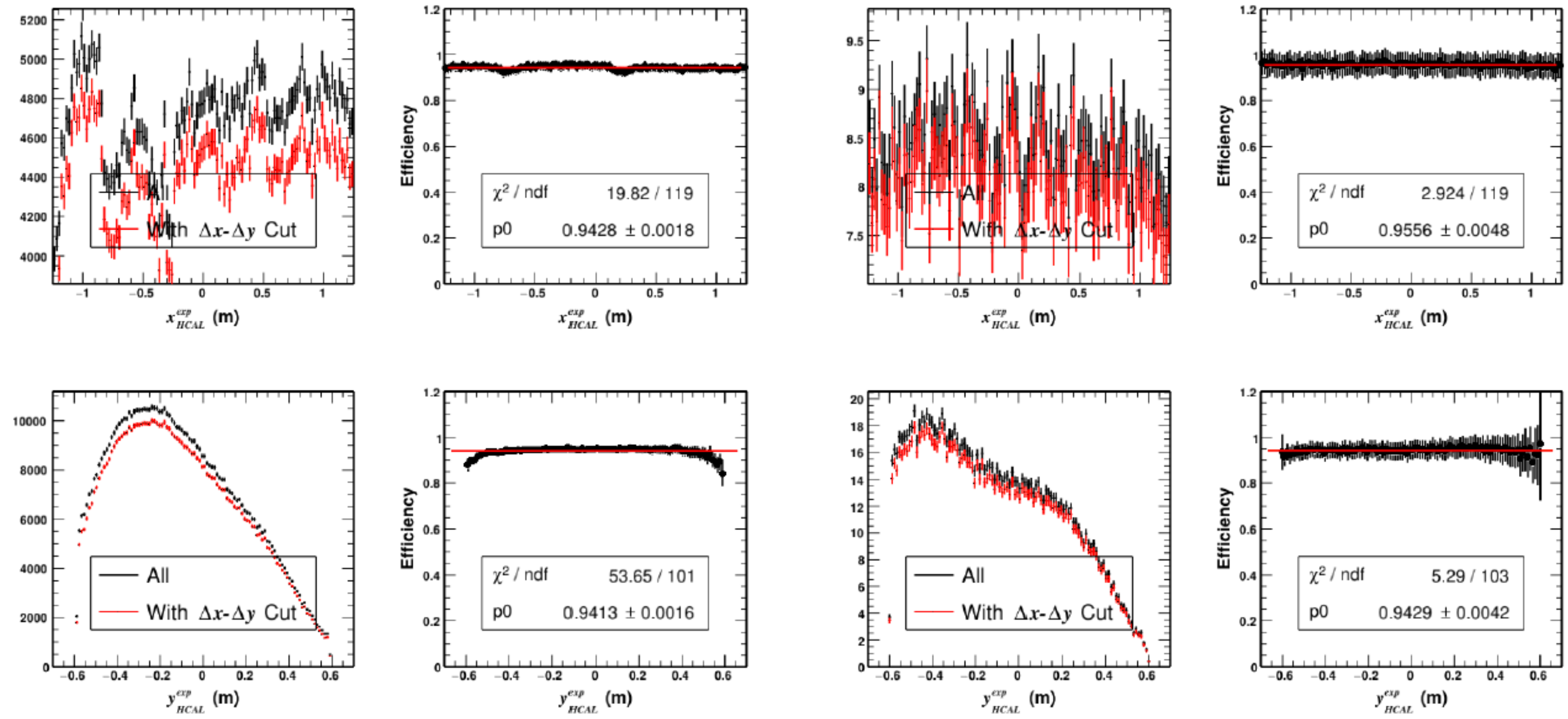

n/p Ratio Uniformity (comparing SBS-8/SBS-9 (nTPE kinematics))

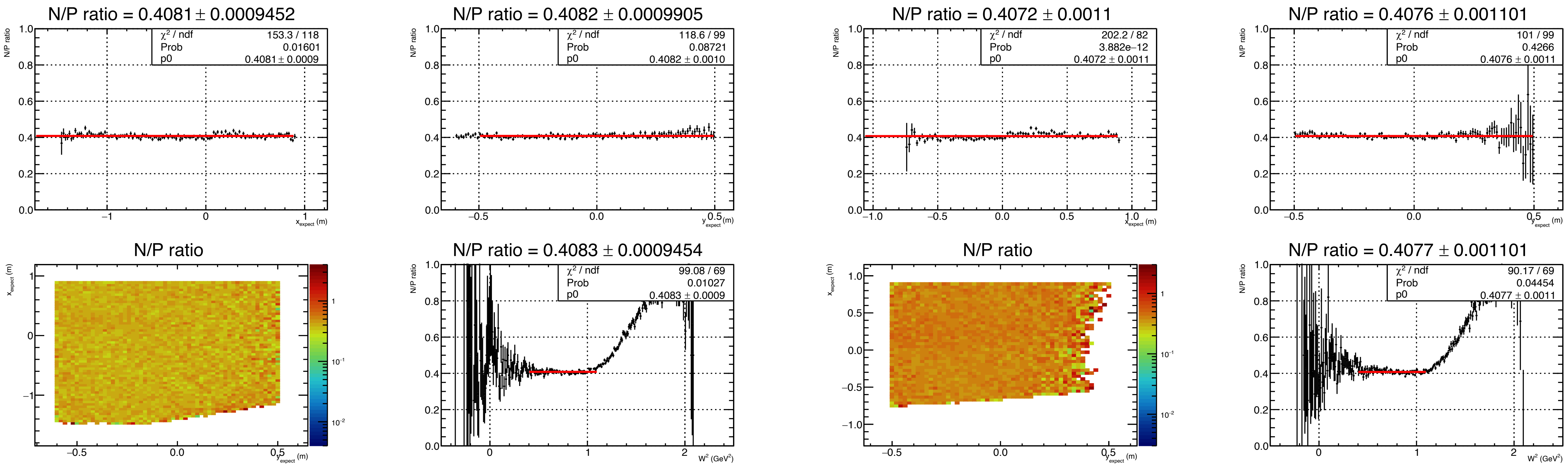

SBS-8 $Q^2 = 4.5\ GeV^2, \epsilon = 0.8$

SBS-9 $Q^2 = 4.5\ GeV^2, \epsilon = 0.5$

- For ”low” Q^2 data, we can extend the cut-based method for proton efficiency analysis to neutron/proton ratios from LD2 (aggressive cuts to obtain a “clean” quasi-elastic sample) and select proton and neutron events using cuts on θ_{pq} and/or $\Delta x, \Delta y$. As long as n/p separation is sufficient, we can also obtain clean $(e, e'n)$ and $(e, e'p)$ samples.
- n/p ratios for nTPE kinematics exhibit non-statistical fluctuations corresponding to regions of known lower efficiency of HCAL
- With acceptance-matching cuts, we expect near-total cancellation of HCAL efficiency systematics in the “super ratio” between two ϵ points at the same Q^2 (Indeed, the projected accuracy of the Rosenbluth slope depends implicitly on this assumption)

nTPE "Super-Ratio" position dependence (pure cut-based method)

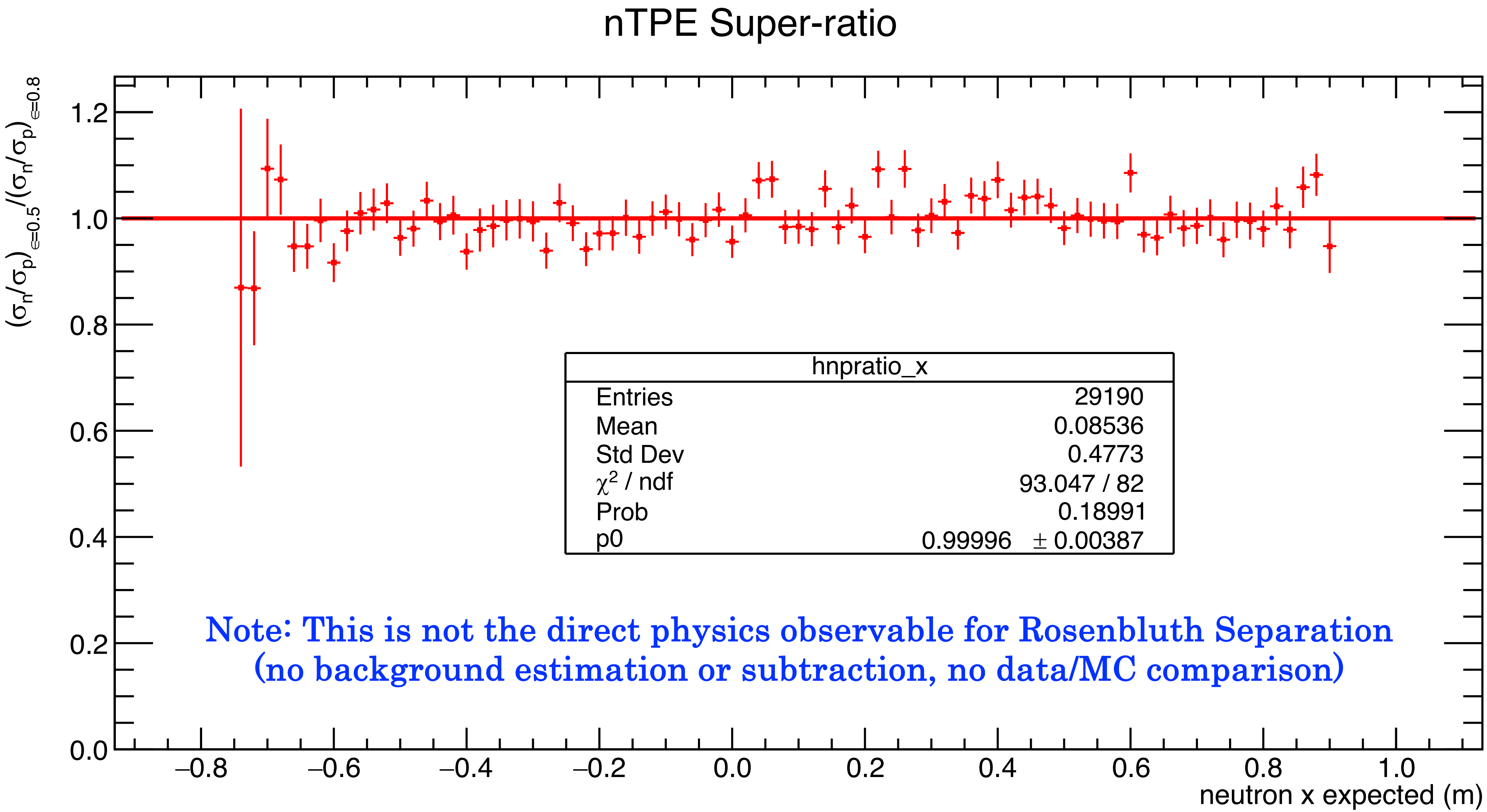

Note: This is not the direct physics observable for Rosenbluth Separation (no background estimation or subtraction, no data/MC comparison)

Absolute yield analysis, I (Provakar Datta)

Yield per Run – SBS4 0% LD2

Yield per Run – SBS4 30% LD2 (Excluding 1st 3 Runs)

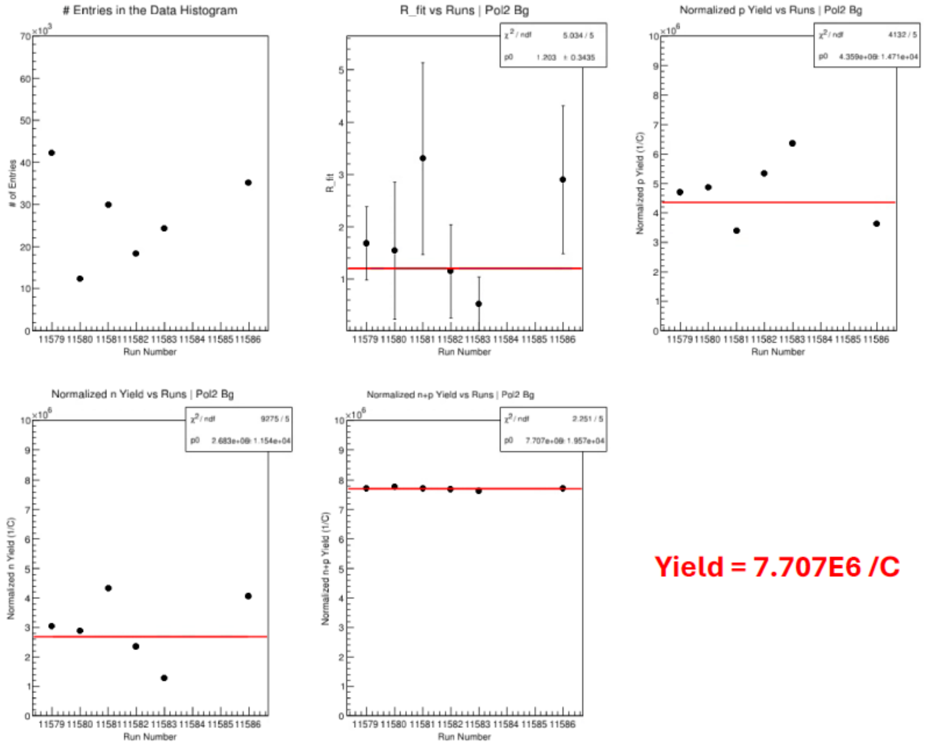

Yield = 7.707E6 /C

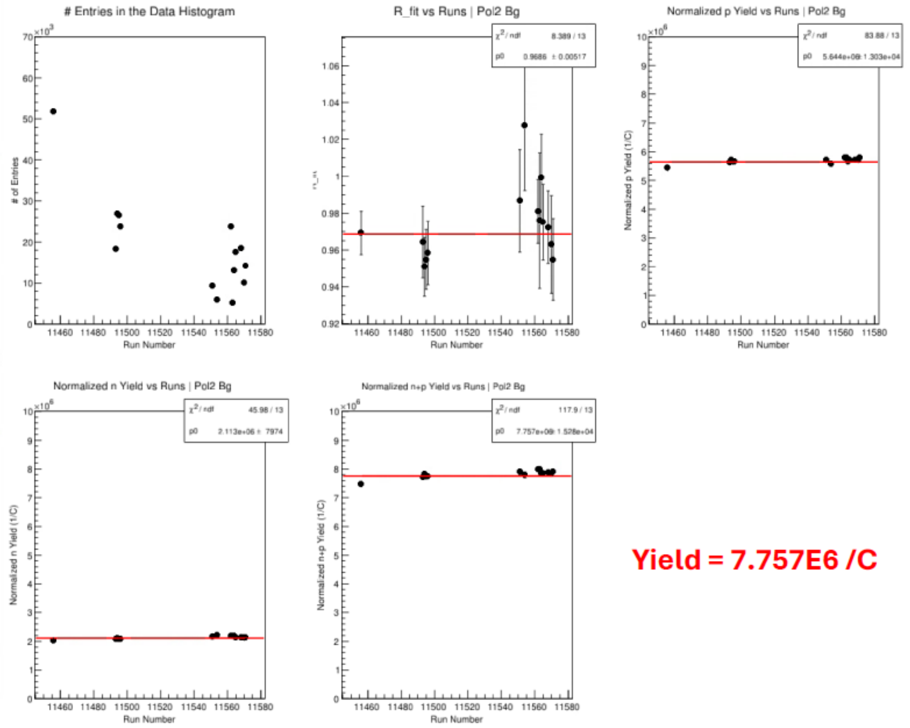

Yield = 7.757E6 /C

- $Yield_{0\%}$ = 7.707E6 /C
- $Yield_{30\%}$ = 7.757E6 /C
- **Agrees within 0.6%!**

- Comparison of charge-normalized, live-time corrected quasi-elastic yields for LD2 runs with SBS magnet OFF and ON shows good agreement/consistency.
- QE yield (n+p) from LD2 with p and n with field off agrees with sum of n and p yields (field on) to better than 1%

Absolute yield analysis, II (overall reconstruction efficiency)

SBS14 70% LD2 and LH2 Runs

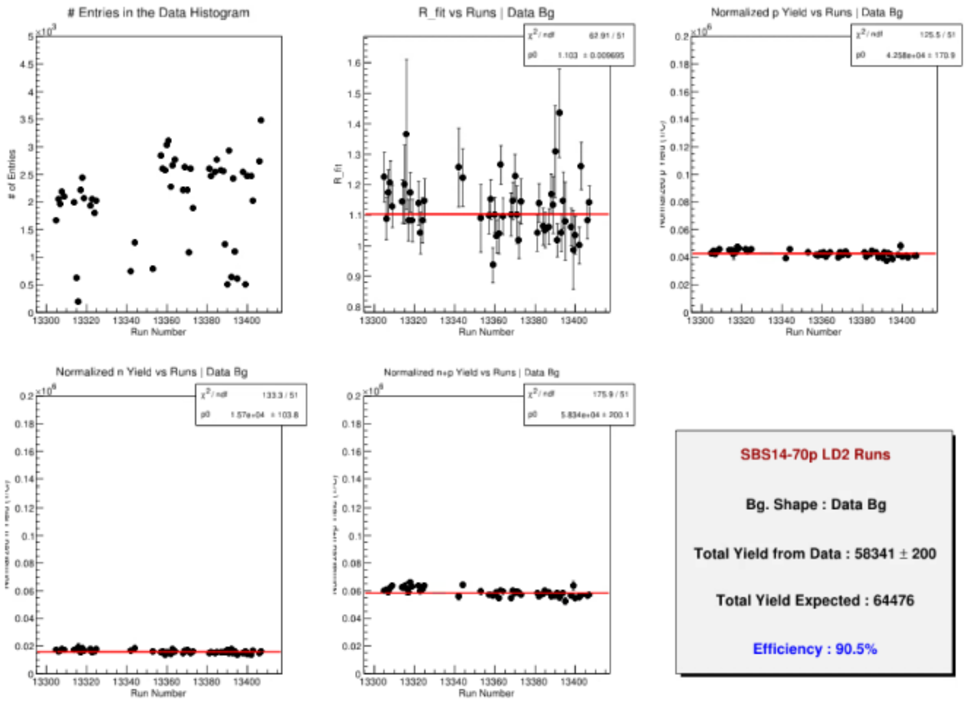

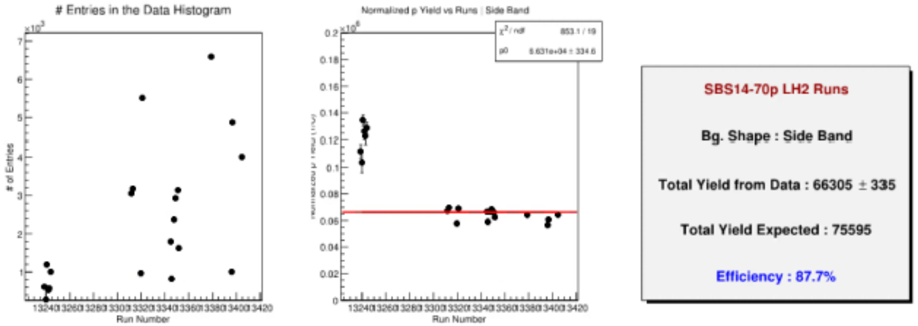

Comparison of absolute yield between data and MC for LH2 elastic and LD2 quasi-elastic shows high overall reconstruction efficiency during GMN (~90%)

GMn “Pre-preliminary” Results (Collecting Various Thesis “Results”)

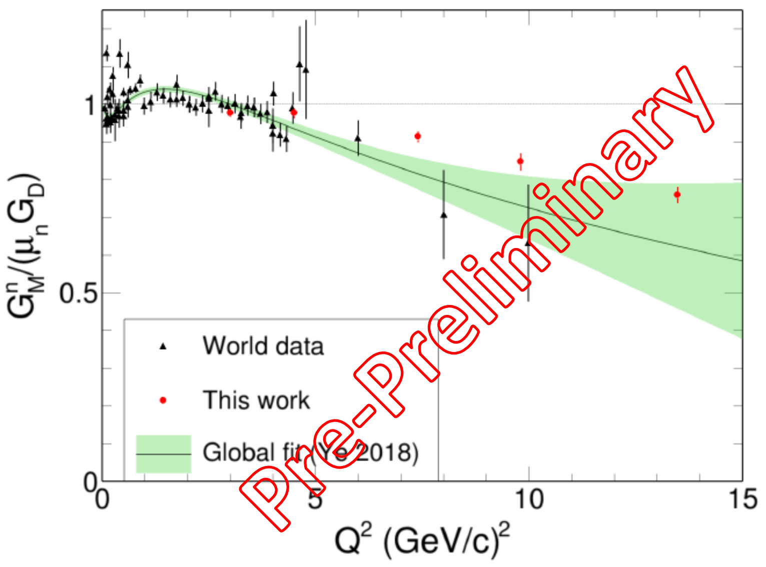

Figure 5.4.1: E12-09-019 world data including the results obtained from this work. The error bars represent the total error obtained by adding the statistical and systematic errors in quadrature.

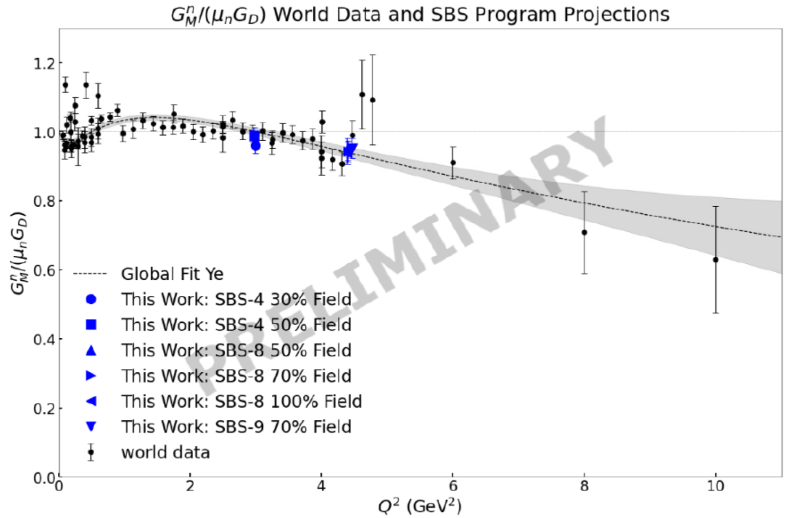

Figure 109: $G_M^n/(\mu_n G_D)$ extractions from this work plotted along with world data taken from [87] and Ye et al. fit[184].

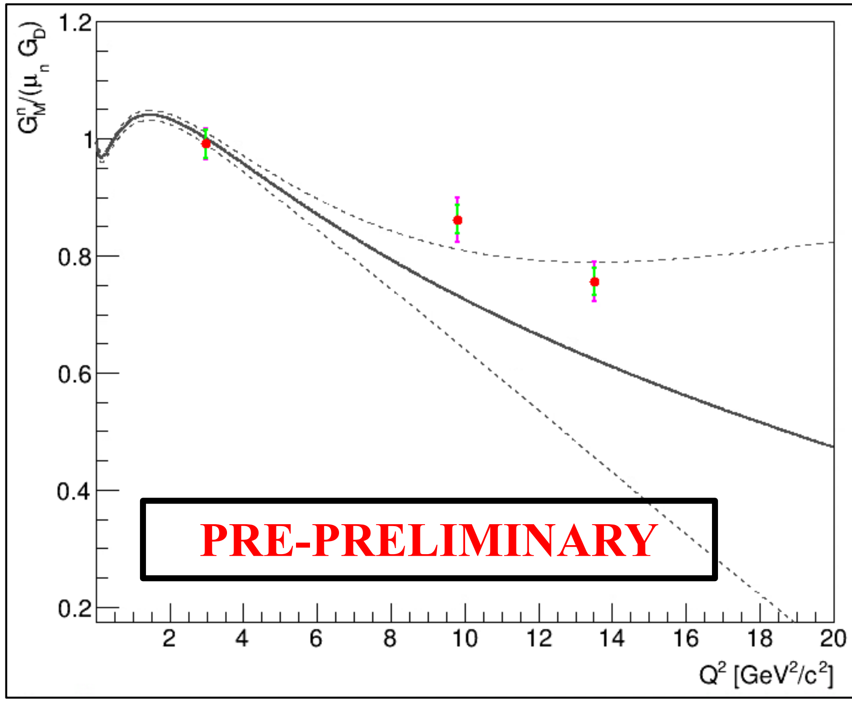

- Above, left: Provakar Datta (UConn)
- Above, middle: Sebastian Seeds (UConn)

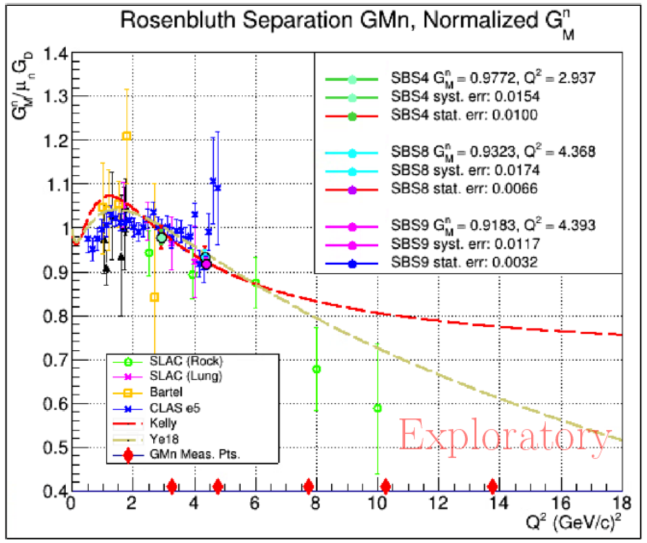

Figure 7-2: [Exploratory] Experimental G_M^n values overlaid with world G_M^n data.

- Below, middle: John Boyd (UVA)
- Above, right: Anuruddha Rathnayake (UVA)

Revisiting GEM Gain drop and Efficiency during GMN—role of trigger?

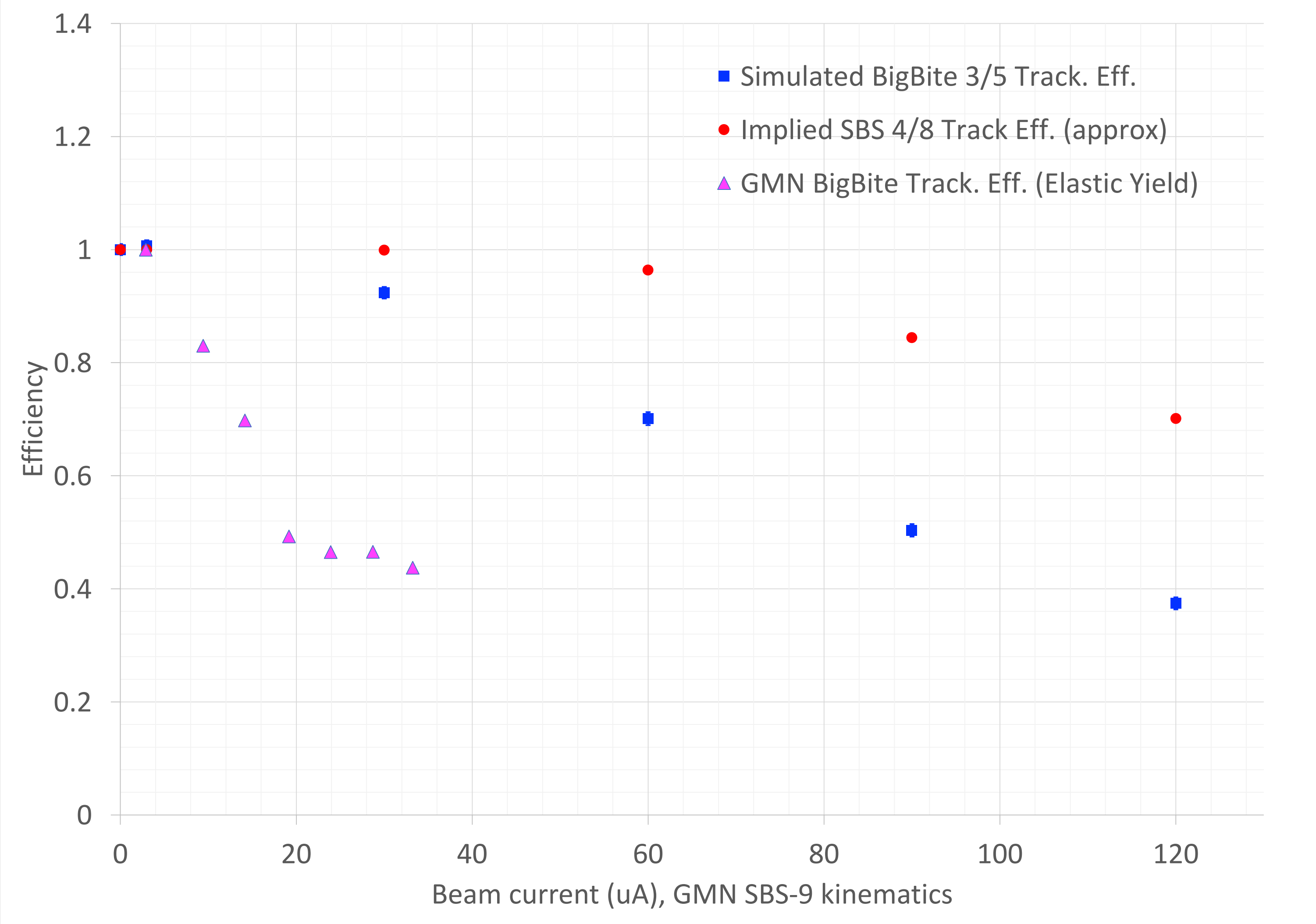

Beam Current	BBCAL Trigger Threshold
3	-428
10	-512
15	-554
20-35	-607

- We observed a significant drop of elastic yield with beam current during test runs taken at the end of GMN
- "Flattening" at high beam current was not fully understood
- Changing trigger threshold with beam current suggests trigger efficiency plays an important role
- Potentially changes the story significantly on GEM tracking efficiency during GMN!

GMN analysis roadmap

- Two full reconstruction passes completed
- Calibrations are relatively mature, but significant room for improvement exists in two areas:
  - HCAL energy and timing calibration
  - Timing hodoscope calibrations and analysis
  - Coincidence timing
- There *will* be a third cooking pass of GMN/nTPE before publication, BUT:
- Pass 2 cooking results are of sufficient quality for the extraction of preliminary physics results.
- Monte Carlo simulation and physics analysis machinery is fully developed and mature
- We are in the process of chasing down remaining small inconsistencies between the experiment and the MC simulation, which I won't belabor here.

E12-09-016: G_E^n/G_M^n to 10 GeV^2 using polarized ^{3}He(e,e'n)pp

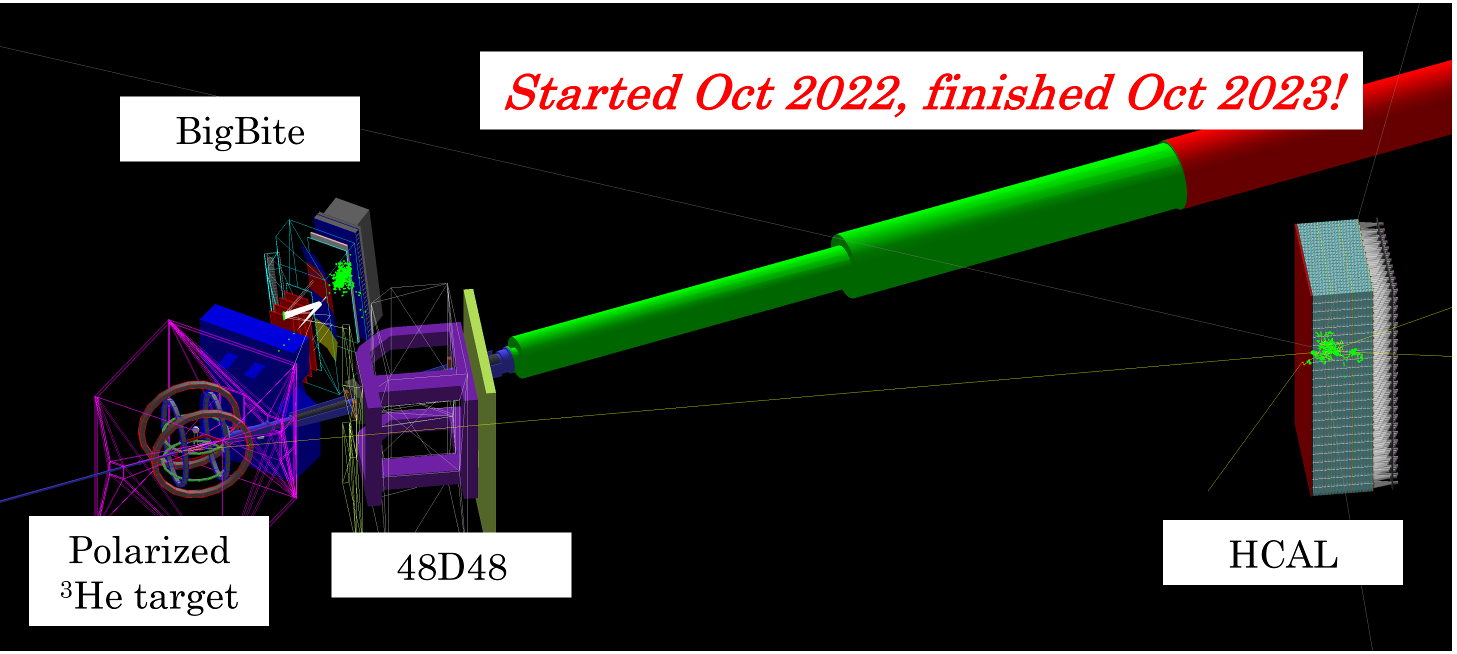

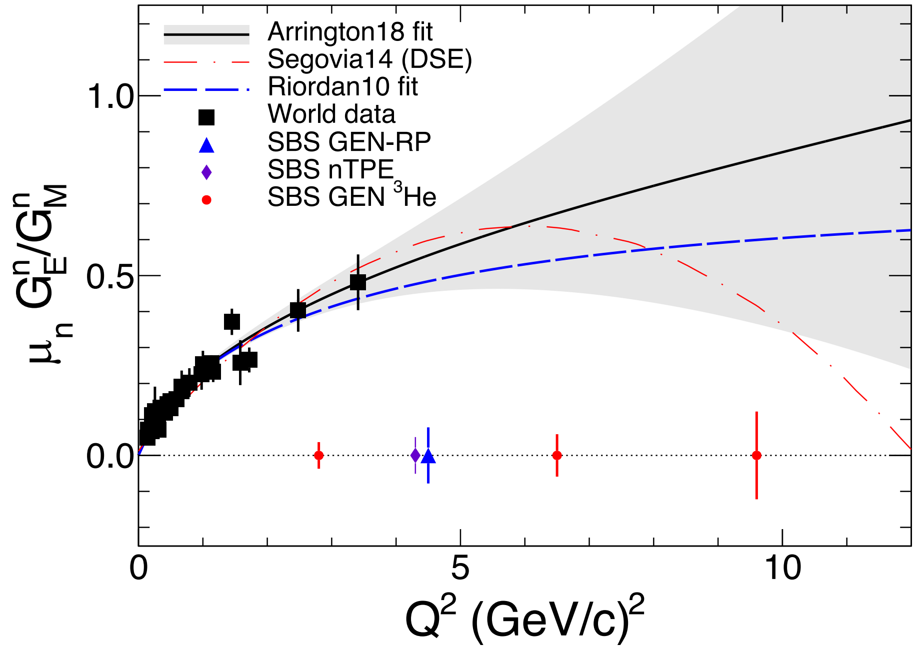

- Same detector configuration as GMN (E12-09-019) (with GEMs added to SBS for commissioning)
- High-luminosity polarized ^{3}He target with convection-driven circulation of polarized gas.
- Measurement to 10 GeV^2 has enormous discrimination power among theoretical models
- **Data-taking completed Oct. 29, 2023!**

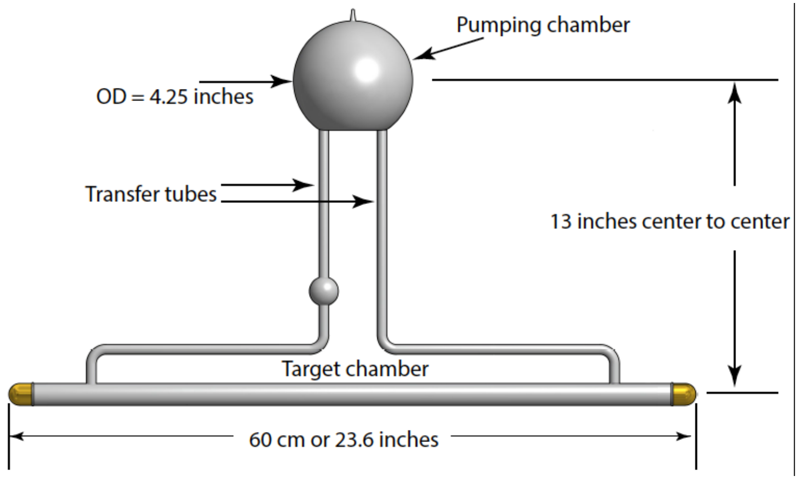

Polarization Observables in Elastic $eN \to eN$ Scattering

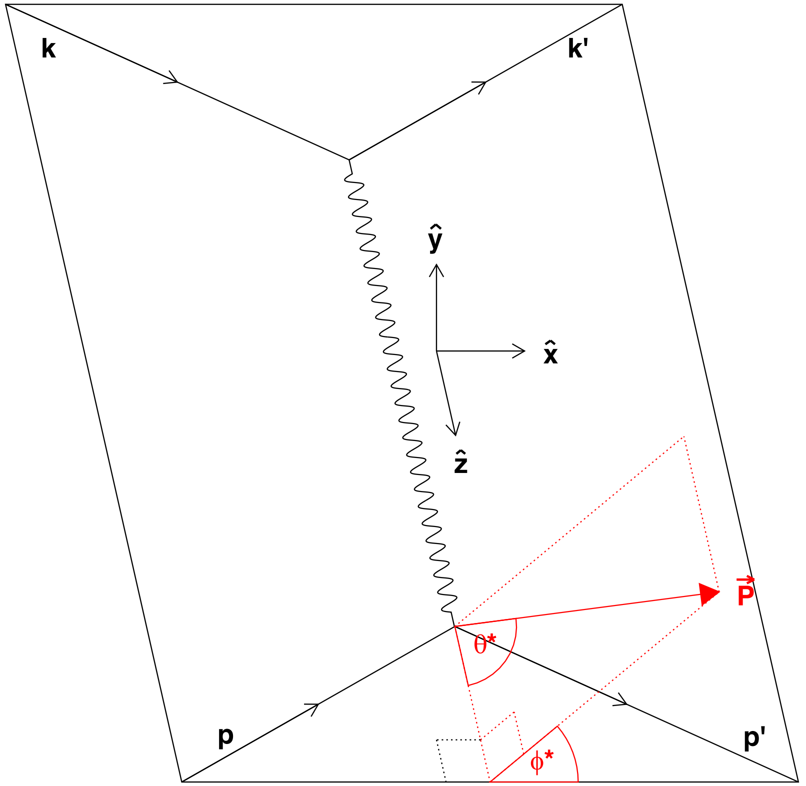

Standard coordinate system and angle definitions for nucleon polarization components in $eN \to eN$

$$A_{eN} \equiv \frac{\sigma_+ - \sigma_-}{\sigma_+ + \sigma_-} = P_{\text{beam}} P_{\text{targ}} \left[A_t \sin\theta^* \cos\phi^* + A_\ell \cos\theta^*\right]$$

$$A_t = -\sqrt{\frac{2\epsilon(1-\epsilon)}{\tau}} \frac{r}{1+\frac{\epsilon}{\tau}r^2}$$

Target spin is oriented to measure this asymmetry in ^{3}He(e,e'n)!

$$A_\ell = -\frac{\sqrt{1-\epsilon^2}}{1+\frac{\epsilon}{\tau}r^2}$$

$$r \equiv \frac{G_E}{G_M}$$

$$P_t = P_{beam} A_t$$

$$P_\ell = -P_{beam} A_\ell$$

$$\frac{G_E}{G_M} = -\frac{P_t}{P_\ell}\sqrt{\frac{\tau(1+\epsilon)}{2\epsilon}} = -\frac{P_t}{P_\ell}\frac{E_e + E'_e}{2M}\tan\left(\frac{\theta_e}{2}\right)$$

- Polarized beam-polarized target double-spin asymmetry or polarization transfer observables in OPE are sensitive to the electric/magnetic form factor *ratio*, giving enhanced sensitivity to $G_E(G_M)$ for large (small) values of Q^2, as compared to the Rosenbluth method

The SBS-GEN polarized Helium-3 target

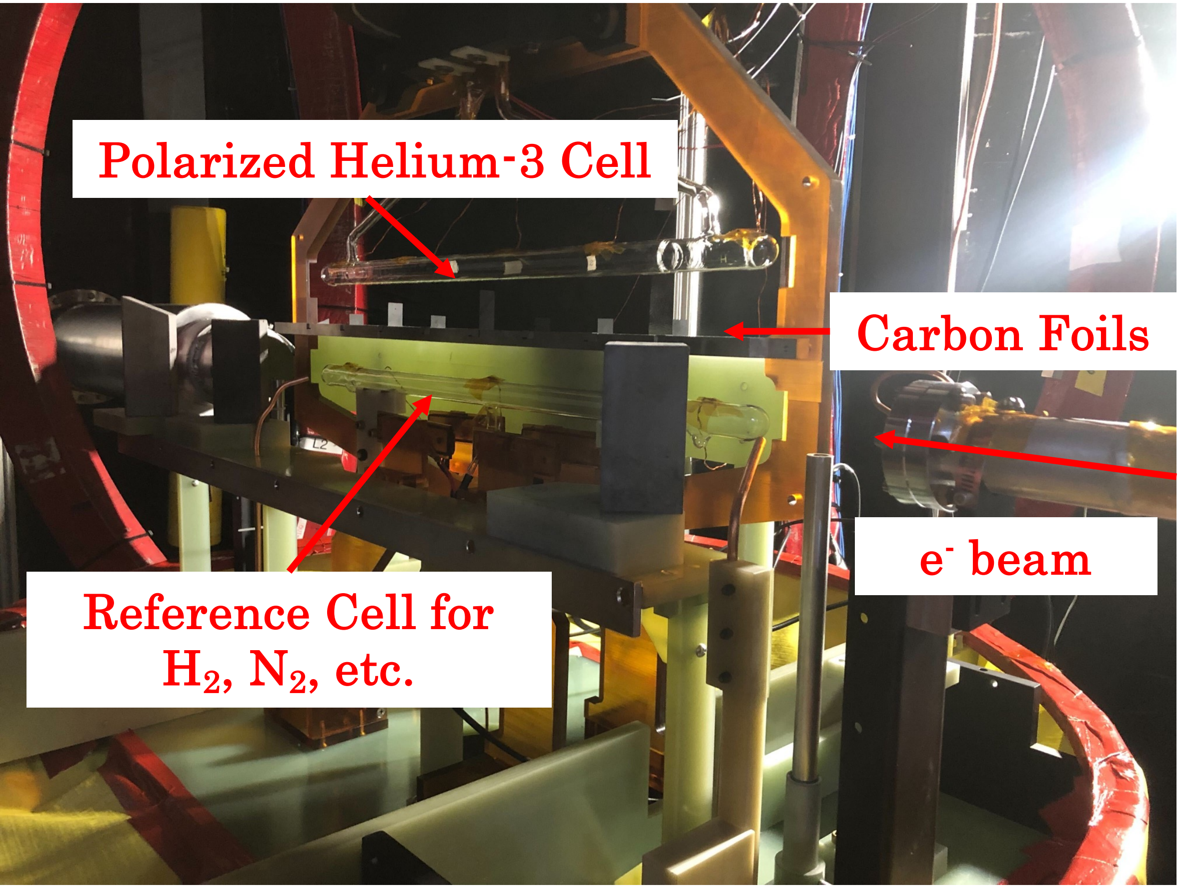

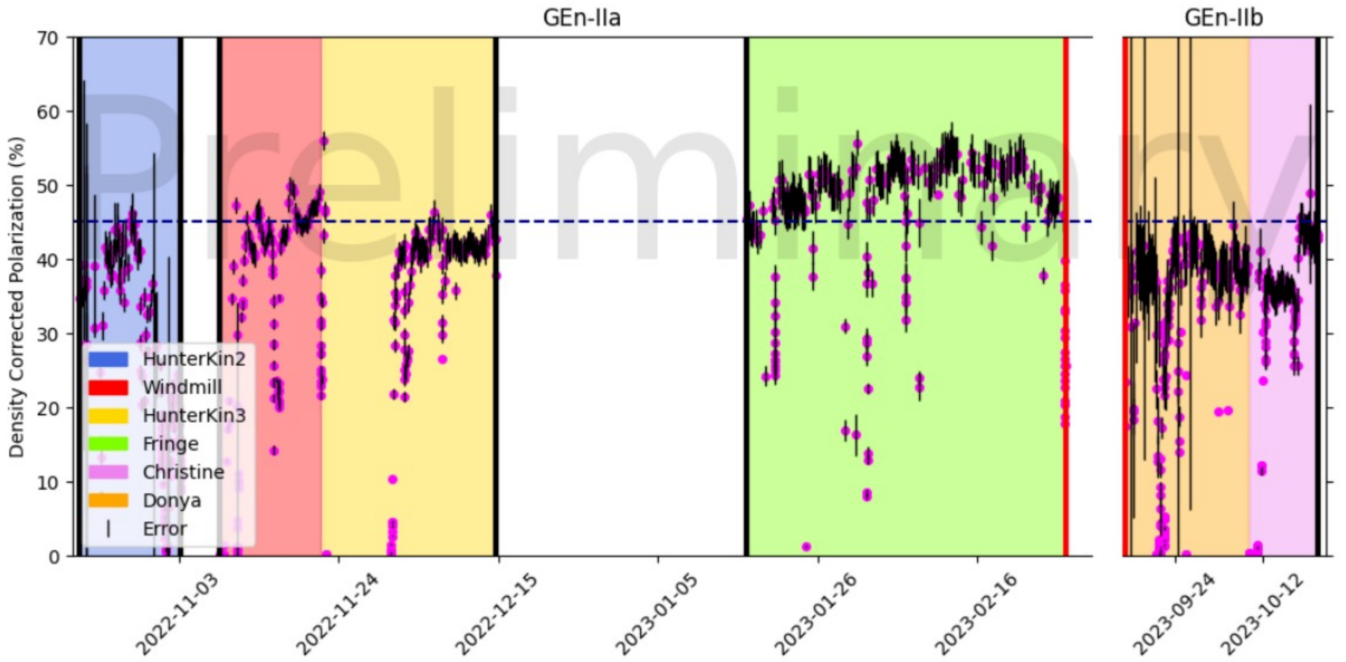

- Above, left: Inside the target enclosure
- Above, right: preliminary target polarization results
- Below, right: estimated FOM compared to previous experiments

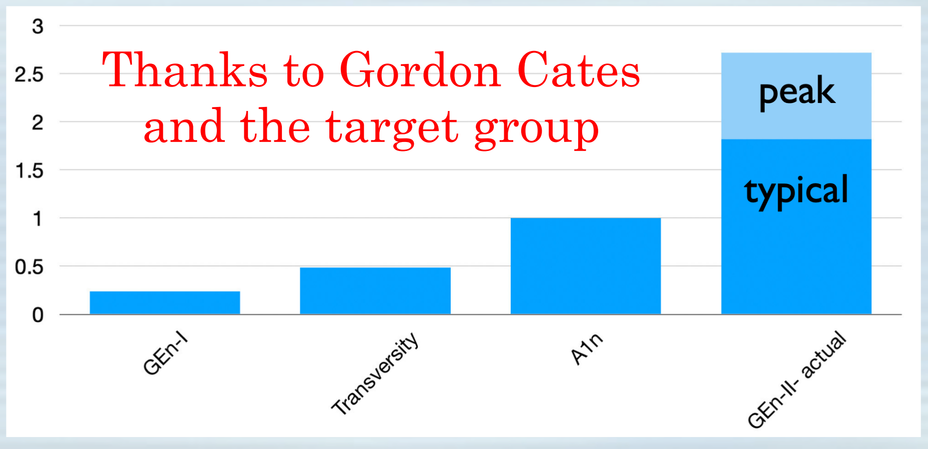

SBS GEN analysis: Moller Polarimetry: Faraz Chahili and Don Jones

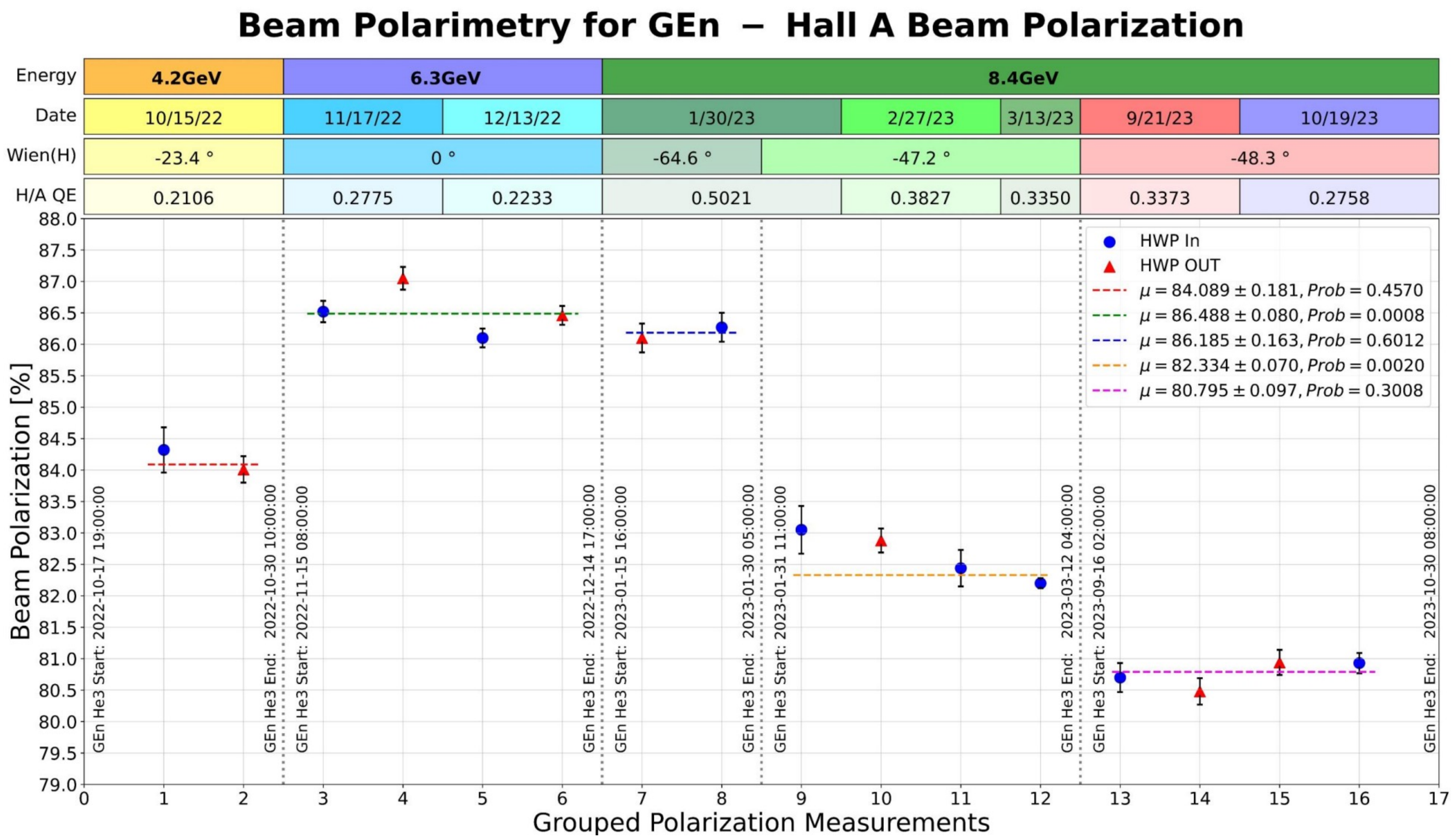

SBS GEN analysis: Quasi-elastic ^{3}He(e,e'n)pp event selection

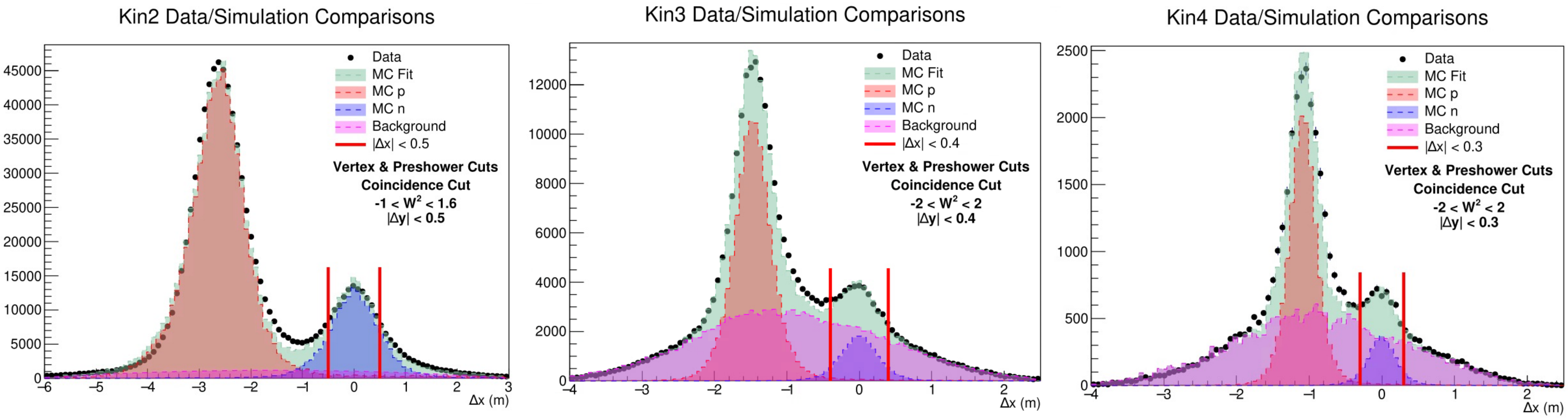

$Q^2 = 3.0\ \text{GeV}^2$ $Q^2 = 6.8\ \text{GeV}^2$ $Q^2 = 9.8\ \text{GeV}^2$

- Plots/analysis credit: Sean Jeffas (UVA)
- Histograms include all (or substantially all) of the data from the first reconstruction pass (does not include Fall 2023 data which are expected to roughly double statistics at the highest Q^2)
- n/p separation for quasi-elastic scattering is very clean due to magnetic deflection
- Substantial, essentially irreducible inelastic background is present, especially at large Q^2

Preliminary raw ^{3}He(e,e'n) asymmetries (Sean Jeffas)

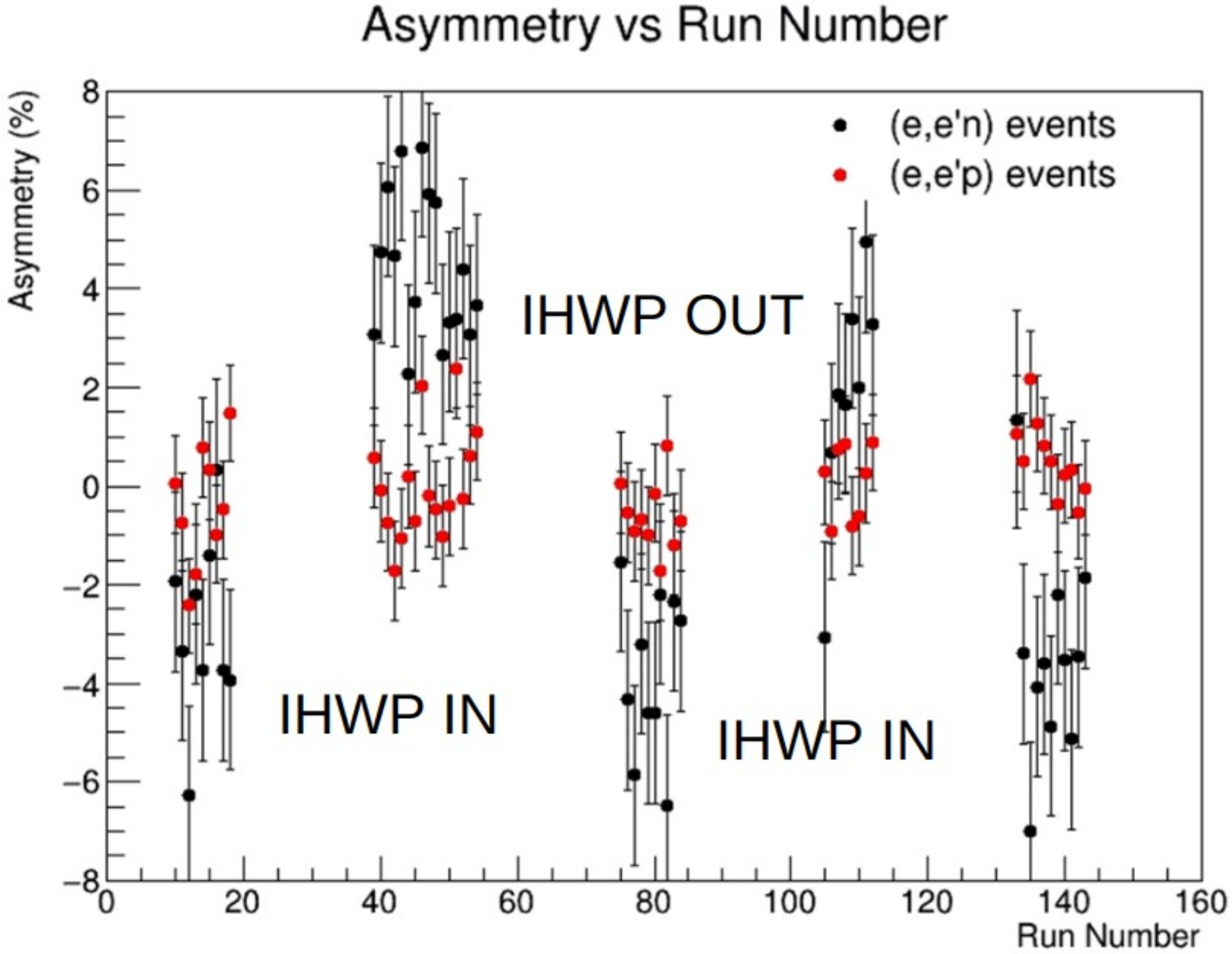

$$Q^2 \quad = \quad 3.0 \text{ GeV}^2$$

- Preliminary (e,e'n) asymmetries at lowest Q^2 (overlapping existing GEN data) consistent in sign, magnitude with expectatation
- Neutron asymmetries large, change sign with IHWP as expected
- Proton asymmetries small

Path forward for GEN analysis

- Detector calibrations still require substantial work toward a 2nd full reconstruction pass—expect significant increase in statistics (and somewhat improved resolution) for higher Q^2's with improved calibrations
- Nuclear corrections: updated Generalized Eikonal Approximation code obtained from Misak Sargsian
- Proper definition of estimators, background contamination, background asymmetry, background subtraction
- Finalize polarimetry
- Substantial remaining analysis work—students graduating → we are several years from publishable physics results from GEN

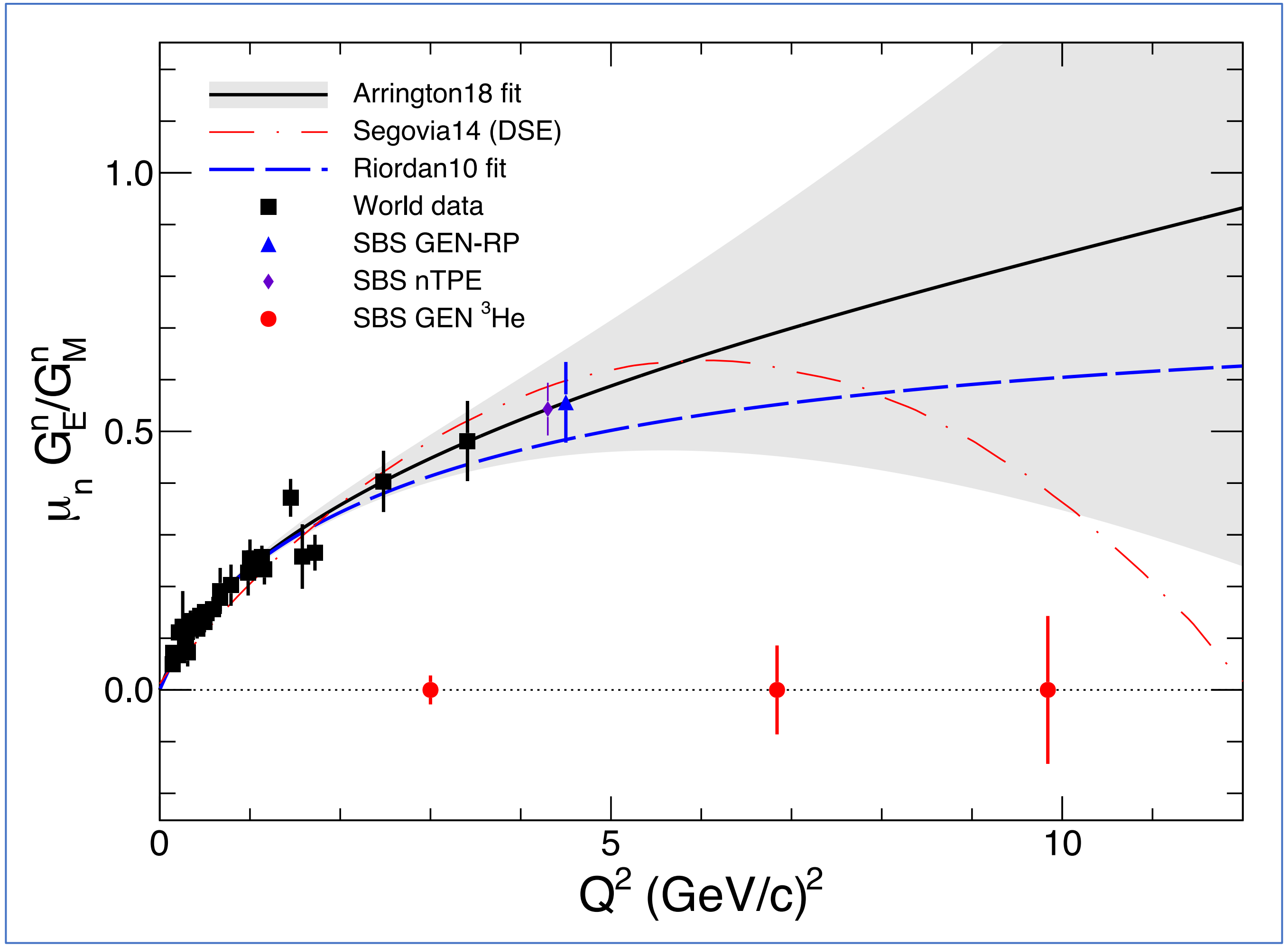

Current uncertainty projections (may prove too optimistic)

Improving SBS Timing Analysis, I

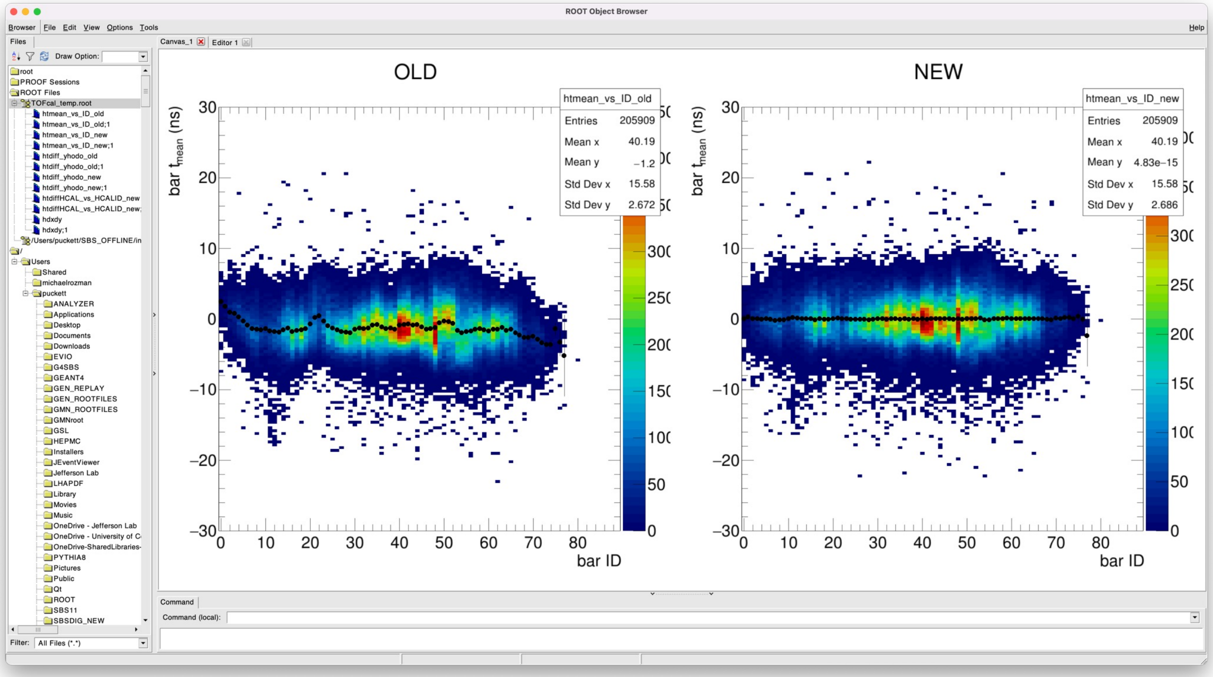

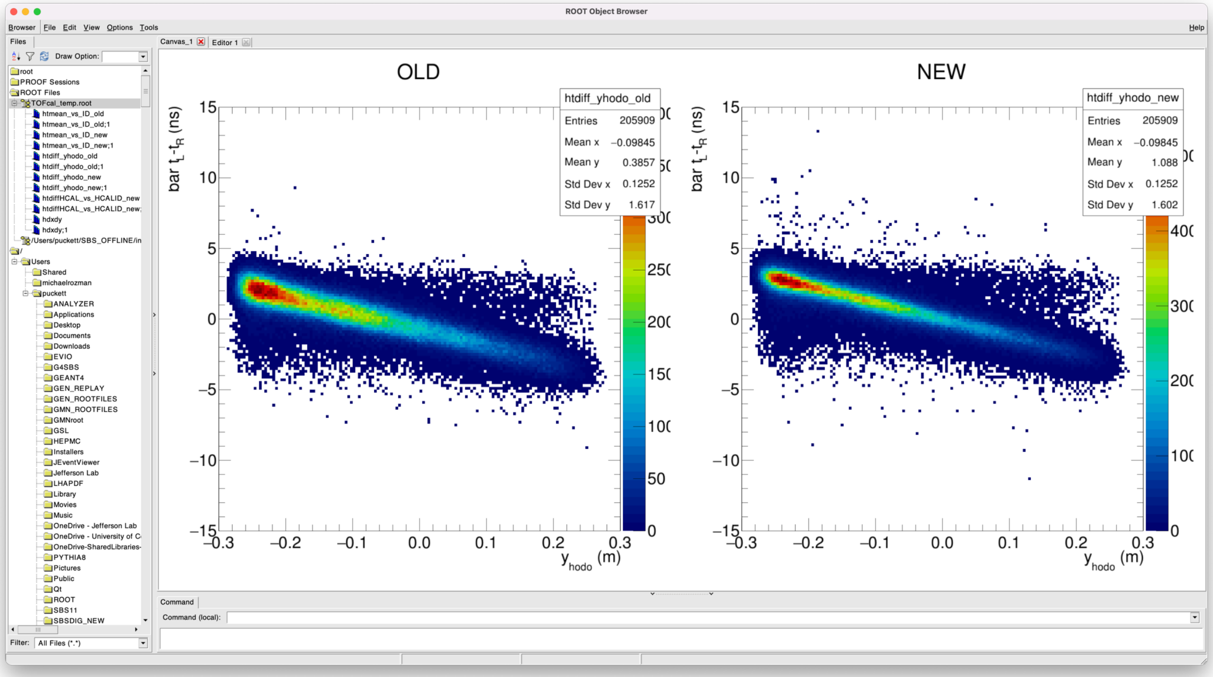

- Seen as crucial for improving signal/background for GEN analysis
- Proof of concept for simultaneous global fit of all hodoscope calibration constants (offset, walk correction, propagation speed, time-of flight variation)
- See https://sbs.jlab.org/cgi-bin/DocDB/private/ShowDocument?docid=540
- Gary Penman working on incorporating HCAL

Improving SBS Timing Analysis, II: Resolving Beam RF structure

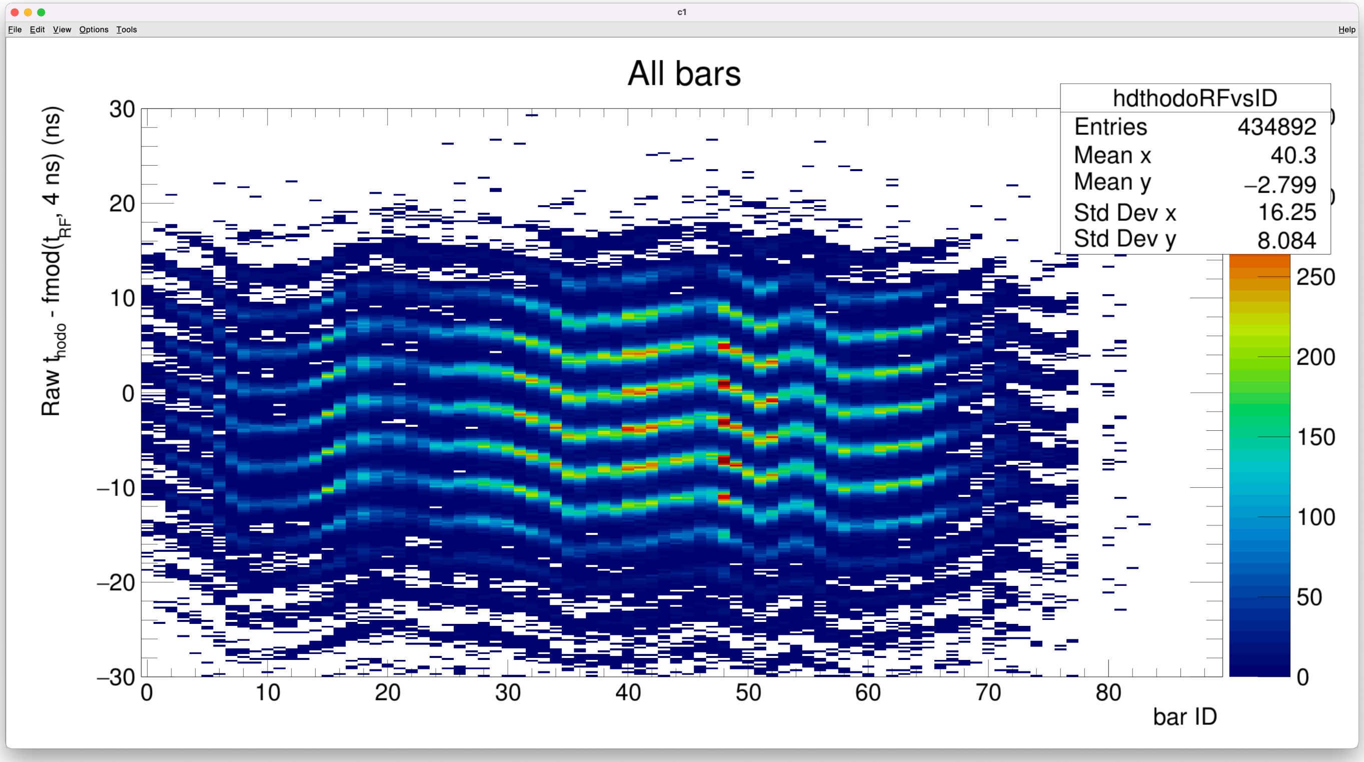

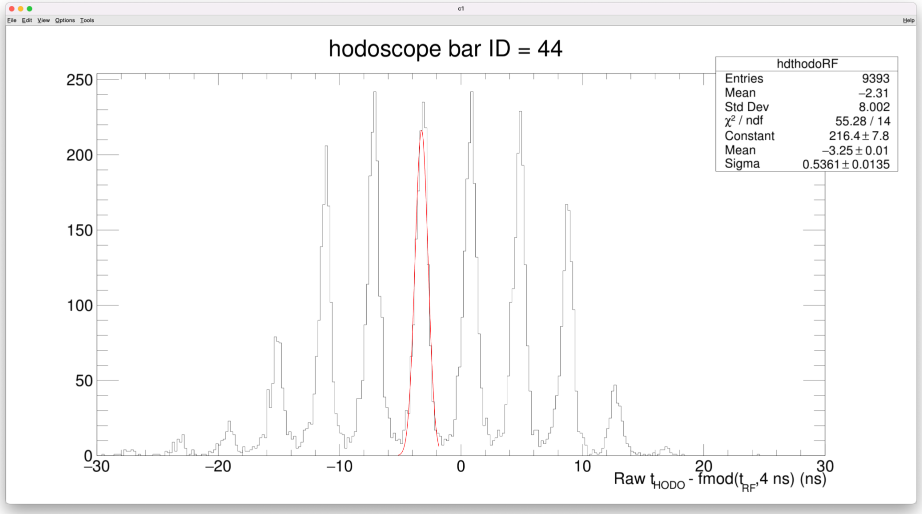

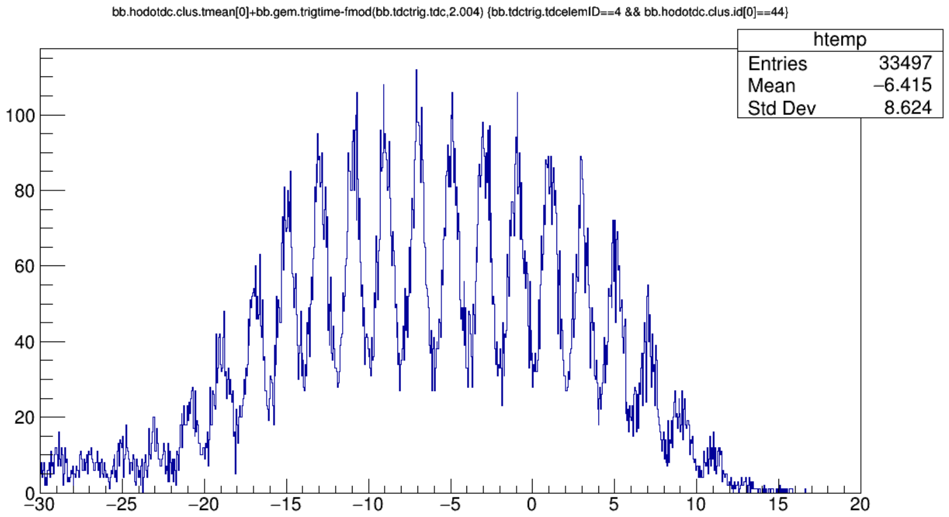

- Above, left: Raw hodoscope mean time minus RF time modulo 4 ns versus hodoscope bar number
- Above, right: for a single bar
- Below, right: for the same bar during GEN (which used 2-ns bunch spacing)

Summary and Conclusions

- GMN/nTPE analysis is converging; thesis students graduating, systematics evaluation making rapid progress, Monte Carlo fine-tuning, formalism for HCAL efficiency corrections, etc.
  - Estimated time to publication ~1-2 years
- GEN analysis is less mature
  - Significant work on detector calibrations is still needed to improve resolution and signal/background ratio—especially in the area of time-of-flight and HCAL energy reconstruction
  - Sean Jeffas already graduated, other GEN students, guided by Arun, carrying the torch
  - Estimated time to publication ~2-4 years
- See more detailed summary talks by Provakar (GMN) and Hunter (GEN)

Backups

Ratios of quasi-elastic n/p yields to total quasi-elastic electrons

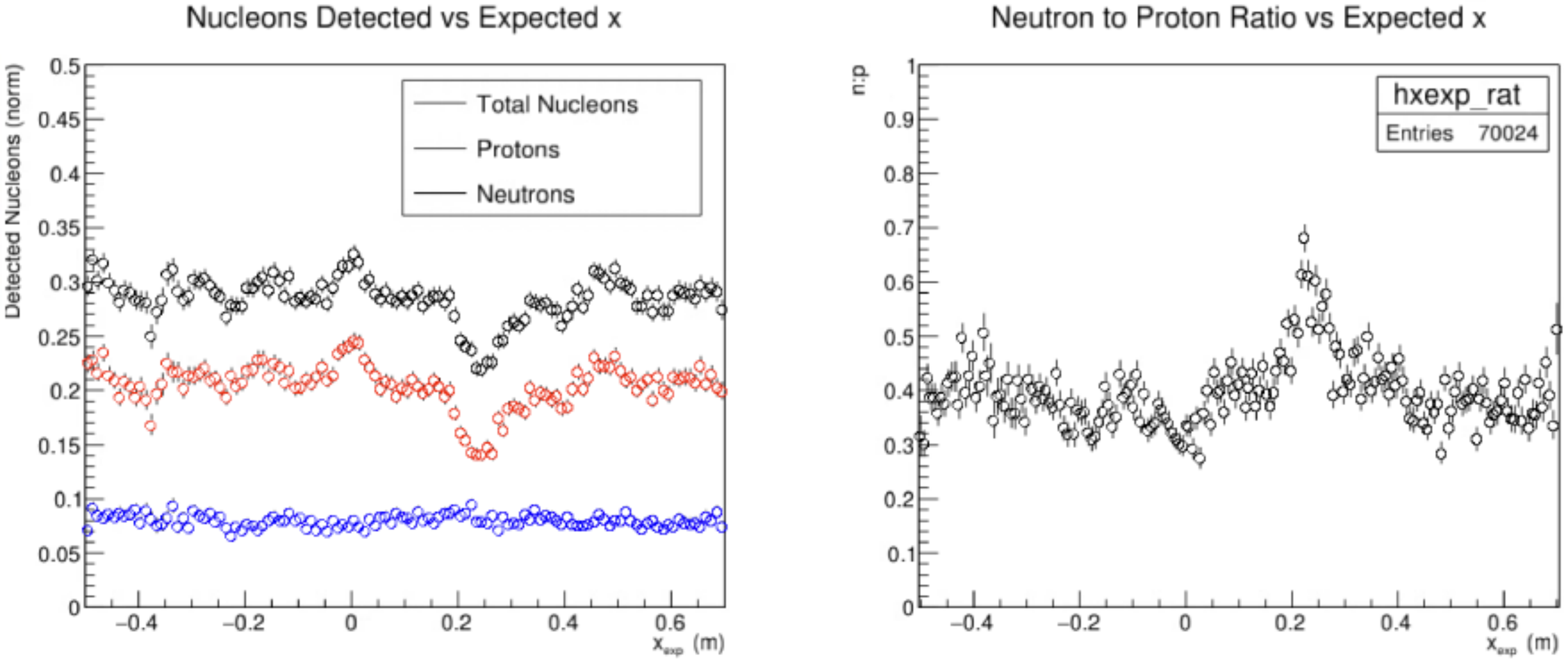

Figure 107: Nucleon detections and n:p ratio vs expected nucleon x position (SBS-9, 70% field). Both plots are bounded by the fiducial cut on this kinematic setting. The y-axis on the left plot includes an arbitrary normalization. The significant variation in detected protons is strongly pronounced for this kinematic setting at $x_{exp} = 0.25$ and results in a systematic upward shift in the n:p ratio at the same expected x position.

- Note: neutrons fall outside the "dip" region for the most part, ratio distribution more uniform

- Figure from Sebastian Seeds' thesis
- Cuts include "good electron" in BigBite, aggressive fiducial y cut, and W^2
- Aggressive fiducial cut in y enhances the "dip" region for protons in SBS-9
- "Proton" and "neutron" events are selected with aggressive "spot" cuts (2σ elliptical)
- Form ratio of n and/or p events to total "quasi-elastic" electron events as a function of *expected* neutron x position.
- This is not a detection efficiency, but we can attempt to reproduce these ratios in MC as a proxy for "efficiency"

Cancellation of position-dependent efficiency systematics in nTPE “super-ratio”

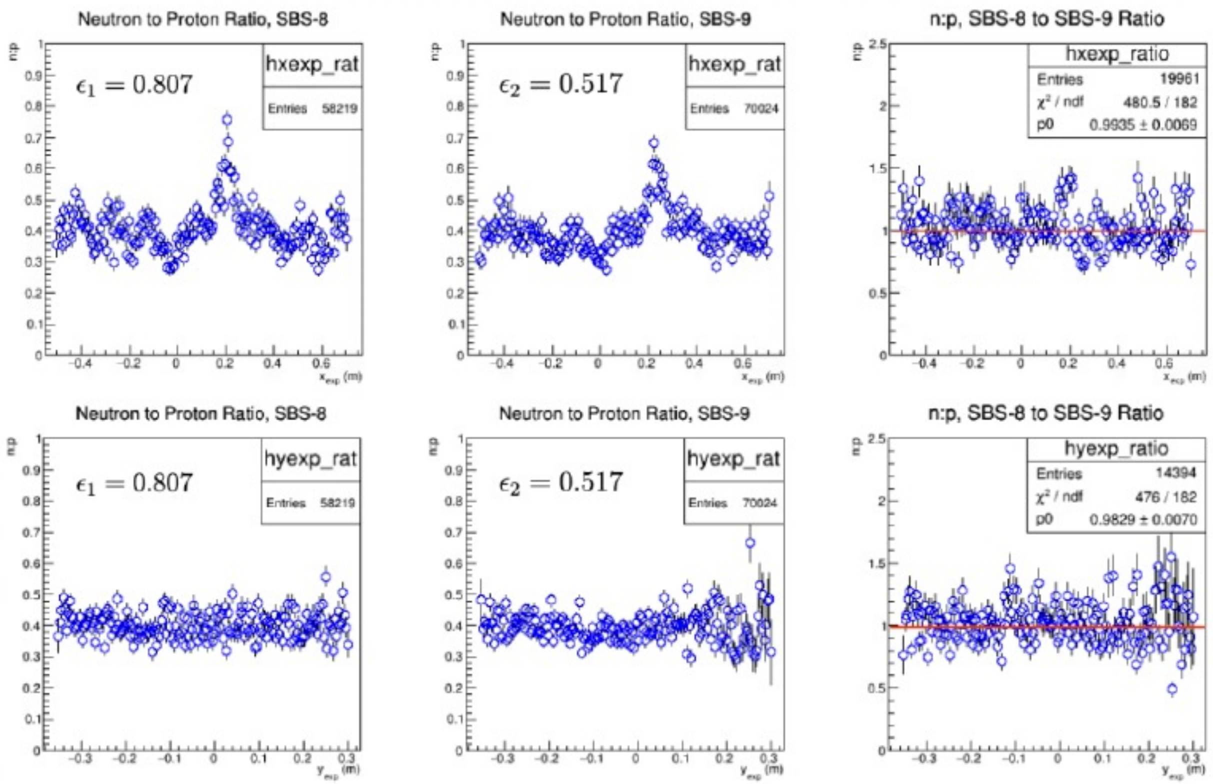

Figure 108: The top row plots are neutron to proton ratio vs expected x from e' projections. The bottom row plots are the same, except vs expected y from e' projections. The first column plots are from SBS-8 ($\varepsilon_1 = 0.807$). The second column plots are from SBS-9 ($\varepsilon_2 = 0.517$). The third column plots are ε_1 n:p ratio (SBS-8, 70% field) divided by ε_2 n:p ratio (SBS-9, 70% field). The pronounced systematic effects, consistent with losses in detection efficiency, are shared across kinematics and largely cancel in the super-ratio.

- Figure is from Sebastian Seeds’ thesis.
- Top row x axis is expected (neutron) x position
- Bottom row x axis is expected (neutron) y position
- Left (middle) column y axis is SBS-8(9) n/p ratio
- Right column y axis is double ratio $\frac{\left(\frac{n}{p}\right)_{SBS8}}{\left(\frac{n}{p}\right)_{SBS9}}$, illustrating (partial) cancellation of efficiency non-uniformity in the double-ratio.
- Fiducial cuts are aggressive (especially for SBS-8) to match smaller envelope of elastic events on HCAL for SBS-9.
- This artificially enhances the “dip” region.
- Wider fiducial cuts reduce sensitivity to the dip region in the acceptance-averaged ratios

Data/SIMC comparison of PDE (SBS-8, 70% field), I (Provakar)

SBS8 – SBS70p H(ee'p)

Data

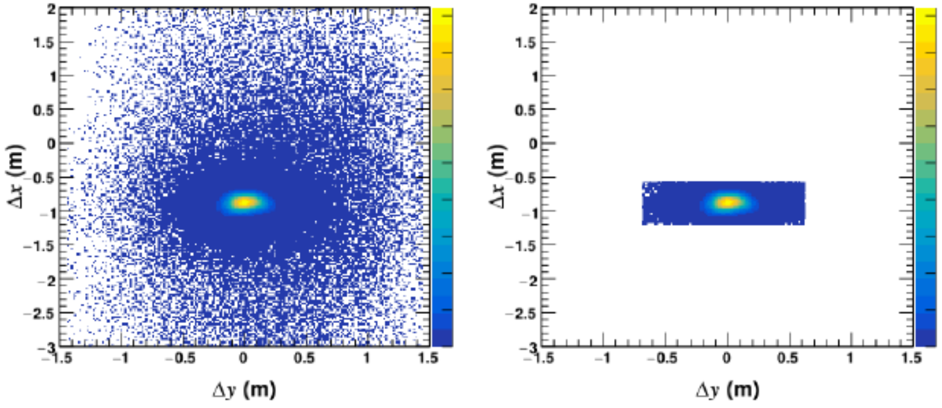

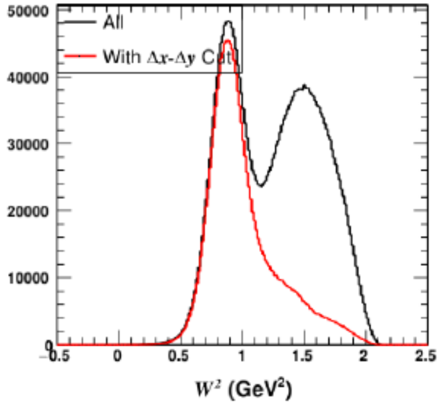

Denominator:
Good e- track cuts
Fiducial Cut
0.65 < W2 < 0.95

Numerator:
Good e- track cuts
Fiducial Cut
0.65 < W2 < 0.95
pdx_nS < 3.5
dy_nS < 3.5
eHCAL>0

SIMC

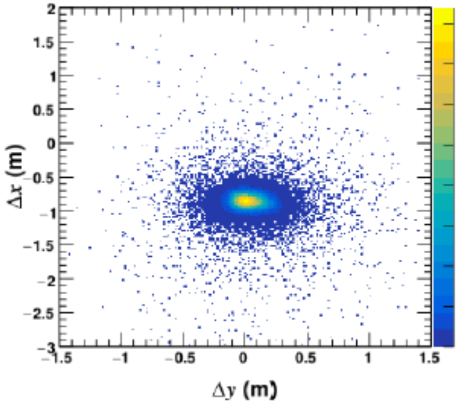

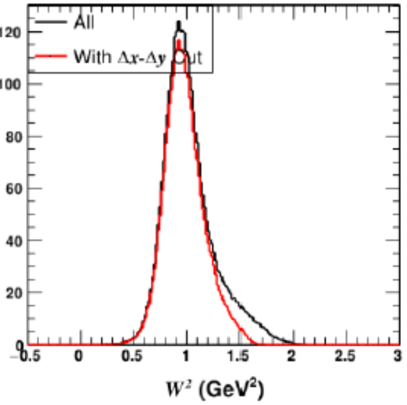

Denominator:
Good e- track cuts
Fiducial Cut
0.65 < W2 < 0.95

Numerator:
Good e- track cuts
Fiducial Cut
0.65 < W2 < 0.95
pdx_nS < 3.5
dy_nS < 3.5
eHCAL>0

* Identical event selection cuts have been applied to data and MC

Statistics requirements: asymmetries vs. cross section measurements

Cross sections:

$$\sigma \propto N$$

$$\Longrightarrow \frac{\Delta\sigma}{\sigma} = \frac{1}{\sqrt{N}}$$

To measure a cross section with a relative statistical precision of 1%, you need 10,000 events.

Asymmetries:

$$\Delta A = \sqrt{\frac{1-A^2}{N}}$$

$$\frac{\Delta A}{A} = \sqrt{\frac{1-A^2}{NA^2}}$$

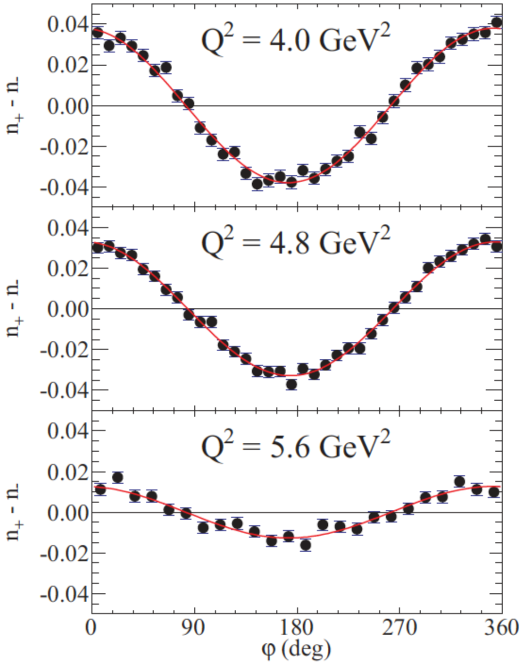

FIG. 6. (Color online) Focal-plane helicity-difference asymmetry $n_+ - n_- \equiv (N_{\text{bins}}/2)[N^+(\varphi)/N_0^+ - N^-(\varphi)/N_0^-]$, where N_{bins} is the number of φ bins and $N^\pm(\varphi)$, $N_0^\pm$ are defined as in Eq. (4), for the three highest Q^2 points from GEp-II. Curves are fits to the data. See text for details.

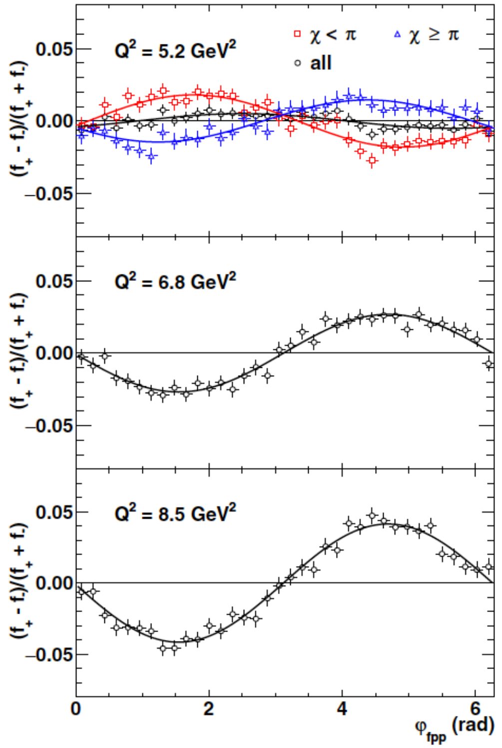

FIG. 10. Focal plane helicity difference/sum ratio asymmetry $(f_+ - f_-)/(f_+ + f_-)$, defined as in Eq. (20), for the GEp-III kinematics, for FPP1 and FPP2 data combined, for single-track events selected according to the criteria discussed in Sec. III B 2. Asymmetry fit results are shown in Table V. The asymmetry at $Q^2 = 5.2$ GeV^2 is also shown separately for events with precession angles $\chi < \pi$ and $\chi \geqslant \pi$, illustrating the expected sign change of the sin(φ) term.

- Example: Typical asymmetry magnitude in a recoil proton polarimeter at "high" momentum is ~few percent.
- To measure a 5% asymmetry with a relative precision of 1%, one needs $N = 10{,}000 \times \frac{1-A^2}{A^2} \approx 4\times10^6$ events!

→ Asymmetry measurement must maximize beam and/or target polarization, and luminosity × acceptance!

SBS/BigBite with GEMs—Hall A enters the "Big Data" era

SBS G_M^n Data Acquisition (DAQ) Facts

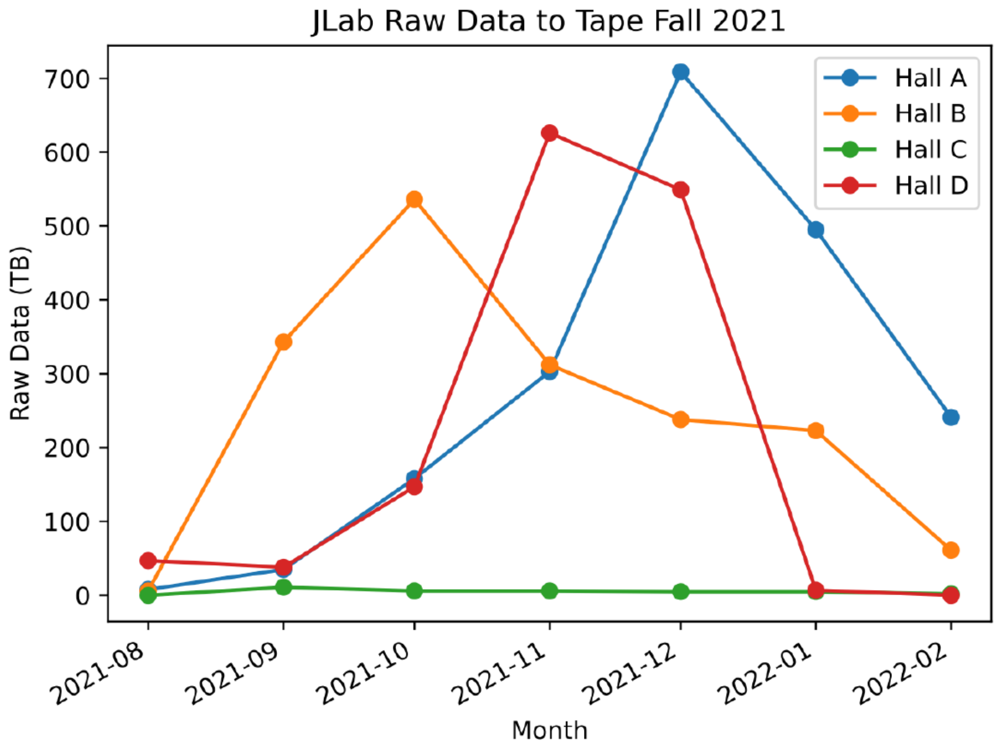

- Data Acquisition challenges:
  - 43,000+ detector readout channels!
  - Very high luminosity, $\sim 10^{38}\ cm^{-2}s^{-1}$
- During 5 months (Oct 2021 - Feb 2022) of SBS G_M^n running, Hall A has recorded ~2 PB worth of raw data!
  - This is more than any other Hall.
  - Also, 5 times more data than all prior Hall A experiments combined in 25 years!

[*] Graphic from Ole Hansen (JLab), Jan 2022

APS April Meeting, 04/11/2022 7

GEM-based tracking in BigBite: what we're up against (run 13727, 12 uA LD2, $Q^2 = 4.5\ GeV^2, E = 4\ GeV$)

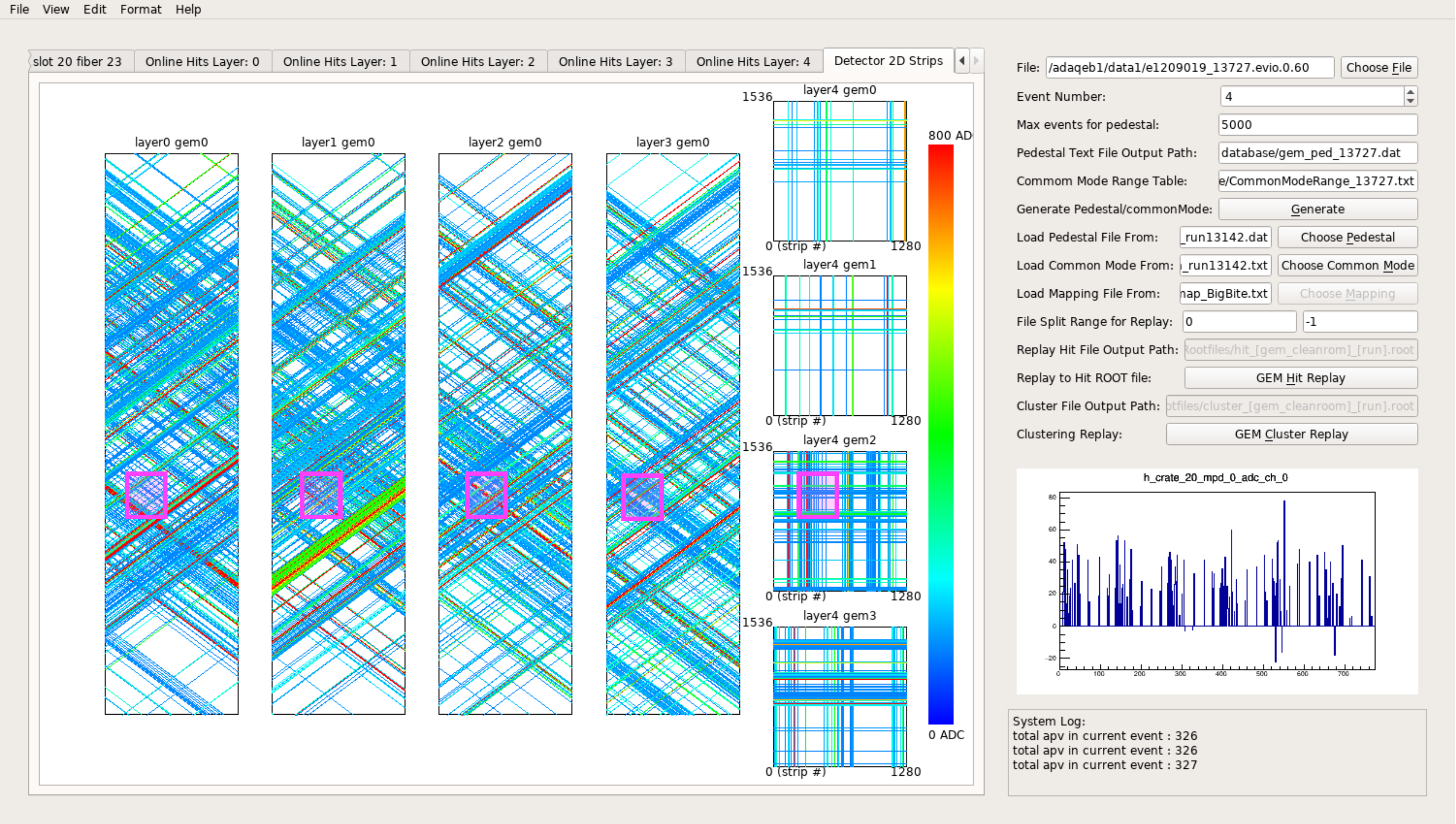

- Single-event display from BigBite GEM trackers during typical SBS GMN production run

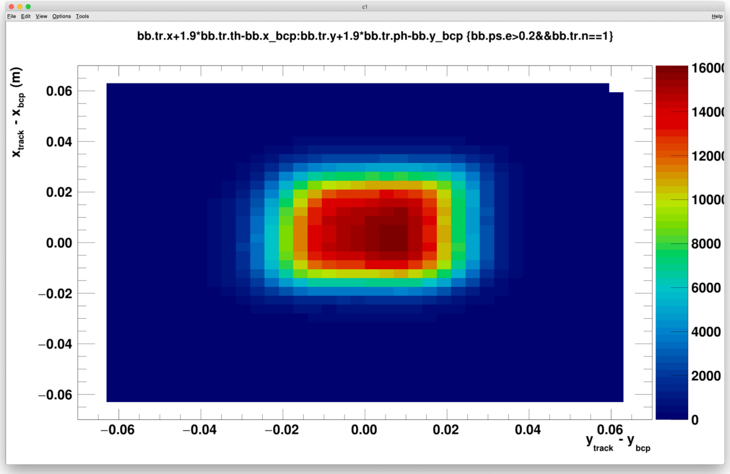

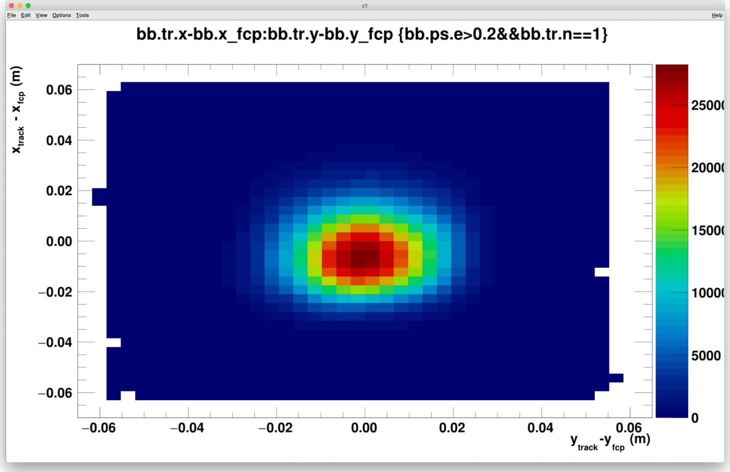

BigBite calorimeter narrows search region for tracking

= approximate size of calorimeter-constrained track search region at each layer

High-Q^2 G_M^n and quark flavor FFs

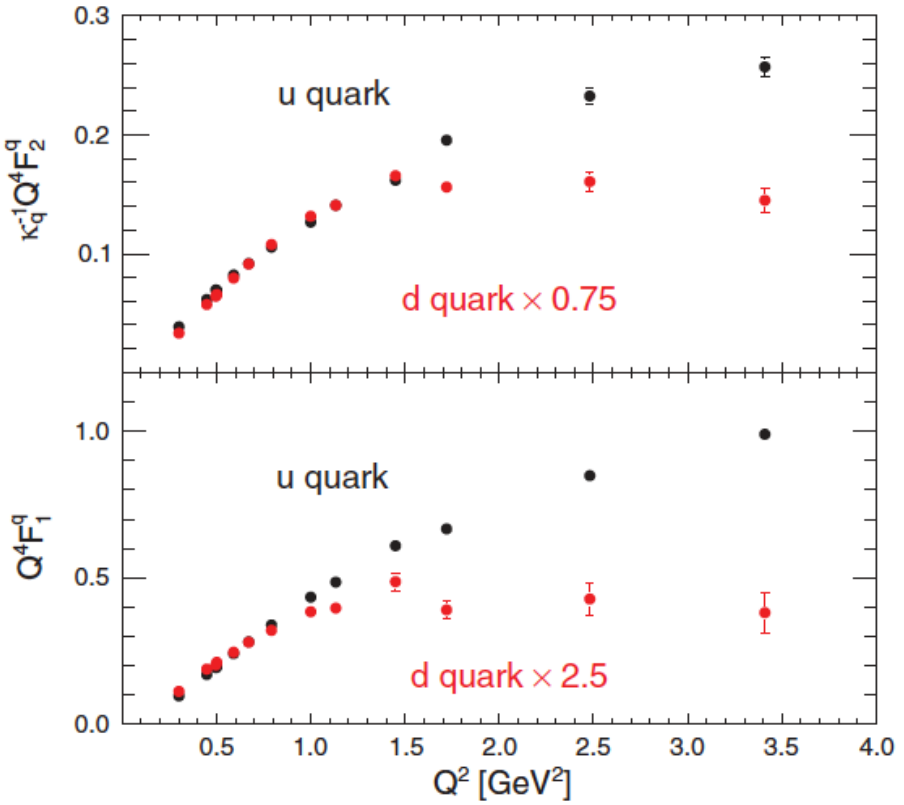

FIG. 3 (color). The Q^2 dependence for the u and d contributions to the proton form factors (multiplied by Q^4). The data points are explained in the text.

Cates *et al.*, PRL 106, 252003 (2011)

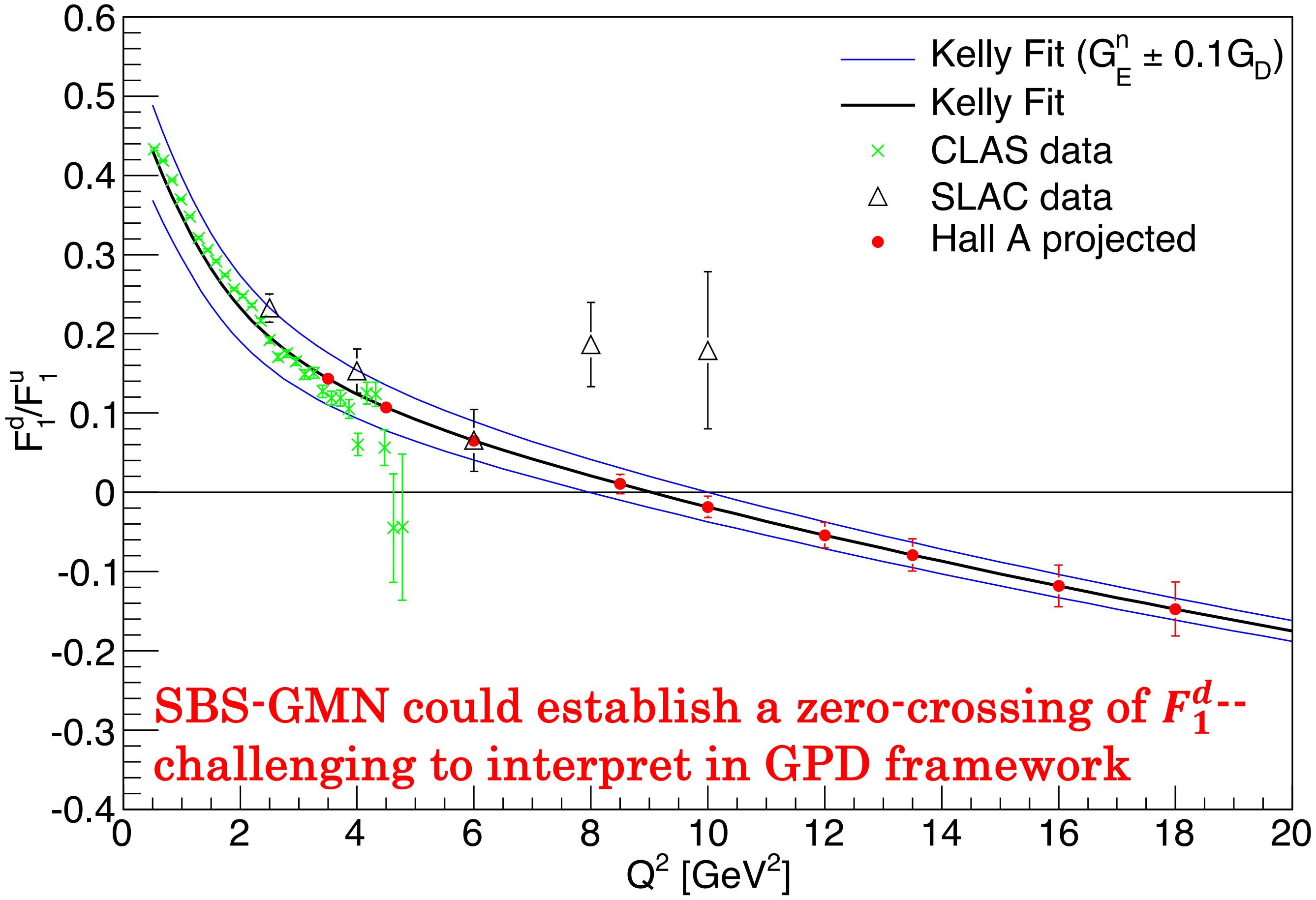

- Notable behaviors: d and u quark FFs show dramatically different Q^2 dependence.
- Flavor FF ratios F_2^q/F_1^q almost constant for both u and d above 1 GeV²

The SBS high-Q^2 Form Factor Program in Hall A

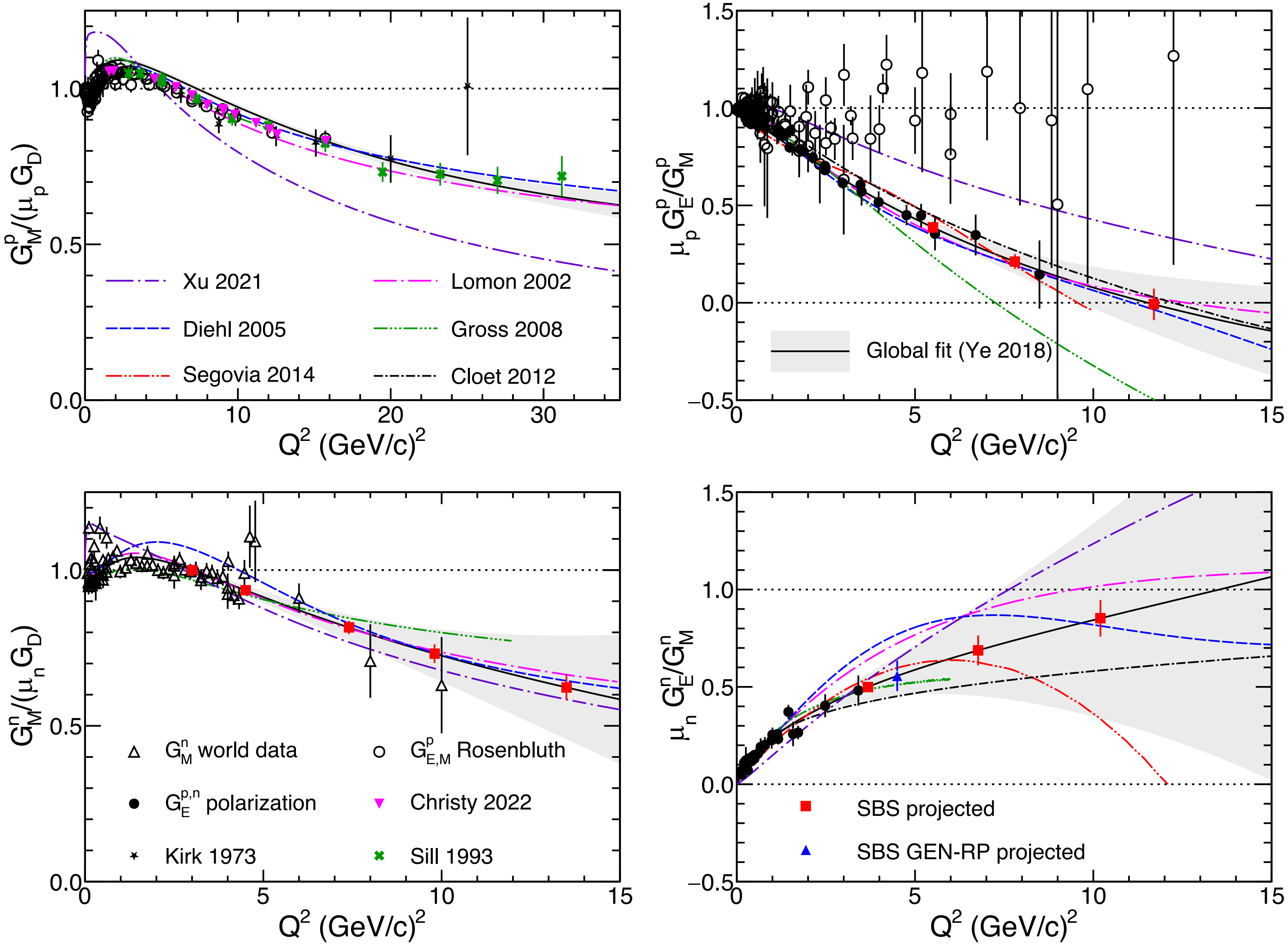

- Figure from "50 Years of QCD" (EPJ C 83, 1125 (2023)): https://inspirehep.net/literature/2617065
- GMN/nTPE (E12-09-019/E12-20-010) using "ratio" method on deuterium: Completed Oct. 2021-Feb. 2022
- GEN Helium-3: Completed Oct. 2022-Oct. 2023)
- GEN-RP: Completed April-May, 2024
- GEP: Projected run 2025
- Except for G_M^n, all SBS form factor measurements are based on polarization observables.
  - Small elastic cross sections and asymmetries require as large as possible FOM (= Luminosity × Polarization² × Acceptance)